THE IMPACT OF RARE EARTH ELEMENTS ON WASTEWATER MICROBIAL COMMUNITIES

by

Stephanie Aurelius

A thesis submitted to the Faculty and the Board of Trustees of the Colorado School of Mines in partial fulfillment of the requirements for the degree of Master of Science (Environmental Engineering Science).

Golden, Colorado

Date _____

Signed: _____

Stephanie Aurelius

Signed: _____

Dr. Junko Munakata Marr
Thesis Advisor

Golden, Colorado

Date _____

Signed: _____

Dr. Junko Munakata Marr
Professor and Department Head
Department of Civil and Environmental Engineering

ABSTRACT

Rare earth elements (REEs) are essential in the manufacture and development of modern technologies. REEs reach water resource reclamation facilities (WRRFs) from hospital and industrial wastewater effluents. The increasing prevalence of REEs motivates the need to understand how they affect the activities and community structure of wastewater microorganisms. Additionally, REEs exhibit antimicrobial properties comparable to heavy metals, which have been shown to co-select for antibiotic resistance.

Plate assays were performed to determine the effect of REE recycling waste on microbial growth. Culturing of REE-resistant cells evaluated the potential for REEs to co-select for antibiotic resistance in wastewater microorganisms. Growth of REE-resistant cells in the presence of antibiotics was explored, and predominant taxa and resistance genes were investigated. The acute effect of REEs and metals on biological nitrification was tested in batch experiments. Additionally, the microbial community was characterized before, during, and after REE-induced inhibition of nitrification in long-term aerobic bioreactor experiments.

Activated sludge growth was inhibited in plates amended with REE recycling waste, though acidity was the main contributor to toxicity. Growth of REE-resistant cultures was similar to, or greater than, unamended sludge growth in the presence of antibiotics. Predominant resistance genes differed between samples exposed to different forms of lanthanum. Compared to the control, lanthanum-resistant samples had higher abundances of kasugamycin resistance genes, with the lanthanum nanoparticle-resistant sample also showing increased fosmidomycin resistance. In batch reactors, lanthanum nanoparticle additions did not affect nitrification, but 1000 μM of aqueous lanthanum, dysprosium, and copper reduced ammonia oxidation. Inhibition of nitrification was associated with diminished abundance of nitrifying microbes in aerobic bioreactors amended with high concentrations of yttrium or gadolinium. Abundance of nitrifying microbes returned to pre-treatment levels once additions were stopped in the yttrium-amended reactor, but not in the gadolinium-amended reactor. Our results indicate that high concentrations of REEs may impact community composition and nitrification in wastewater communities.

TABLE OF CONTENTS

LIST OF FIGURES

LIST OF TABLES

LIST OF ABBREVIATIONS

Centers for Disease Control and Prevention . . . . . CDC

Clinical and Laboratory Standards Institute . . . . . CLSI

Colorado School of Mines . . . . . CSM

Half maximal effective concentration EC50

Luria-Bertani . . . . . LB

Mueller-Hinton . . . . . MH

Promethium . . . . . Pm

United States Environmental Protection Agency . . . . . EPA

Waste 1A W1A

Waste 1B W1B

Waste 2A W2A

Waste2B W2B

ammonia as N . . . . . NH_3-N

ammonia as nitrogen . . . . . NH_3-N

ammonia uptake rate . . . . . AUR

ammonia-oxidizing archaea . . . . . AOA

ammonia-oxidizing bacteria . . . . . AOB

amplicon sequence variant . . . . . ASV

antibiotic resistance gene . . . . . ARG

antibiotic-resistant bacteria . . . . . ARB

below detection limit . . . . . BDL

biochemical oxygen demand . . . . . BOD

cadmium . . . . . Cd

cerium . . . . . Ce

chemical oxygen demand . . . . . COD

complete ammonia oxidation . . . . . comammox

confidence interval CI

copper . . . . . Cu

copper (II) chloride . . . . . $CuCl_2$

degrees Celcius . . . . . °C

dysprosium . . . . . Dy

dysprosium chloride . . . . . $DyCl_3$

erbium . . . . . Er

europium . . . . . Eu

gadolinium . . . . . Gd

gram . . . . . g

holmium . . . . . Ho

hydraulic residence time . . . . . HRT

hydrochloric acid . . . . . HCl

inductively coupled plasma with atomic emission spectroscopy detection . . . . . ICP-AES

iron . . . . . Fe

kilogram . . . . . kg

lanthanum . . . . . La

lanthanum chloride . . . . . $LaCl_3$

lanthanum oxide . . . . . La_2O_3

liter L

lutetium . . . . . Lu

micro (10^{-6}) . . . . . μ

microgram . . . . . μg

microliter . . . . . μL

micrometer . . . . . μm

micromoles per liter . . . . . μM

milligram . . . . . mg

milliliter . . . . . mL

millimeter . . . . . mm

minimum inhibitory concentration . . . . . MIC

mixed liquor suspended solids . . . . . MLSS

mixed liquor volatile suspended solids . . . . . MLVSS

moles per liter . . . . . M

nanogram . . . . . ng

nanometer . . . . . nm

neodymium . . . . . Nd

nitrate as N . . . . . NO_3-N

nitrate as nitrogen . . . . . NO_3-N

nitric oxide . . . . . NO

nitrite as N . . . . . NO_2-N

nitrite as nitrogen . . . . . NO_2-N

nitrogen gas . . . . . N_2

nitrous oxide . . . . . N_2O

parts per million . . . . . ppm

permutational multivariate analysis of variance . . . . . PERMANOVA

polyethersulfone . . . . . PES

potassium . . . . . K^+

potassium . . . . . K^+

praseodymium . . . . . Pr

principal coordinates analysis . . . . . PCoA

rare earth element . . . . . REE

rare earth oxide basis . . . . . REO

revolutions per minute . . . . . rpm

samarium . . . . . Sm

scandium . . . . . Sc

sodium . . . . . Na

solubility product constant . . . . . K_{sp}

specific oxygen uptake rate . . . . . SOUR

sulfur . . . . . S

synthetic wastewater . . . . . SWW

terbium . . . . . Tb

thulium . . . . . Tm

total suspended solids . . . . . TSS

tri-n-butyl phosphate . . . . . TBP

volume per volume . . . . . v/v

water resource reclamation facility . . . . . WRRF

ytterbium . . . . . Yb

yttrium . . . . . Y

ACKNOWLEDGMENTS

I would like to thank everyone who has supported me throughout graduate school. First, I would like to thank my advisor, Dr. Junko Munakata Marr, for her guidance, feedback, and patience throughout this process. I would also like to thank Dr. Linda Figueroa for serving on my committee and helping me produce the best possible version of my thesis. I am very grateful to Dr. Gary Vanzin for serving on my committee and for the reassurance (and extreme patience) while I learned the ins and outs of microbiology and data processing.

I would also like to thank Dr. Yoshiko Fujita, from Idaho National Laboratory, for providing expertise and insight to this research. I appreciate all of the encouragement and support of new ideas and experimental investigations.

I am also grateful to my GEM lab mates for their support and advice. I am always amazed by their work and have learned so much from them, despite the pandemic pushing us to virtual meetings. A special thank you to undergraduate researchers Diana Teran, Leonard Igberaese, and Erin Taggart for their time and efforts in the lab, which helped further this research.

The research presented was possible through the financial support of the Critical Materials Institute. I am incredibly grateful for the opportunities to work with, and learn from, collaborators within the organization. Additional support was provided by the Edna Bailey Sussman Foundation, which allowed me to deepen my knowledge and further my investigation into rare earths and wastewater microbial communities.

Finally, I would like to thank my friends and family for their endless support. I feel incredibly lucky to have great friends to vent to, and celebrate with, as we navigate graduate programs and post-graduate life. A big thank you to my parents, John and Lani, for always encouraging me to challenge myself and to follow each adventure, even if takes me away from California.

CHAPTER 1

INTRODUCTION

Rare earth elements (REEs) are essential in the manufacture and production of modern technologies, including cell phones, engine exhaust catalysts, and batteries. Because REEs are used in a variety of modern and emerging products, the demand for these resources is increasing. In the United States, REEs are ranked high on the criticality factor for raw materials, as they are essential to technologies and economies while also being at risk for supply disruptions [1]. The United States does not produce enough REEs to support domestic use and relies heavily on imports. To meet demand, researchers and organizations have invested in domestic mining and recycling technologies. The development of these technologies brings the need to understand the effects of their resulting waste streams.

Mountain Pass Mine in San Bernardino County, California was once the leading global producer of REEs. The mine has recently restarted operation after prior owners left the site in the 1990s [2]. Today, Mountain Pass is the only REE mining facility in the United States and produces 15% of the global supply of REEs, though it currently sends intermediate products to be further processed in Asia [2]. With the expected relaunch of its onsite processing facilities in 2022, it is expected to support the United States' rare earth demand. In addition to increased production, researchers have developed economically viable methods to recycle REEs for reuse. REEs can be recovered from end-of-life products through separation processes, resulting in high purity REE. As the manufacturing and use of REEs continues to increase, so does the likelihood of REEs ending up in water resource reclamation facilities (WRRFs). REEs reach WRRFs through industrial and hospital wastewater effluents, and are used in WRRFs as a phosphate reduction strategy.

Biological processes like activated sludge are crucial in the effective treatment of wastewater. Aerobic microorganisms in activated sludge are essential in the transformation and degradation of contaminants in the wastewater. The introduction of a contaminant, like REEs, could impair or inhibit the functions of the microbial communities, possibly affecting the effectiveness of the treatment process. The impact of REEs on biological wastewater treatment has not been widely

studied.

In addition to REEs, WRRFs serve as collection points for contaminants from industrial and domestic effluents [3]. These waste streams contain stressors (e.g. antibiotics, heavy metals) that could lead to the enrichment of resistant bacteria in wastewater microbial communities. Resistance develops when stressors provide a selective pressure for bacteria to evolve and develop resistance mechanisms. In the United States, conventional WRRFs are not designed to remove or monitor pharmaceutical concentrations [4]. Heavy metals have been shown to select for antibiotic resistance due to the shared resistance mechanisms between heavy metals and antibiotics, and REEs have been shown to exhibit antimicrobial properties comparable to some heavy metals [5]. Once resistance develops, it can proliferate through the microbial community via horizontal gene transfer due to the high density of microorganisms in biological wastewater treatment processes [6]. Links between heavy metal tolerance and antimicrobial resistance have been explored, but the relationship between REEs and antibiotic resistance has not been investigated. If REEs co-select for antibiotic resistance, the presence of REEs in WRRFs may contribute to the spread of antibiotic-resistant microorganisms. In addition to discharging treated wastewater to receiving bodies of water, many facilities participate in programs where their biosolids are used for fertilizer, potentially releasing resistant bacteria and/or genes into the terrestrial environment. While aerobic digestion can reduce antibiotic resistance genes, efficacy is dependent on reactor design and gene type [7].

The goal of this study was to investigate the impact of REEs on the function and composition of biological wastewater microbial communities. Specifically, I aimed to evaluate the following questions:

1. Does REE recycling waste affect the growth of wastewater microorganisms?

2. Does lanthanum affect nitrification in wastewater microorganisms?

3. If so, are impacts different between aqueous lanthanum and lanthanum nanoparticle additions?

4. Do REEs exert a selective pressure for antibiotic resistance in wastewater microorganisms?

5. How does microbial community composition change during, and after, REE-induced inhibition of nitrification?

I hypothesized that, at high concentrations, lanthanum would adversely impact wastewater microbial communities by inhibiting growth and nitrification. Based on literature describing the adverse effects of REE ions, I hypothesized that aqueous lanthanum would exhibit a greater inhibitory effect than lanthanum nanoparticles. I further hypothesized that aqueous lanthanum and lanthanum nanoparticles would co-select for antibiotic resistance. We designed multiple experiments to investigate our hypotheses. The first study evaluated the toxicity of rare earth recycling waste streams on activated sludge. The study consisted of preparing aerobic culture plates amended with REE recycling waste at varying dilutions. The plates were inoculated with activated sludge from a local WRRF and colony growth was evaluated.

The second study aimed to determine if REEs selected for antibiotic resistance by preparing culture tubes amended with antibiotics and metals at varying concentrations. Antibiotics included chloramphenicol, erythromycin, kanamycin, nalidixic acid, nitrofurantoin, novobiocin, penicillin, streptomycin, sulfamethoxazole, and tetracycline. Metals included heavy metal cadmium and REEs lanthanum and dysprosium. Metal-resistant cells were then used as inoculum for culture tubes amended with antibiotics. Metal-resistant cells were also used as inoculum to evaluate inhibition caused by antibiotic discs on agar plates. The effect of REEs on antibiotic resistance was further investigated using an Oxford Nanopore MinION sequencing device. Metagenomic sequencing data were analyzed to compare taxonomy and resistance genes between cells exposed to metals and cells exposed to both metals and antibiotics.

The third study investigated the acute impacts of REE to nitrification. Batch reactors inoculated with activated sludge from a local WRRF were dosed with increasing concentrations of aqueous lanthanum, lanthanum nanoparticles, aqueous dysprosium, and copper as a positive control. Samples were collected every 30 minutes for 120 minutes to measure nitrification activity.

The final study was conducted to investigate the change in microbial community composition during and after REE exposure. Following increasing amendments of either gadolinium (Gd) or yttrium (Y) to batch-fed aerobic bioreactors, REE additions to the synthetic wastewater (SWW) were discontinued. Samples were collected regularly for treatment performance measurements and DNA sequencing.

The findings of this research are intended to inform REE waste generators and WRRF operators. If WRRF performance is shown to be adversely impacted by REE-containing waste

streams, discharges to WRRFs will need to be pre-treated or limited. In addition, if REEs co-select for antibiotic resistance, the U.S. Environmental Protection Agency (EPA) will need to consider implementing effluent and biosolid limitations for REEs to protect receiving environments. This research will further the investigation into the impacts of REEs on biological treatment processes. This thesis describes further background information on treatment processes, antibiotic resistance, and REEs in WRRFs in Chapter 2. Methodology and results are described in Chapters 3 and 4, respectively, which inform the conclusions and recommendations in Chapter 5.

CHAPTER 2

BACKGROUND

The widespread use of rare earth elements (REEs) increases the likelihood of these materials reaching the microbial communities in water resource reclamation facilities (WRRF), potentially affecting the composition and activity of these communities.

2.1 Biological Wastewater Treatment

Biological wastewater treatment is essential in the degradation of contaminants in wastewater. In the activated sludge process, water from primary treatment is pumped into an aeration basin. The aeration basin is constantly aerated to provide enough oxygen for the microorganisms to carry out their functions. The water has a biochemical oxygen demand (BOD), which is a measure of how much oxygen is required to break down the contaminants. The aeration basin holds microorganisms in suspension as they degrade the organic matter. Activated sludge is comprised of a diverse group of microorganisms. The bacteria oxidize the organic matter and ammonia in the water into carbon dioxide, water, and nitrate. Nitrification is a key process in biological treatment, as nitrogen compounds are harmful to receiving surface waters. Ammonia-oxidizing bacteria, like *Nitrosomonas*, transform ammonia into nitrite, while nitrite-oxidizing bacteria, like *Nitrobacter*, transform nitrite into nitrate. The mass of bacteria in the aeration basin is called mixed liquor volatile suspended solids (MLVSS). All suspended solids, including bacteria and non-biodegradable suspended matter is called mixed liquor suspended solids (MLSS), which describes total suspended solids (TSS). Facility operators must control dissolved oxygen levels, MLVSS, and hydraulic residence time (HRT) to ensure effective treatment.

Biological treatment is crucial in the overall wastewater treatment process and for meeting regulatory effluent standards. Due to the importance of this process, it is necessary to understand how REEs may impact the growth or functions of the activated sludge microbial community.

2.2 Antibiotic-Resistant Bacteria

The Centers for Disease Control and Prevention (CDC) estimates that, annually, over 35,000 deaths and 2.8 million illnesses are attributed to antibiotic-resistant infections in the U.S. [8].

This is due in part to the misuse and overuse of antibiotics, along with the lack of new antibiotic development. Thirty to fifty percent of patients are inappropriately prescribed antibiotics in terms of choice of agent or treatment duration [9]. The COVID-19 pandemic also contributed to antibiotic overuse; though few hospitalized patients had a bacterial co-infection, the majority received antibiotics as treatment [10, 11]. Antibiotics are also widely used for livestock as growth supplements to increase yield and improve animal health. This misuse and overuse contributes to the observed resistance, as widespread use leads to the evolution and emergence of resistant bacteria. Today, there are a number of species that are resistant to widely-available antibiotics [8]. Bacteria of interest, termed ESKAPE pathogens, are highly virulent and antibiotic-resistant. ESKAPE pathogens were defined by Dr. Louis B. Rice, former director of the Infectious Diseases Society of America. The group is made up of *Enterococcus faecium*, *Staphylococcus aureus*, *Klebsiella pneumoniae*, *Acinetobacter baumannnii*, *Pseudomonas aeruginosa*, and *Enterobacter* species. [12]

Literature reports that microbial exposure to heavy metals can co-select for antibiotic resistance. When a microorganism is exposed to heavy metals, it may develop resistance to the metal as well as antibiotics. This occurs because metal and antibiotic-resistance genes are commonly co-located on mobile genetic elements, particularly plasmids [13]. Co-resistance to metals and antibiotics is achieved through various mechanisms. A single pathway may provide resistance to multiple compounds, or the expression of resistance systems may be controlled by a common regulator. Once a microorganism develops resistance, resistance can proliferate through a microbial community through horizontal gene transfer, where genes are exchanged via mobile genetic elements. Following exposure to a range of heavy metals, *Bacillus* sp. was resistant to antibiotics kanamycin, ampicillin, and methicillin [14]. Further testing indicated that the genes for heavy metal and antibiotic resistance were located on plasmid DNA [14]. Wastewater treatment processes are not designed to remove antibiotic resistant bacteria (ARB) or resistance genes, and WRRFs can harbor antimicrobials in addition to the metals and REEs that may enter through the influent [15]. The combination of multiple stressors facilitates resistance. In activated sludge bioreactors, the addition of 5 mg/L zinc increased tylosin resistance [16]. Tylosin, oxytetracycline, and ciprofloxacin resistance was amplified further when antibiotics were introduced in addition to zinc [16].

Like some heavy metals, REEs have been shown to exhibit antimicrobial properties. All rare earth ions (with the exception of promethium) have shown antibacterial and antifungal activity comparable to copper and silver ions [17]. Heavy REEs, which have atomic numbers higher than 63 (including scandium and yttrium), exhibited stronger toxic effects than light REEs [17]. Due to their similar antimicrobial properties, it is possible that REEs may exert a selective pressure, like heavy metals, that may lead to antibiotic resistance. A study showed that pre-exposure to 10 to 100 milligrams of rare earth oxide nanoparticles (La_2O_3, Nd_2O_3, Gd_2O_3) per kilogram of soil increased the abundance and richness of antibiotic resistance genes in soil microorganisms throughout the 60 day experiment [18]. The number of resistance genes and the number of mobile genetic elements were significantly correlated, indicating that horizontal gene transfer facilitated the spread of resistance in the soils [18].

Amplification of antibiotic resistance genes in response to rare earth nanoparticle exposure has been demonstrated in soil microorganisms but has yet to be investigated in wastewater microbial communities. If REEs are found to co-select for antibiotic resistance, implications for WRRFs could be large. If resistance develops in the aeration basin, it could spread through the microbial population through horizontal gene transfer. The resistant bacteria and resistance genes could then be released into the environment through wastewater effluents and biosolids.

2.3 Presence of REEs in WRRFs

Elevated concentrations of REEs have been measured in WRRFs and surface waters. Kaegi et al. (2021) compared REE concentrations from 63 WRRFs in Switzerland to background REE levels. The study found that the fluxes of REEs in wastewater is dominated by industrial point sources [19]. Kulaksız and Bau (2013) found that the Rhine River in Germany may carry up to 730 kg gadolinium (Gd), 5700 kg lanthanum (La), and 584 kg samarium (Sm) annually. With an average annual discharge of 2,300 m^3, the Rhine contains 2.02 μM, 17.8 μM, and 1.69 μM of Gd, La, and Sm, respectively [20]. The anthropogenic La and Sm were found to originate from a facility along the Rhine that produces catalysts for petroleum refining [21]. Verplanck (2010) collected samples from four metropolitan WRRFs in the United States to determine the fate of REEs within a treatment facility. Total REE concentrations in the wastewater influent ranged from 1.76 to 3.82 nM, while effluent concentrations ranged from 1.29 to 1.88 nM [22]. Gadolinium

was the most abundant REE in all of the collected samples. Gadolinium is commonly used in medical facilities as a contrast agent in magnetic resonance imaging and has been detected in wastewater effluents and surface waters [23]. Unusually high Gd concentrations (up to 2.1 nM) in four WRRFs were consistent with the use of magnetic resonance imaging in the metropolitan areas that the facilities serve [22]. Detection of high levels of Gd in hospital wastewater is not uncommon; effluent from the Freiburg University Hospital in Germany contained up to 55 µg/L (0.35 µM) Gd [24]. Gadolinium is used in hospitals in a chelated form, meaning that the metal bonds with organic molecules and is transformed into an inert, stable form that moves through the patient's body without causing harm. In this thermodynamically stable form, the chelated gadolinium is more difficult to treat in WRRFs and, therefore, more prevalent in effluent streams and receiving waters [25]. Other rare earths, like lanthanum and cerium, commonly occur in nanoparticle form, which is easier to remove in treatment facilities due to increased aggregation of particles and settling [26].

Rare earths are commonly used in manufacturing as rare earth oxides; therefore, they may enter WRRFs as nanoparticles. A study examining five Swiss WRRFs determined that the majority of anthropogenic cerium (Ce) in digested sewage sludge existed as cerium oxide nanoparticles [27]. Gomez-River et al. (2012) investigated the fate of cerium nanoparticles in activated sludge treatment and found that the nanoparticles aggregated at the pH levels maintained in WRRFs. Batch reactors were amended with 55 mg/L (392 µM) Ce and roughly 2 mg/L (14.3 µM) Ce was detected in the effluent. A fraction of the Ce was found in biomass, as the nanoparticles sorb to the outer membranes of bacteria. [26]

REEs are trivalent and are unlikely to exist as free ions in wastewater. If REEs did reach WRRFs in their dissolved forms, they would readily precipitate out as rare earth phosphates ($K_{sp} = 10^{-26.15}$) [28]. Since these rare earths have a high affinity for phosphate, they are being intentionally added to WRRFs as a phosphate reduction strategy. Lanthanide salts have been investigated for phosphate removal since the 1970s [29]. Research by Recht and Ghassemi (1970) led to a patent which includes a combination treatment of alum and lanthanum, with lanthanum concentrations ranging from 13 to 82 mg/L (93 to 590 µM) [30]. In the past decade, lanthanide salt solutions have been added directly to WRRF primary clarifiers at REE concentrations ranging from 5 to 42 mg/L (36 to 302 µM) [31]. A patent for a rare earth clarifying agent claimed

REE concentrations ranging from 0.001 to 1.0 mM, which includes REEs Ce, La, Sm, praseodymium (Pr), neodymium (Nd), promethium (Pm), and yttrium (Y) [32]. In addition to precipitation techniques, adsorption of phosphate using rare earths is currently being investigated to meet effluent limitations in WRRFs [33, 34].

As technology continues to advance, the use, and reuse, of REEs will continue to increase. While rare earths do occur naturally in the earth's crust, literature suggests that WRRFs and surface waters receive substantial REE inputs from anthropogenic sources. This is attributed to the increase in the use and manufacturing of products that use REEs [35, 36]. Due to the high domestic demand for REEs, researchers have developed methods to recycle these resources for reuse. However, recycling methods create waste streams potentially discharged to WRRFs. Traditional recycling methods are effective in REE recovery but have disadvantages. They use strong acids, have a high energy demand, and produce a large volume of waste [37]. A recently developed recycling process maximizes REE recovery while reducing hazardous waste generation. The new approach involves dissolving electronic waste into an acid-free solution and allows the selective leaching of REEs. Though the waste is not as harsh as the waste from traditional recycling methods, it still contains trace concentrations of REEs that may contribute to REE loads currently detected in wastewater influents. This may lead to a higher prevalence of REEs in WRRFs, heightening the need to understand how these materials may affect WRRF biological processes.

2.4 Effect of REEs on Wastewater Microbial Communities

REE salts have been shown to be toxic to microorganisms. Técher et al. (2020) performed dose-response inhibition assays of *Escherichia coli* growth under REE exposure. All 16 REEs were tested in this experiment. Half maximal effective concentration (EC50) values ranged from 1.1 to 27.4 µM, with scandium exhibiting the highest toxicity. Bacterial growth monitoring showed that heavy REEs were more toxic than light REEs. A bacterial injury assessment indicated that REEs have a toxicity potential through cell membrane damage, involving lipid peroxidation, enhanced membrane permeability and depolarization, and impaired ATP production. [38]

REEs have also been shown to adversely impact the activities of activated sludge. Fujita et al. (2016) investigated the impact of europium (Eu), Y, and an organic complexant, tri-n-butyl

phosphate (TBP), on biological activity of activated sludge. TBP is commonly used in REE extractions. Synthetic wastewater (SWW) was amended with concentrations of Eu or Y at 0, 6.6, 66, and 660 µM (1, 10, 100 mg/L Eu; 0.59, 5.9, 59 mg/L Y). The SWW was placed in an incubator with orbital shaking and was sampled over the course of the 37-day experiment. The specific oxygen uptake rate (SOUR) decreased significantly at all Eu concentrations. Only the 660 µM amendment resulted in reduced SOUR values for the Y-amended flasks. The addition of the complexant TBP enhanced inhibition by Eu at all concentrations and by Y at the 660 µM (59 mg/L Y) concentration. Addition of Eu was associated with higher concentrations of ammonia in the SWW, with reduced concentrations of nitrate. Addition of Y did not affect ammonia or nitrate levels. [39] The results indicated that Eu and Y have the potential to negatively affect sludge activity in different ways and to different degrees.

Rare earth oxide nanoparticles also impact microbial community structure and function. Kamika and Tekere (2017) evaluated the impact of CeO_2 nanoparticles on the microbial community in activated sludge in an enhanced biological phosphorus removal system. Reactors were amended with 10 to 40 mg/L (58 to 232 µM) CeO_2 and incubated for 5 days before analysis. Compared to the control, species richness decreased by approximately 97% in the treated reactors. Dominant phyla changed in the treated reactors, suggesting that cerium nanoparticles may promote the growth of certain microorganisms while inhibiting the growth of others, i.e. selective growth. Scanning electron microscope images showed a decrease in microbial biomass as cerium concentration increased. In the reactors amended with 40 mg/L CeO_2, total phosphate and nitrate reduction was only 1.83% and 35.15%, respectively, compared to 89.2% phosphate removal and 99.6% nitrate removal in the control. These substantially lower removal rates suggest the inhibition of microbial functions. [40] Yue et al. (2020) investigated the effect of REE nanoparticle exposure on ammonia oxidation by soil microorganisms. Soil was amended with 10 to 100 mg/kg of La_2O_3, Nd_2O_3, or Gd_2O_3 nanoparticles and incubated for 60 days. Samples were taken on the first, seventh, and final day of the experiment. All amendments substantially decreased soil potential ammonia oxidation. Ammonia-oxidizing archaea (AOA) communities were different in the treated soils when compared to the control on the first day of incubation, however, only La_2O_3-treated soils had a different AOA community on the sixtieth day. The persistence of La_2O_3 toxicity until the final day of incubation indicates a higher toxicity than the

other nanoparticles. The relative abundance of ammonia-oxidizing bacteria (AOB) increased in soils amended with intermediate doses of Nd_2O_3 and Gd_2O_3 after the first day of incubation, suggesting Nd and Gd nanoparticles may promote nitrification at these concentrations. [41] Activities of ammonia-oxidizing microorganisms may be inhibited after exposure to La_2O_3 nanoparticles, thus inhibiting nitrification.

2.5 Tools for Investigating Microbial Community Characteristics

DNA sequencing has served as an essential scientific tool since its creation in the 1970's. It has been used to construct genomes, detect changes in genes associated with disease, and identify species and certain genes within a sample. 16S rRNA gene sequencing is commonly used for bacterial analysis because the 16S rRNA gene can be compared among all bacteria, and since the gene is highly conserved, universal primers can be used in analyses [42]. These primers target certain sections of the gene, known as hypervariable sections. The V4-V5 section is commonly targeted due to its reliability and high resolution in representing the full-length sequence for phylogenetic analysis [43, 44].

The Illumina sequencing platform is widely used for 16S rRNA analysis due to its low cost and high accuracy reads. It is used for phylogenetic classification to determine the species present in diverse microbial populations. Once taxonomy is determined, the data can be used for downstream analysis like alpha diversity and principal coordinates analysis (PCoA). PCoA is a method used to evaluate similarities or dissimilarities in data. It can visualize the clustering or divergence of microbial communities in response to treatments. While Illumina is effective for phylogenetic analysis, it has its disadvantages. Illumina sequencing produces short reads, which is usually not sufficient to construct an entire genome or identify specific locations of resistance or virulence genes [45, 46].

Recently, Oxford Nanopore's MinION sequencing is gaining popularity due to its long sequence reads, which aid in the assembly of whole genomes. Unlike Illumina, Nanopore sequencing is a real-time analysis that can be performed in a few hours. It works by tracking changes to an electrical current as nucleic acids pass through. The changes in the current are decoded to produce a sequence read. The data are immediately available for download and downstream analysis. MinION sequencing has been used to identify taxonomy and antibiotic

resistance genes (ARGs) in stormwater, dust, and sewage [47–49]. Due to the long read lengths obtained by this sequencing method, researchers can get information down to the species level [48]. This not only provides more detailed information about the microbial community, but it also aids in antimicrobial resistance investigations, as specific species have been highlighted as emerging concerns by the Centers for Disease Control and Prevention (CDC) [8]. Analyses like ARGpore use antibiotic resistance databases to identify ARGs, resistance types, and their hosts [49]. Other analyses can determine whether ARGs are associated with plasmids, or co-located with other resistance genes, like metal-resistant genes.

Since MinION technology is new, there have been concerns about accuracy. Multiple studies have analyzed the same DNA samples using Illumina and Nanopore technology, and the results are not significantly different [46, 50]. One study found no difference in the results, but saw that the MinION output had more detailed taxonomic information [48]. Both tools are frequently used simultaneously to get high resolution microbial data, where Illumina is used for taxonomy and MinION technology is used to resolve genomic structure [45, 51]. Both Illumina and MinION sequencing have proven effective in microbial community analysis.

CHAPTER 3

METHODOLOGY

Multiple experiments were designed to evaluate the impact of rare earth elements (REEs) on the structure and activities of wastewater microbial communities. Plate assays were conducted to evaluate the toxicity of REE recycling waste to activated sludge. Antibiotic studies investigated the potential for REEs to co-select for antibiotic resistance in wastewater microbes. Batch reactor experiments evaluated the impact of acute REE exposure on biological nitrification, and microbial analysis was conducted to investigate any microbial shifts during and after chronic REE exposure in aerobic bioreactors.

3.1 Recycling Waste Investigation

A recycling waste investigation was conducted to evaluate the effect of REE-impacted waste on the growth of mixed microbial communities. Plates were amended with two dilutions of wastes generated from a Terfenol-D recycling process. Terfenol-D is a magnetostrictive alloy containing iron and rare earths, terbium (Tb) and dysprosium (Dy) [52]. Its unique properties make Terfenol-D useful for underwater acoustic transducers and actuators [53]. Plates amended with two dilutions of Terfenol-D recycling waste were inoculated and evaluated for cell colony growth.

3.1.1 Waste Materials

We received four wastes from two waste streams from a Terfenol-D recycling method developed by Ames Laboratory in Ames, Iowa. The generation of the two waste streams is depicted in Figure 3.1.

This recycling process includes the dissolution of Terfenol-D scrap into a copper(II) solution, leading to the formation of Fe^{2+}, Fe^{3+}, and REE^{3+} ions in the leachate. Anhydrous Na_2SO_4 was added to precipitate the REE as sulfates, and the remaining solution was termed Waste 2A (W2A). Waste 2A is neutralized with Na_3PO_4/$NaHCO_3$, resulting in precipitation of much of the Fe, and the residual solution was termed Waste 2B (W2B). Waste 1A (W1A) is the aqueous phase resulting from the reaction between $(NH_4)_2C_2O_4$ to the REE sulfates to convert them into

REE oxalates (insoluble). Waste 1B (W1B) is generated through neutralizing Waste 1A with calcium hydroxide. Estimated concentrations for various constituents were provided by Ames Laboratory, and measurements of rare earths and numerous other elements were made using inductively coupled plasma with atomic emission spectroscopy detection (ICP-AES).

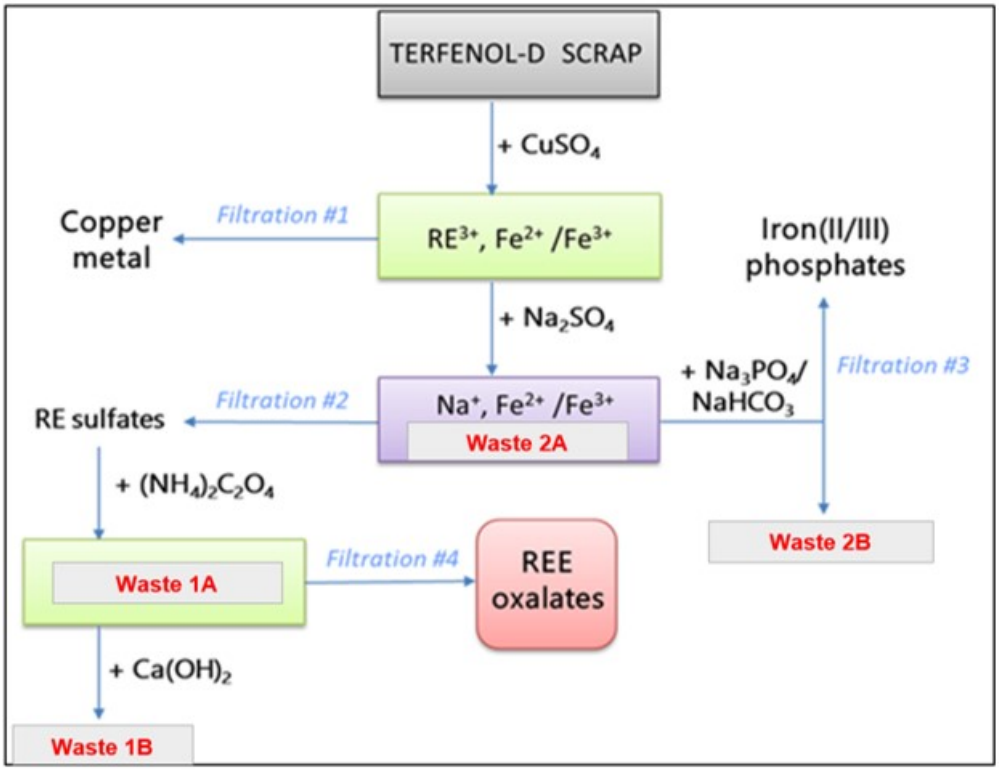

Figure 3.1 Waste generation during the Terfenol-D recycling process.

3.1.2 Aerobic Plates

Aerobic plates amended with two dilutions of four recycling wastes were prepared and inoculated with activated sludge from a local water resource reclamation facility (WRRF) to evaluate the effect of REE recycling waste on cell colony growth. Growth inhibition was assessed by conducting plate counts for each waste and dilution.

3.1.2.1 Plate Media

Aerobic culture plate medium was prepared from Luria-Bertani (LB) broth (Sigma Aldrich, St. Louis, MO) and agar. LB medium is a commonly used medium for growth of heterotrophic

organisms in the laboratory. LB broth was added at 25 grams or 31.25 grams per liter (g/L) of distilled water for untreated and treated plates, respectively. Agar was added at 15 g/L or 18.75 g/L for untreated and treated plates, respectively. Each plate had a final volume of 25 mL. Control plates had 20 mL of LB broth and agar medium and 5 mL of MilliQ water, amended plates had 20 mL of LB agar medium and 5 mL of REE waste diluted with MilliQ water to achieve final dilutions in the plates of either 2.5% volume per volume (v/v) or 5% v/v.

The LB broth and agar, along with clean glass beakers, were autoclaved at 121°C for 15 minutes. The LB agar medium was then pipetted into the autoclaved beakers so that each beaker contained 60 mL of medium (20 mL per plate). The REE waste (15 mL after dilution, as described in 3.1.2.2) was then poured into each respective REE-amended beaker. The beakers were swirled to mix the contents, prior to pouring into the plates. Plates were prepared in triplicates.

3.1.2.2 REE Waste Dilutions

REE waste dilutions are described in Table 3.1. REE waste was filter-sterilized, using 0.22 µm polyethersulfone (PES) filters, into Falcon tubes to achieve 2.5% v/v and 5% v/v final concentrations (Table 3.1). Filter-sterilized MilliQ water was added to dilute the wastes, and the contents of the tube mixed prior to addition to the LB agar medium.

Table 3.1 REE waste dilutions in REE-waste-amended media.

Waste Dilution (v/v)	**Volume (mL)**			
	LB agar	**REE waste**	**MilliQ water**	**Final volume**
2.5%	60	1.875	13.125	75
5%		3.75	11.25	

3.1.2.3 Inoculum

Activated sludge was collected from an aeration basin at a local WRRF. The activated sludge was placed on ice immediately after collection, and plates were inoculated the same day. Following inoculation of plates with 100 µL of the 3-log diluted activated sludge (diluted with MilliQ water), the plates were placed in a 30°C incubator. Inoculum was distributed across the plate using sterilized glass beads. Preliminary tests indicated that these conditions should result

in an appropriate number of distinct colonies for unambiguous counting by 24 to 72 hours of incubation.

3.1.3 pH-Adjusted Aerobic Plates

Because Waste 1A and 2A were acidic, pH-adjusted plates were prepared to test if acidity alone was responsible for inhibition of microbial growth. To investigate this, the pH of the 2.5% v/v media was adjusted with 1M hydrochloric acid (HCl) until it reached the pH of the 5% v/v media. This procedure was only performed on the acidic Wastes 1A and 2A, as Wastes 1B and 2B were already at neutral pH.

3.1.3.1 pH-Adjusted Plate Medium

LB agar medium was prepared as described in 3.1.2.1. After sterilization by autoclave, the medium was measured and poured into autoclaved glass beakers, where each beaker represented one dilution. REE waste dilutions, described in 3.1.2.2, were added to their respective beakers. pH values were measured and recorded (Table 3.2). Three unamended control beakers were prepared: a neutral pH control, a control amended to the pH of Waste 1A at 5% v/v, and a control amended to the pH of Waste 2A at 5% v/v. Incremental volumes of 1M HCl were added to the acidified controls and the 2.5% v/v dilutions until their respective pH values were approximately equivalent to the 5% v/v dilution pH value (Table 3.2). An agar-tolerant pH electrode was used to validate pH values throughout the experiment. Once solidified, the pH of the plates was measured (Table 3.2). Plates were then inoculated per 3.1.2.3.

Table 3.2 Measured pH values of media throughout the second round of pH-adjusted plates.

Amendment		**pH of liquid media after waste addition**	**Volume of 1M HCl added (mL)**	**pH of liquid media following HCl addition**	**Final pH of plates**
Control		6.38	-	6.38	8.64
Control acidified to W1A 5% v/v		6.37	1.2	4.52	4.70
Waste 1A	2.5% v/v	5.59	0.5	4.52	4.71
	5% v/v	4.51	-	4.51	4.66
Control acidified to W2A 5% v/v		6.34	1.3	4.25	4.42
Waste 2A	2.5%	5.16	0.7	4.27	4.36
	5% v/v	4.27	-	4.22	4.19

3.1.3.2 Plate Count Protocol and Statistical Analysis

Culture plates were photographed 24 hours and 72 hours after inoculation and photographs from the 72-hour incubation were used for culture plate count analysis. The imager package (https://CRAN.R-project.org/package=imager) in RStudio (R Foundation for Statistical Computing, Vienna, Austria) was used to crop the photos and convert the photographs to a binary black and white image. The cropped photographs were then analyzed using the Cell Colony Edge macro in ImageJ software, which calculates the number of microbial colonies on each plate [54]. RStudio packages ggpubr (https://CRAN.R-project.org/package=ggpubr) and multcomp [55] were used to perform Kruskal-Wallis rank sum tests and post-hoc Dunnett's tests to compare the mean colony counts between the control and 2.5% v/v, the control and 5% v/v, and 2.5% v/v and 5% v/v.

3.2 Antibiotic Resistance Investigation

Liquid and plate culturing experiments were developed to investigate the effect of REEs on the wastewater microbial community and the potential for REEs to co-select for antibiotic resistance. Culturing was performed to compare the growth of REE-resistant and unamended cells in the presence of antibiotics. DNA from lanthanum-resistant and multi-resistant (lanthanum (La) and antibiotics) cultures was then sequenced to investigate the effect of lanthanum exposure on predominant taxa and resistance genes.

3.2.1 Liquid Culturing of Metal- or Antibiotic-Resistant Cells

Mueller-Hinton (MH) medium was prepared according to a Millipore recipe consisting of casein hydrolysate, starch, and meat extract (Sigma-Aldrich, 2018). MH medium is commonly used for antibiotic susceptibility testing, as the components do not interfere with antibiotics. The Mueller-Hinton medium was then amended with increasing concentrations of either metal (La, Dy, or cadmium (Cd)), or antibiotic. Stock solutions were prepared for both metals and antibiotics, which were filter sterilized through 0.2 µm PES filters. Metal stock solutions were prepared from lanthanum chloride (99.99% rare earth oxide basis (REO), Alfa Aesar, Haverhill, MA), dysprosium chloride (99.9% REO, Alfa Aesar, Haverhill, MA), and cadmium chloride (99.9% pure, Cerac, Inc., Milwaukee, WI). Antibiotics tested included chloramphenicol,

erythromycin, kanamycin, nalidixic acid, nitrofurantoin, novobiocin, penicillin, streptomycin, sulfamethoxazole, and tetracycline. Concentration ranges were chosen based on literature and published minimum inhibitory concentrations (MIC). Concentrations tested are listed in Table 3.3. Culture tubes were performed in triplicate for each condition; 2.5 mL of amended media were added to 5 mL culture tubes.

The culture tubes were inoculated with 10 µL of 3-log diluted activated sludge from a local WRRF. The inoculant was diluted in unamended MH media. The culture tubes were placed in an incubator shaker running at 200 revolutions per minute (rpm) at room temperature for 48 hours.

One mL of culture was measured to evaluate growth as absorbance at 600 nanometer (nm) wavelength, using a Hach DR3600 Spectrometer (Loveland, CO). Unamended MH media was used as a baseline for turbidity evaluation. Culture tubes with absorbance values over 0.5 after 60 hours were saved for future experimentation.

Table 3.3 Added concentrations of metals or antibiotics in MH medium. An asterisk (*) denotes MIC breakpoint values according to CLSI M100 [56]. A dagger (†) denotes MIC values based on a range of published MICs for different microorganisms [57, 58]. A double dagger (‡) denotes inhibitory values based on ciliates found in activated sludge [59]. A paragraph (¶) denotes inhibitory values based on gram-negative EC50 values determined from a dose-response experiment [38].

Amendment	Concentration 1	Concentration 2	Concentration 3	Concentration 4	Concentration 5
Antibiotics (mg/L)					
Chloramphenicol	4	8*	16	32	64
Erythromycin	0.25	0.5*	1	2	4
Kanamycin	8	16*	32	64	128
Nalidixic Acid	8	16*	32	64	128
Nitrofurantoin	32	64*	128	256	512
Novobiocin	8	16 †	32	64	128
Penicillin	4	8*	16	32	64
Streptomycin	8	16 †	32	64	128
Sulfamethoxazole	19	38*	76	152	304
Tetracycline	2	4*	8	16	32
Metals (µM)					
Cadmium ‡	50	100	200	400	800
Lanthanum¶	50	100	200	400	800
Dysprosium ¶	50	100	200	400	800

3.2.2 Liquid Culturing of Multi-Resistant Cells

The goal of this experiment was to see if metal-resistant bacteria were also resistant to antibiotics. This experiment included three antibiotics: streptomycin, erythromycin, and penicillin. These antibiotics were chosen because the microbes showed the highest resistance to them, shown by growth beyond their MICs. Mueller-Hinton media was prepared and amended per 3.2.1. The inoculum for the second experiment was the metal-resistant cells in the saved culture tubes that had growth at the highest concentration in 3.2.1. For example, if there was growth in media amended with 400 µM La, but not 800 µM La, the 400 µM-resistant culture was used as inoculum. Metal-resistant cells were added to antibiotic-amended media, using the antibiotic concentrations listed in Table 3.3.

Incubation and absorbance measurements were performed as per 3.2.1. The growth of unamended activated sludge was then compared to the growth of metal-resistant sludge in antibiotic-amended media.

3.2.3 Agar Plate Culturing of Multi-Resistant Cells

The goal of this experiment was to investigate the antibiotic resistance of metal-resistant bacteria on agar medium, and to compare results to liquid medium experiments. Figure 3.2 depicts the experimental procedure. MH medium was amended with different concentrations of lanthanum, dysprosium, and cadmium (Table 3.4). Metal-resistant bacteria were cultured in 5 mL tubes, per 3.2.1, and incubated at room temperature for 48 hours.

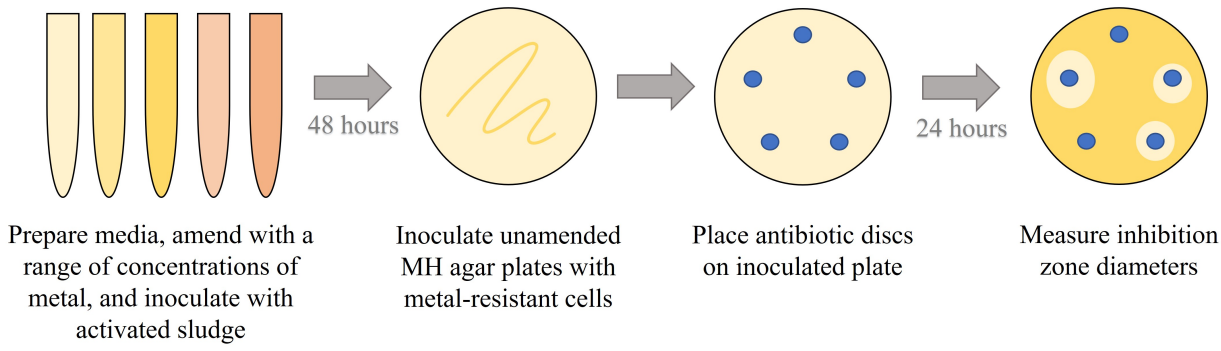

Figure 3.2 Antibiotic disc procedural diagram.

Unamended MH agar plates were prepared for each inoculum. Agar was added to the MH medium at a concentration of 17 g/L. MH agar medium was autoclaved for 15 minutes at 121°C and cooled before pouring. A total volume of 25 mL of MH agar was added to each plate. Metal-resistant cells were washed with unamended MH medium before being used as inoculum for the plates. The experiment included two controls: activated sludge inoculated directly onto the plate, and growth from a culture tube that contained MH medium without metals (0 µM in Table 3.4).

Table 3.4 Metal concentrations for resistant growth of activated sludge in culture tubes.

Metal amendment	**Added Concentrations (µM)**
La	0, 100, 250, 500, 1000
Dy	
Cd	

Duplicate plates were inoculated with 100 µL metal-tolerant bacteria, using sterilized glass beads to form a lawn. Following inoculation, five antibiotic discs were placed on each plate (Figure 3.2). Each disc contains a standard potency of antibiotic (Table 3.5). Plates were incubated for 24 hours at 30°C before inhibition zones around each antibiotic disc were evaluated. Inhibition zone diameters around each antibiotic disc were measured in millimeters using a ruler. Inhibition zone diameters around each antibiotic disc were compared across plates to evaluate the effect of increasing metal resistance on antibiotic resistance.

Table 3.5 Potencies of antibiotic discs used in disc diffusion assays.

Antibiotic	**Disc potency (µg)**
Chloramphenicol	30
Erythromycin	15
Kanamycin	30
Nalidixic Acid	30
Nitrofurantoin	300
Novobiocin	30
Penicillin	10 units
Streptomycin	300
Sulfamethoxazole	23.75
Tetracycline	30

3.2.4 Microbial Community Analysis

The goal of this experiment was to investigate the effect of lanthanum exposure on predominant taxa and resistance genes in activated sludge. LB broth media was prepared and amended with 1000 µM of lanthanum, as aqueous lanthanum chloride ($LaCl_3$) or lanthanum oxide (La_2O_3) nanoparticles (Type A: 30-50nm, ACS Material, Pasadena, CA). The lanthanum chloride stock solution was sterile-filtered using a 0.2 µm PES filter, but the lanthanum oxide was not filtered to ensure nanoparticles remained in the solution. An unamended control was maintained throughout the experiment. LB agar plates were amended with three antibiotics, described in Table 3.6. These antibiotics were chosen based on their varying cellular targets.

Culture tubes were inoculated with activated sludge from a local WRRF and incubated per 3.2.1. Metal-resistant cells were stored for DNA analysis and used to inoculate antibiotic-amended plates, simultaneously. Two milliliters of each sample was centrifuged at 10,000 rpm for 3 minutes, the supernatant was pipetted off, and the pellet was stored at -20°C. Sterilized glass beads were used to form a lawn from 100 µL of inoculum on antibiotic-amended agar plates. After 48 hours of incubation at 30°C, composites of colonies were collected by scraping the diameter of the lawn with an inoculation loop. The composite was resuspended in 2 mL of unamended LB broth and immediately centrifuged at 10,000 rpm for 3 minutes. The supernatant was removed, and the pellet was stored at -20°C . Metal and antibiotic exposure of the final samples are described in Table 3.6.

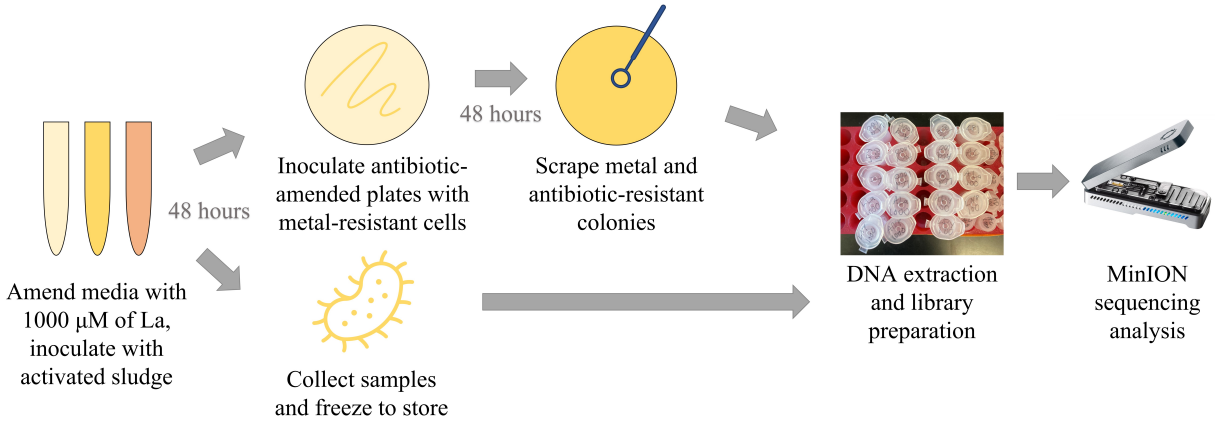

Figure 3.3 MinION sequencing protocol.

DNA from resistant cultures was prepared for sequencing using the Oxford Nanopore Genomic DNA by Ligation protocol [60]. Per the protocol, each sample was loaded on a MinION flow cell for a minimum of 72 hours (Oxford Nanopore, Oxford, UK). Following sequencing, the output data was downloaded from the MinION device for downstream analysis.

Table 3.6 Nomenclature and resistance of samples sequenced on an Oxford Nanopore MinION flow cell.

Sample name	**Metal Resistance**	**Antibiotic resistance**
Control	-	-
LLa	1000 µM La (as $LaCl_3$)	-
LNP	1000 µM La (as La_2O_3)	-
ALa	1000 µM La (as $LaCl_3$)	100 mg/L erythromycin
		100 mg/L penicillin
		10 mg/L tetracycline
ANP	1000 µM La (as La_2O_3)	100 mg/L erythromycin
		100 mg/L penicillin
		10 mg/L tetracycline

3.2.5 Data Analysis

Statistical analysis was performed in RStudio to evaluate growth of resistant cells. Plots were made using the ggpubr package in R. Dunnett's tests were performed using the multcomp package in R to determine if growth of resistant cultures was significantly different than growth from the original activated sludge, at each amendment concentration. For example, in liquid media amended with 200 µM of lanthanum, the average absorbance (at 600 nm wavelength) of the growth from activated sludge inoculation was compared to growth from inoculation with streptomycin-resistant, erythromycin-resistant, and penicillin-resistant cultures. Inhibition zone diameters around discs on plates inoculated with unamended activated sludge were compared to diameters around discs on plates inoculated with cells with increasing resistance to metals.

Sequencing data were analyzed on Oxford Nanopore's EPI2ME software (Oxford, UK). The samples were analyzed for taxonomy and antibiotic resistance genes. Data were further assessed using ARGpore, which identifies antibiotic resistance genes and carrier populations on nanopore reads [49]. NanoARG software was used to identify any co-occurrence between antibiotic-resistant genes, metal-resistant genes, and mobile genetic elements [61].

Results from the control sample were compared to the samples resistant to lanthanum alone, and to samples resistant to lanthanum and antibiotics. Results from both lanthanum sources were also compared to each other. Sankey diagrams displaying associations between sample, genera, resistance type, and resistance gene were created using the ggvis (https://CRAN.R-project.org/package=ggvis) package in RStudio.

3.3 Acute Impacts to Nitrification in Batch Reactors

Batch reactors amended with increasing concentrations of REE were inoculated with activated sludge from a local WRRF and sampled to evaluate nitrification. Inhibition of nitrification was measured through ammonia, nitrite, and nitrate measurements throughout the 2-hour experiment. Ammonia uptake rates (AUR) in reactors amended with copper (II) chloride ($CuCl_2$) (99.999% trace metals basis, Sigma Aldrich, St. Louis, MO), dysprosium chloride ($DyCl_3$), lanthanum chloride, and lanthanum oxide were compared.

3.3.1 Reactor Composition

Synthetic wastewater (SWW) was prepared per Table 3.7, which was developed based on guidelines from the Organization of Economic Cooperation and Development Method 209 [62]. The SWW was autoclaved for 1 hour at 121°C.

Table 3.7 Synthetic wastewater composition. An asterisk (*) denotes a reagent prepared in advance as a dry stock pellet. A dagger (†) denotes a reagent prepared in advanced as filter-sterilized, concentrated stock solution. A double dagger (‡) denotes a reagent added after autoclave-sterilization.

Reagent	**Concentration (mg/L)**
$CaCl_2 \bullet 2H_2O$ *	175
Peptone*	160
Meat Extract*	110
$MgSO_4 \bullet 7H_2O$ *	134
$(NH_3)_2Fe(SO_4)_2$ *	7.6
NH_4Cl †	105
KH_2PO_4 †	28
$NaHCO_3$ † ‡	336

SWW was amended with an appropriate volume $LaCl_3 \bullet 7H_2O$, La_2O_3, $DyCl_3 \bullet 6H_2O$, or $CuCl_2 \bullet 2H_2O$ stock solution to reach a volume of 25 mL (Table 3.8). Metal stock solutions were

filter-sterilized with a 0.2 µm PES filter. Activated sludge was collected from a local WRRF and added to the amended SWW (Table 3.9). Each amendment was performed in triplicate.

Table 3.8 Metal stock solution composition.

Metal	**Stock Solution**	
	µM	**g/L**
La	0.005	0.695
Dy		0.813
Cu		0.318

Table 3.9 Batch reactor composition.

Amendment (µM)	**Volume (mL)**			
	Metal Stock	**SWW**	**MilliQ Water**	**Activated Sludge**
0	0	15	10	25
1	0.01	15	9.99	25
10	0.1	15	9.9	25
100	1	15	9	25
1000	10	15	0	25

3.3.2 Sampling

Sampling parameters are described in Table 3.10. Samples were taken at time 0, 30, 60, 90, and 120. Total suspended solids (TSS) was collected immediately following incubation (prior to time 0 sampling event) and measured according to Standard Methods 2540D [63]. After sampling, the bottles were capped with aluminum foil and placed in an incubator shaker set at 200 rpm at 20°C. Every 30 minutes, reactors were removed from the incubator shaker and allowed to settle for 1 minute. Samples were taken from above the settled sludge and pipetted into Hach vials. NH_3-N, NO_2-N, and NO_3-N were analyzed with Hach TNT 832, 840, and 835 kits, respectively.

Table 3.10 Sampling parameters and frequency of sampling during the 120 minute experiment.

Parameters	**Samples collected per reactor**	**Sample collection time**
TSS	1	Immediately after inoculation
NH_3-N	5	Every 30 minutes
NO_2-N	5	Every 30 minutes
NO_3-N	5	Every 30 minutes

3.3.3 Data Analysis

AUR was calculated using Equation 3.1 [64]. Boxplots were created using the ggpubr package in R.

$$AUR(\frac{mgNH3}{gTSS-hr}) = \frac{NH3removed(\frac{mgNH3}{L-hr})}{TSS(\frac{gTSS}{L})} \tag{3.1}$$

Dunnett's tests, performed using the multcomp package in RStudio, were conducted determine if AUR was significantly different at each amendment concentration compared to the control. Data was visualized using the rstatix (https://CRAN.R-project.org/package=rstatix), plyr [65], and tidyverse [66] packages in R Studio. Analysis also compared AUR values and extent of ammonia removal within each treatment at different concentrations.

3.4 Recovery of Microbial Community Composition and Function After REE-Induced Inhibition of Nitrification

DNA sequencing was conducted to identify any shifts in the microbial community in response to REE-induced inhibition of nitrification. Experimentation by Salmon (2019) found that 25 ppm yttrium (Y) and 50 ppm gadolinium (Gd) inhibited nitrification in bench-scale bioreactors. One reactor served as a control, one was amended with Gd, and one was amended with Y. Increasing concentrations of Gd or Y were added to SWW throughout the duration of the experiment. REE amendments over time are described in Table 3.11. Reactors were sampled biweekly for ammonia as N (NH_3-N), nitrate as N (NO_3-N), TSS, chemical oxygen demand removal (COD), and DNA. DNA (sludge pellet) samples were stored at -20°C for future analysis. [67]

Figure 3.4 shows the impact of increasing concentrations of REEs on nitrification over the course of the experiment. Nitrification was inhibited 3 weeks after continuous exposure to 25 ppm Y began. Inhibition continued through 50 ppm Y additions, but nitrification recovered shortly after Y additions were stopped. Gadolinium partially inhibited nitrification at 50 ppm. Similar to the Y-amended reactor, nitrification recovered after Gd additions were stopped. COD removal varied throughout the experiment and no substantial trends were identified. High concentrations of REEs impaired the activity of nitrifying wastewater microorganisms, but it was unclear if the population of nitrifying microbes was able to return to pre-treatment levels after additions were discontinued.

Table 3.11 REE addition concentrations over the course of the experiment.

REE Concentration (ppm)	**Days from Startup**
0	0-16
25	17-55
50	56-93
0 (Recovery)	94-143

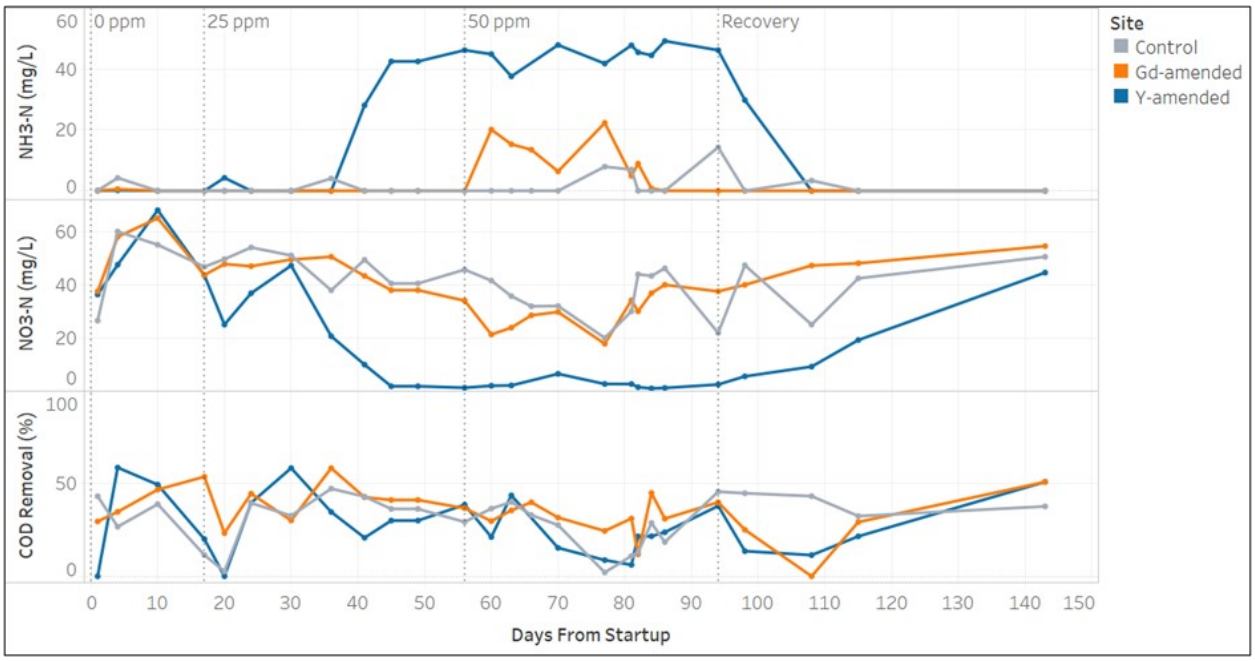

Figure 3.4 Wastewater treatment performance parameters during and following REE exposure.

3.4.1 16S rRNA Microbial Community Analysis

DNA sequencing was performed on the stored sludge pellets from the Salmon (2019) experiment to investigate the effect of increasing concentrations of Gd or Y on microbial community composition. DNA was extracted from sludge pellets using a Qiagen DNeasy PowerLyzer PowerSoil kit and following the corresponding protocol (Germantown, MD). In the bead beating step in the protocol, pellets were disrupted for 90 seconds using a BioSpec BeadBeater (Bartlesville, OK). Extracted DNA was then quantified using a Qubit broad-range assay kit (Invitrogen, Carlsbad, CA).

A two-step PCR protocol, as described in [68] , was used for amplification. The samples were amplified per the Parada et al. (2016) protocol, using primers 515_Y and 926R that cover the V4-V5 region between 515 and 926 base pair. Primer 515_Y has a 5' extension corresponding to the M13 forward primer (GTA AAA CGA CGG CCA G) [69]. A bead cleaning was performed using KAPA PureBeads at a concentration of 0.8x v/v (Kapa Biosystems, Wilmington, MA). Amplicons were barcoded using 5 Prime Hot MasterMix (Quanta BioSciences Inc., Gaithersburg, MD) and 926R reverse primer. Four µL of each DNA amplicon was added to 43.5 µL of MasterMix solution, and 2.5 µL of 4 µM stock barcode solution was added into respective wells in a 96-well plate. The well plate was placed into a Techne TC-412 thermocycler (Cole-Parmer, Vernon Hills, IL), where samples underwent an initial denaturation at 94°C for 2 minutes, followed by 6 cycles of: 45 seconds at 94°C, 45 seconds at 50°C, 90 seconds at 68°C, followed by final denaturation at 68°C for 5 minutes. A second 0.8x v/v bead clean was performed before samples were pooled equimolarly. The pooled sample was sent to University of Colorado Anschutz's Genomics and Microarray Core for Illumina 2x250 V2 analysis.

3.4.2 Data Analysis

Sequencing data were analyzed to determine taxonomy using R, RStudio, Quantitative Insights into Microbial Ecology (QIIME2) [70], and Tableau (Seattle, WA). The DADA2 R package [71] was used to filter and trim low quality reads, construct reads into a sequence table, and remove chimeras. Taxonomy was assigned using Silva v138 [72]. The QIIME2 plug-in q2-fragment-insertion [73, 74] was used to insert sequences into a curated phylogenetic tree based

on the Silva v128 database. The resulting tree was then merged with the sequence table for downstream data processing and visualization.

Relative abundance of species at each treatment concentration was calculated and imported to Tableau to create time series charts. Time series analysis focused on the relative abundance of nitrifying families Nitrospiraceae and Nitrosomonadaceae.

Principal coordinate analysis (PCoA) was performed to determine dissimilarities of the data as a function of REE amendment, treatment concentration, and time from the start of the experiment. A distance matrix was generated using weighted UniFrac after rarefying for normalization. Principal coordinates were generated from the distance matrix using Phyloseq [75]. Plots were created using a UniFrac distance matrix. Permutational multivariate analysis of variance (PERMANOVA) and beta dispersion statistics were performed using the vegan package (https://CRAN.R-project.org/package=vegan) in RStudio.

CHAPTER 4

RESULTS AND DISCUSSION

Multiple experiments were conducted to investigate the effect of rare earth elements (REEs) on the composition and activities of microbial communities in water resource reclamation facilities (WRRF). Toxicity was assessed through plate assays and antibiotic resistance was investigated through culturing and DNA analysis. The acute and chronic impacts to biological nitrification were evaluated through batch reactor and aerobic bioreactor studies, respectively. Microbial community shifts in response to REE-induced inhibition of nitrification were evaluated through DNA sequencing.

4.1 REE Recycling Waste Investigation

As REE recycling processes continue to develop in the United States, how recycling waste streams may affect wastewater is important to understand. Four wastes from various steps in a samarium-cobalt recycling process were added to plate media at 2.5% v/v and 5% v/v dilutions. Plate culturing experiments were conducted to investigate the effect of REE recycling waste on activated sludge growth.

4.1.1 Recycling Waste Constituents

ICP-AES analysis showed trace concentrations of nearly every REE in each waste (Table 4.1). Concentrations of additional constituents are listed in Table A.1 in Appendix A.

Waste 1A (W1A) mainly consisted of cerium and lanthanum, as well as other constituents like sulfur, sodium, and iron (Table 4.1, Figure 4.1). Waste 2A (W2A) contained relatively high concentrations of REEs, particularly dysprosium and terbium, as well as sulfur, sodium, iron, and copper (Table 4.1, Figure 4.1). REE concentrations in Wastes 1B (W1B) and 2B (W2B) were orders of magnitude lower than those in Wastes 1A and 2A. Waste 2B contained relatively high levels of sulfur and sodium (Figure 4.1). Sodium compounds are used in the process that generates 2B, and the high sulfur concentration could be residual from sulfate additions earlier in the recycling process.

Table 4.1 REE concentrations in each recycling waste, determined from ICP analysis. BDL indicates a measurement below the instrument's detection limit.

REE	**Detection Limit (μM)**	**W1A**	**W1B**	**W2A**	**W2B**
		Concentration (μM)			
Ce	8.90E-02	29.6	BDL	71.8	1.30
Dy	7.77E-03	3.84	0.47	5900	0.39
Er	1.64E-02	BDL	BDL	51.4	0.12
Eu	2.31E-03	2.12	4.06E-03	4.47	0.02
Gd	1.69E-02	8.25	0.03	142	0.11
Ho	5.91E-03	BDL	0.01	200	0.06
La	1.16D-02	25.0	0.03	105	0.08
Lu	2.11E-03	7.04	0.02	25.5	0.03
Nd	5.69E-02	BDL	BDL	71.4	1.00
Pr	3.84E-02	BDL	BDL	10.1	0.24
Sc	1.57E-02	4.08	0.02	38.0	0.03
Sm	4.44E-02	BDL	BDL	13.8	1.40
Tb	2.08E-02	BDL	0.17	832	0.18
Tm	9.10E-03	BDL	BDL	24.5	0.07
Y	4.60E-03	1.64	0.01	15.1	0.03
Yb	1.18E-03	1.00	3.48E-03	5.28	0.02

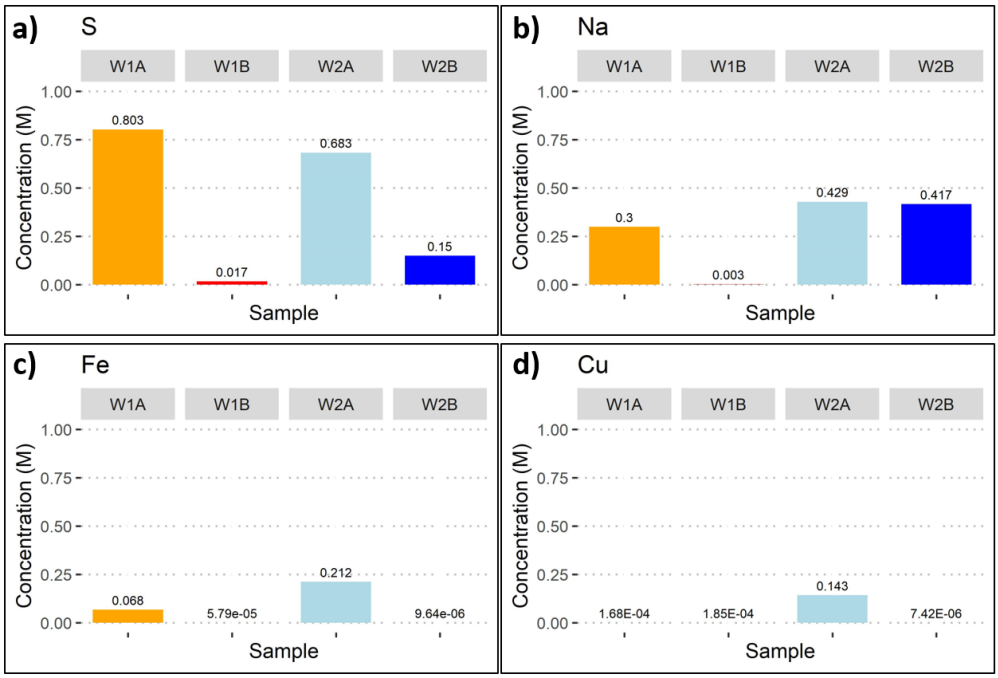

Figure 4.1 Concentrations in moles per liter of a) sulfur, b) sodium, c) iron, and d) copper in REE waste, determined from ICP analysis.

4.1.2 Aerobic Plate Colony Counts

Aerobic culture plates amended with two dilutions of REE recycling waste were prepared to investigate inhibition of activated sludge growth. Inhibition was assessed through colony counts for each waste and waste dilution.

Results indicate partial and complete inhibition of microbial growth on plates treated with 5% v/v of the two acidic wastes (Wastes 1A and 2A), but no inhibition on plates containing neutral pH wastes or plates with 2.5% v/v of acidic waste. The mean colony count was noticeably different between the 2.5% v/v and 5% v/v treatments for Waste 1A and Waste 2A (Figure 4.2). Mean colony counts in Waste 1B and Waste 2B showed no observable differences (Figure 4.2). In addition, differences between the control and the 2.5% v/v/ plates across all wastes did not appear significant.

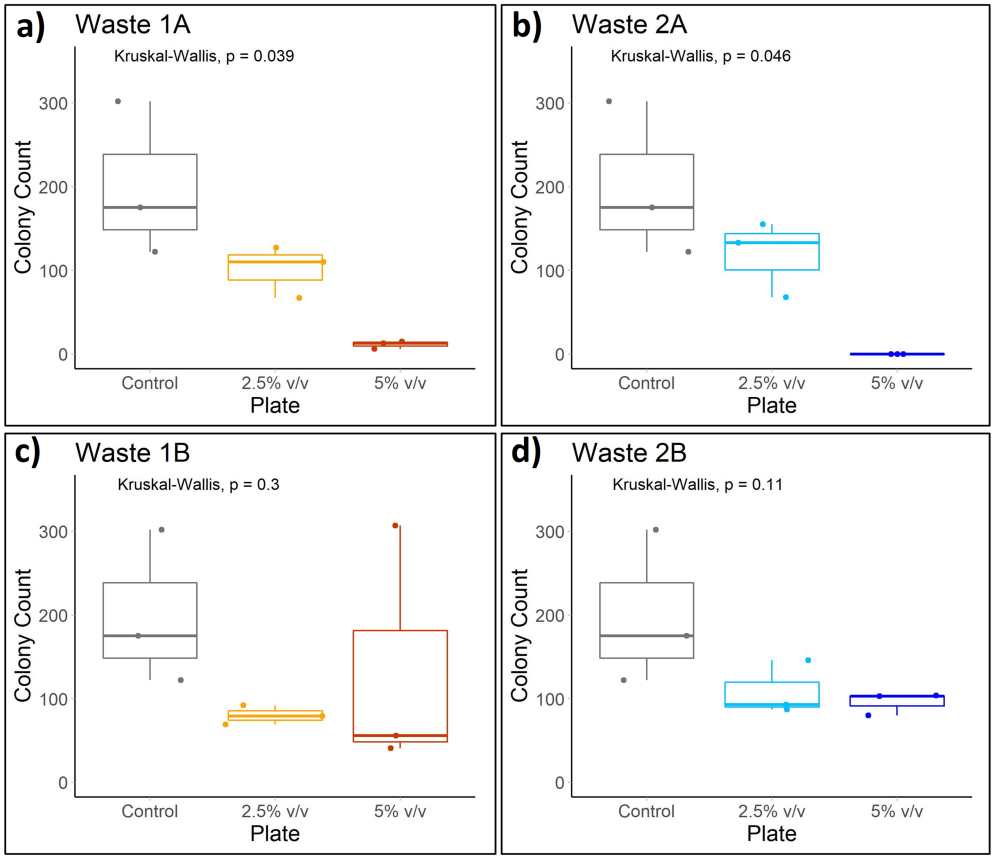

Figure 4.2 Colony counts and statistical analysis on plates with a) Waste 1A, b) Waste 2A, c) Waste 1B, and d) Waste 2B.

The Kruskal-Wallis test evaluates whether differences between the means of treatments are statistically significant. This test determines significance but does not specify which treatments are significantly different. Further statistical analysis was conducted to determine the significance of differences between the control and each wastewater treatment. A Dunnett's test compares means of different treatments against a control group. In Waste 1A, the colony counts on the 2.5% v/v treated plates were not significantly different from the control, suggesting that a 2.5% v/v concentration of this waste does not inhibit microbial growth (Table 4.2). Statistically significant inhibition, compared to the control, was observed when the concentration was increased to 5% v/v (Table 4.2). Similar to Waste 1A, Waste 2A microbial growth was significantly inhibited by 5% v/v of waste compared to the control, but not by 2.5% v/v (Table 4.2).

Table 4.2 Dunnett's test results for colony count differences on REE waste-amended aerobic plates. Significant values are bolded. CI values describe upper and lower confidence intervals.

Comparison	**Difference**	**Lower CI**	**Upper CI**	**p-value**
W1A 2.5% - Control = 0	-98.33	-248.5	51.79	0.3118
W1A 5% - Control = 0	-188.3	-338.5	-38.21	**0.0106**
W1B 2.5% - Control = 0	-119.7	-269.8	30.45	0.1549
W1B 5% - Control = 0	-65.00	-215.1	85.12	0.7152
W2A 2.5% - Control = 0	-81.00	-231.1	69.12	0.5044
W2A 5% - Control = 0	-199.7	-349.8	-49.55	**0.0065**
W2B 2.5% - Control = 0	-91.00	-241.1	59.12	0.3863
W2B 5% - Control = 0	-104.00	-254.1	46.12	0.2616

4.1.3 pH-Adjusted Aerobic Plate Colony Counts

Plates were acidified to uniform pH levels to evaluate inhibition due to waste constituents rather than waste acidity. Colony count analysis was performed on plates amended with Waste 1A or 2A at two dilutions. The 2.5% v/v diluted plate and an unamended plate were acidified to the pH of the 5% v/v diluted plate for each waste. A neutral unamended plate served as a control.

Results show partial inhibition of cell growth on plates amended with both dilutions of Waste 1A (Figure 4.3). While the colony counts on the amended plates were significantly lower than the neutral unamended plate, they were not significantly different than the pH-adjusted control plate (Table 4.3). Plates amended with Waste 2A completely inhibited cell growth at both dilutions

(Figure 4.4). Growth was only partially inhibited on the pH-adjusted control plate, suggesting that the waste itself contributed to the inhibition.

All acidic plates had significantly lower colony counts than the neutral control plates (Table 4.3). Colony counts on plates amended with Waste 1A were comparable to the pH-adjusted control plate (Table 4.3). Plates amended with Waste 2A had significantly lower colony counts than the pH-adjusted control plate (Table 4.3).

Table 4.3 Dunnett's test results for colony count differences on pH-adjusted aerobic plates. Significant values are bolded. CI values describe upper and lower confidence intervals.

Comparison	**Difference**	**Lower CI**	**Upper CI**	**p-value**
W1A pH Control - Control = 0	-229.3	-248.4	-210.3	**4.4E-16**
W1A 2.5% - Control = 0	-227.3	-246.4	-208.3	**<2.0E-16**
W1A 2.5% - W1A pH Control = 0	2.00	-17.93	21.93	0.942
W1A 5% - Control = 0	-229.7	-248.7	-210.6	**<2.0E-16**
W1A 5% - W1A pH Control = 0	-0.333	-20.27	19.60	0.998
W2A pH Control - Control = 0	-247.7	-255.7	-239.7	**<2.0E-16**
W2A 2.5% - Control = 0	-257.7	-265.7	-249.7	**<2.0E-16**
W2A 2.5% - W2A pH Control = 0	-10.00	-11.91	-8.089	**1.0E-05**
W2A 5% - Control = 0	-258.7	-266.7	-250.7	**<2.0E-16**
W2A 5% - W2A pH Control = 0	-11.00	-12.91	-9.089	**5.8E-06**

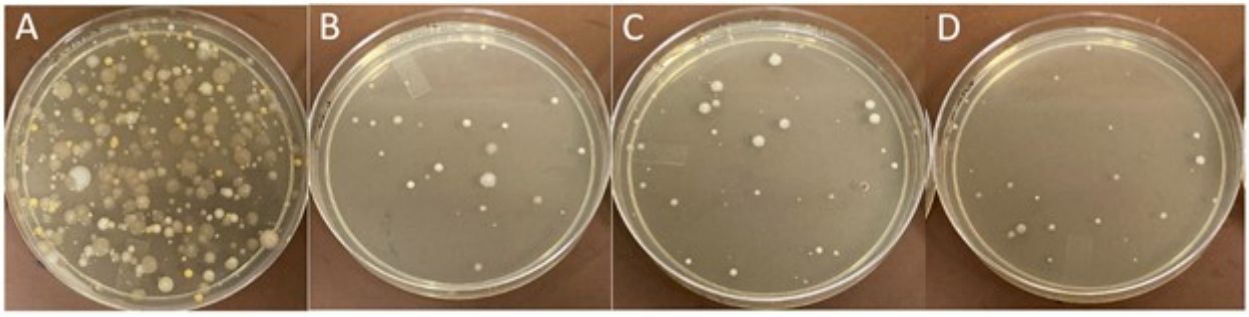

Figure 4.3 Cell growth on a) neutral control plate, b) control plate acidified to 4.70 pH, c) plate amended with Waste 1A 2.5% v/v and acidified to pH 4.71, d) plate amended with Waste 1A 5% v/v (pH 4.66).

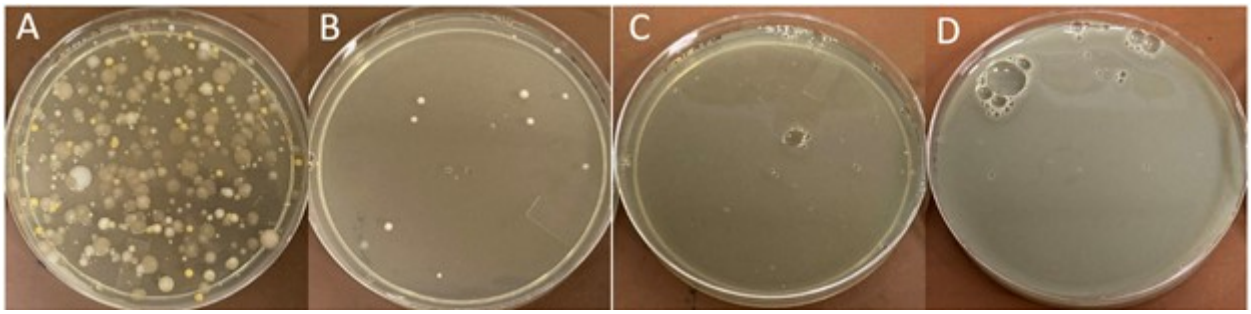

Figure 4.4 Cell growth on a) neutral control plate, b) control plate acidified to 4.42, c) plate amended with Waste 2A 2.5% v/v and acidified to pH 4.4, d) plate amended with Waste 2A 5% v/v (pH 4.2).

4.1.4 Discussion

Microbial growth was not inhibited at either treatment concentration in both Wastes 1B and 2B. This may be due to the pH of the neutralized wastes, as well as their constituents. The optimum pH for biological treatment processes is between 6.5 and 8, and typical wastewater treatment plants maintain a pH between 6 and 8 in their aeration basins [76, 77]. Neutral waste may provide a better growth environment for the wastewater microbes than acidic waste. Wastes 1A and 2A have pH values of 2 and 3, respectively, and low pH values (2.5 to 3.5) have been shown to be detrimental to activated sludge density [76]. In addition, concentrations of the REEs and many other metals decreased by at least an order of magnitude after the neutralization of the acidic wastes Table 4.1.

For both Wastes 1A and 2A, acidity is likely a major factor for microbial growth inhibition. When plates were amended with increasing dilutions of Waste 1A and 2A, cell colony growth noticeably decreased (Figure 4.2). When pH was uniformly 4.7 across control and plates amended with Waste 1A, colony growth between plates was comparable. However, when pH was uniformly 4.4 across control and plates amended with Waste 2A, activated sludge growth was completely inhibited on amended plates while growth occurred on a control plate without waste amendment. This suggests that the waste constituents in Waste 2A contributed to growth inhibition. Waste 2A contains relatively high concentrations of REEs dysprosium, terbium, holmium, and gadolinium (Table 4.1). However, constituents other than REE could contribute to toxicity; in addition to REEs, Waste 2A contains elevated concentrations of heavy metals iron and copper (Figure 4.1).

Elevated iron concentrations are not necessarily concerning, as iron-reducing bacteria have been found in activated sludge [78] and the biological reduction of nitrogen species can take place concurrently with the oxidation of ferrous iron [79]. However, high concentrations of copper may contribute to the inhibition of activated sludge growth. In water, copper exists as Cu^{2+} at low pH levels and $Cu(OH)_2$ at neutral pH [80]. Copper (II) has been shown to be toxic to wastewater microorganisms at concentrations ranging from 15 to 420 μM [81], which is two to three orders of magnitude lower than the copper concentrations found in Waste 2A.

Culture plate results indicate toxicity of acidic rare earth recycling waste at 5% v/v dilutions. Adverse effects were not observed when the waste was neutralized and/or diluted to 2.5% v/v. Results suggest that, in addition to acidity, the constituents of Waste 2A contribute to inhibition of growth of activated sludge microorganisms. Elucidation of the mechanisms of toxicity indicated by the plate assays requires more investigation. The presence of a variety of REEs in the recycling waste, as shown by ICP-AES, motivates an investigation into how these REEs may impact the microbial community composition and functions of wastewater microorganisms.

4.2 Antibiotic Resistance Investigation

Multiple experiments were conducted to investigate the potential for REEs to co-select for antibiotic resistance in wastewater microbial communities. Liquid culturing of metal or antibiotic-resistant cells established a baseline for resistance thresholds and activated sludge growth in amended media. Liquid and plate culturing was conducted to evaluate the growth of metal-resistant growth in the presence of antibiotics. DNA from lanthanum-resistant and multi-resistant (La and antibiotics) growth was sequenced to explore the effect of these pressures on microbial community composition.

4.2.1 Growth of Metal- or Antibiotic-Resistant Cells in Liquid Media

The first experiment consisted of liquid cultures amended with increasing concentrations of either metals or antibiotics to determine inhibition thresholds. Growth was measured as absorbance at 600 nanometers (nm) for each amendment and concentration.

Results show a downward trend in absorbance with increased concentration of the rare earths lanthanum (La) and dysprosium (Dy), and the heavy metal cadmium (Cd) (Figure 4.5).

Lanthanum had less of a downward trend than dysprosium. Absorbance of media amended with cadmium dramatically decreased at the 800 µM concentration (Figure 4.5).

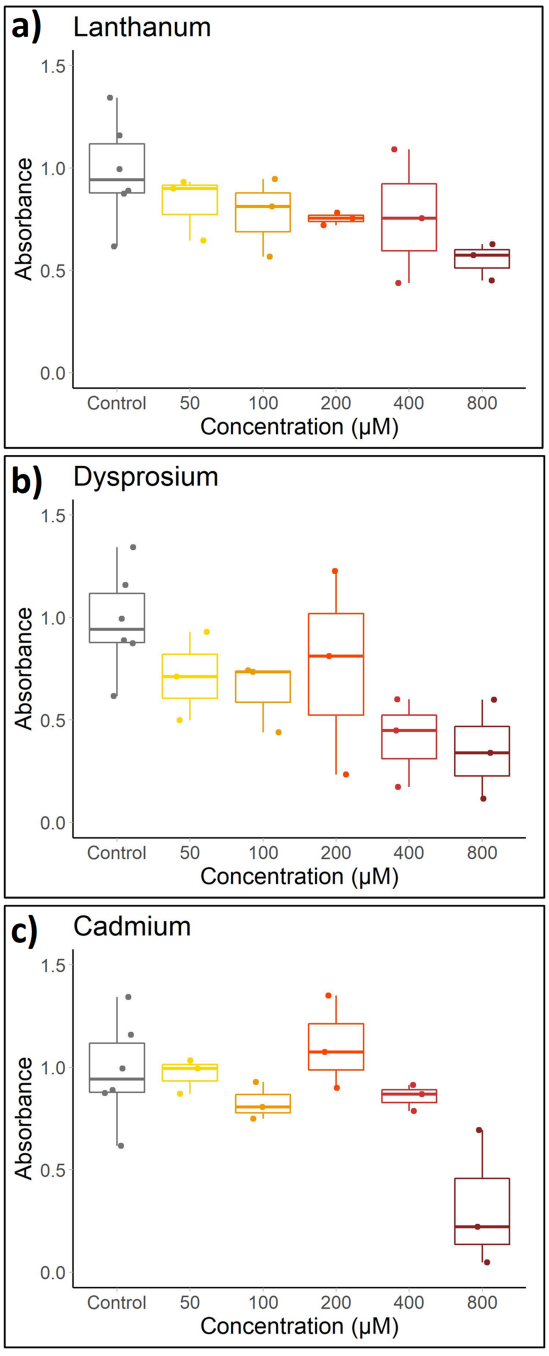

Figure 4.5 Absorbance of growth in media amended with increasing concentrations of a) lanthanum, b) dysprosium, and c) cadmium, after 48-hours of incubation.

Similar to the metal-amended media, media amended with antibiotics showed a downward trend in absorbance with increasing antibiotic concentration. Streptomycin, erythromycin, and penicillin were chosen for subsequent resistance experimentation due to the amount of growth at concentrations beyond their minimum inhibitory concentrations (MIC) (Figure 4.6). Cells did not show growth beyond their respective MICs in media amended with chloramphenicol, nitrofurantoin, novobiocin, sulfamethoxazole, or tetracycline (data not shown). Growth in media amended with streptomycin and penicillin show decreased absorbance at higher concentrations, while growth in media amended with erythromycin shows a sharp decrease in absorbance at 2 mg/L (Figure 4.6).

These results of these culture experiments were used to shape the second experiment. The measurements established a baseline for expected growth of activated sludge at different amendment concentrations. It also shed light on resistance thresholds, as metal-resistant cells were used as inoculum in the multi-resistant culturing experiment.

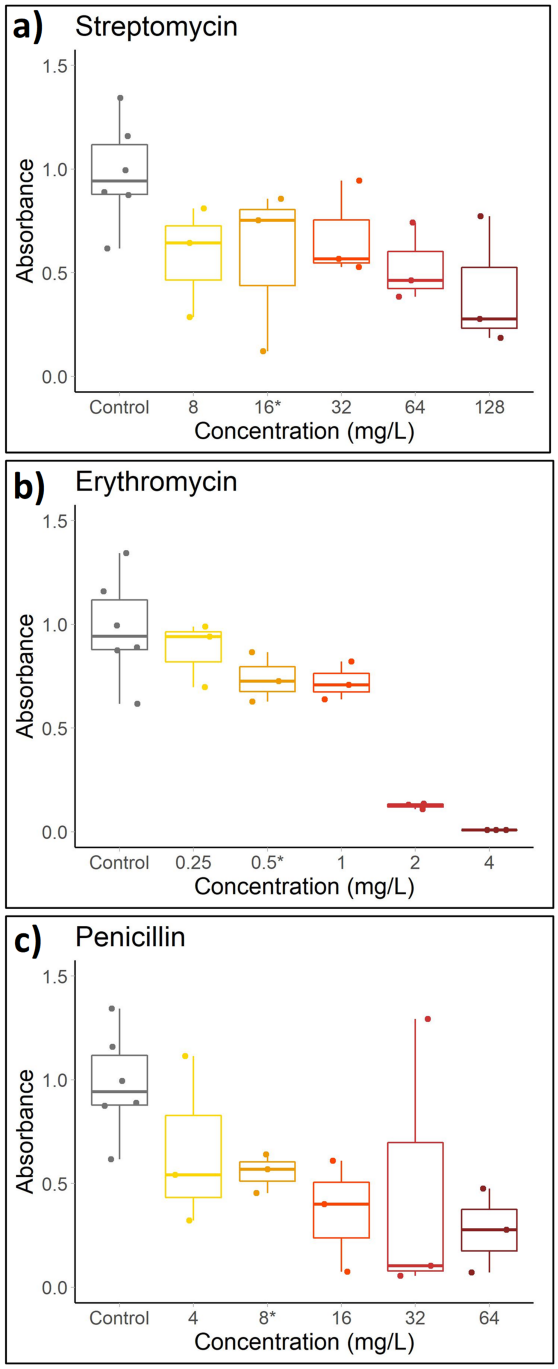

Figure 4.6 Absorbance of media amended with increasing concentrations of a) streptomycin, b) erythromycin, and c) penicillin. MICs are denoted with an asterisk and are based on values published in CLSI M100-ED30:2020 Performance Standards for Antimicrobial Susceptibility Testing, 30th Edition [56].

4.2.2 Growth of Multi-Resistant Cells in Liquid Media

Metal-resistant cells were used as inoculum in antibiotic-amended media to investigate the relationship between metal resistance and antibiotic resistance. Table 4.4 summarizes growth of metal-resistant inoculum in media amended with increasing concentrations of antibiotics. When looking at metal-resistant growth, absorbance decreased at higher antibiotic concentrations (Table 4.4).

Table 4.4 Average absorbance (at 600 nm wavelength) of metal-resistant cells in media amended with increasing concentrations of antibiotics after 48-hours of incubation. Inocula were resistant to 800 μM of metal. Bold values indicate absorbance values significantly different ($p<0.05$) from the absorbance in unamended media.

Amendment concentration (mg/L)	**Absorbance of cultures grown from resistant inocula**		
	Cd	**Dy**	**La**
0 (Control)	1.19	0.705	1.04
Streptomycin-amended media			
8	1.06	0.812	0.921
16	0.973	0.822	**0.813**
32	**0.639**	0.659	**0.730**
64	**0.563**	0.454	**0.291**
128	**0.144**	**0.355**	**0.357**
Penicillin-amended media			
4	0.989	0.919	**0.714**
8	0.984	0.882	0.821
16	**0.747**	0.685	**0.702**
32	**0.720**	**0.429**	**0.597**
64	**0.365**	**0.440**	**0.004**
Erythromycin-amended media			
0.25	0.910	0.904	**0.758**
0.5	**0.781**	0.753	0.862
1	**0.842**	0.820	0.890
2	**0.541**	0.633	**0.539**
4	**0.029**	**0.008**	**0.442**

All metal-resistant bacteria showed a decrease in absorbance at higher streptomycin concentrations (Table 4.4, Figure 4.7). Media with 8 mg/L streptomycin inoculated with cadmium-resistant cells showed significantly higher absorbance when compared to growth from unamended activated sludge inoculum (Figure 4.7). Media inoculated with lanthanum- and dysprosium-resistant cells performed similarly to the media inoculated with activated sludge

(Figure 4.7). The results show that metal-resistant bacteria perform similarly to the original activated sludge with respect to growth in streptomycin-amended media, and that cadmium-resistant bacteria may have higher resistance to 8 mg/L of streptomycin than the original activated sludge.

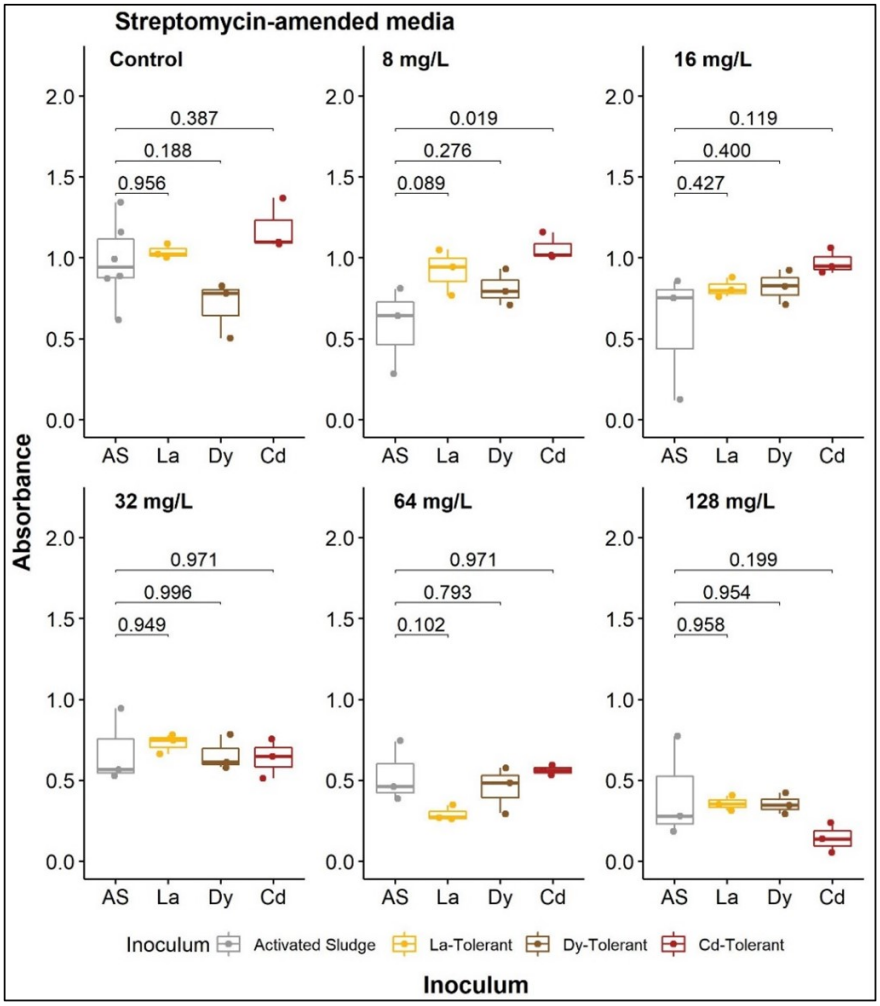

Figure 4.7 Absorbances of media amended with increasing concentration of streptomycin with respect to growth of various inocula. Brackets depict Dunnett's test p-values between the mean absorbance of the activated sludge growth and the metal-resistant growth.

Like streptomycin-amended media, media amended with penicillin showed a decrease in absorbance at higher concentrations for all metal-resistant bacteria (Table 4.4). Absorbances for all three classes of metal-resistant bacteria were significantly higher than absorbance of unamended activated sludge at the 8 mg/L concentration (Figure 4.8). In media amended with 64 mg/L penicillin, Dy- and Cd-resistant growth was significantly higher than La-resistant growth.

The results suggest that metal-resistant bacteria may exhibit greater resistance than activated sludge in regards to growth in penicillin-amended media, and that cadmium and dysprosium-resistant bacteria may be more tolerant to penicillin than lanthanum-resistant bacteria as concentrations increase beyond 32 mg/L.

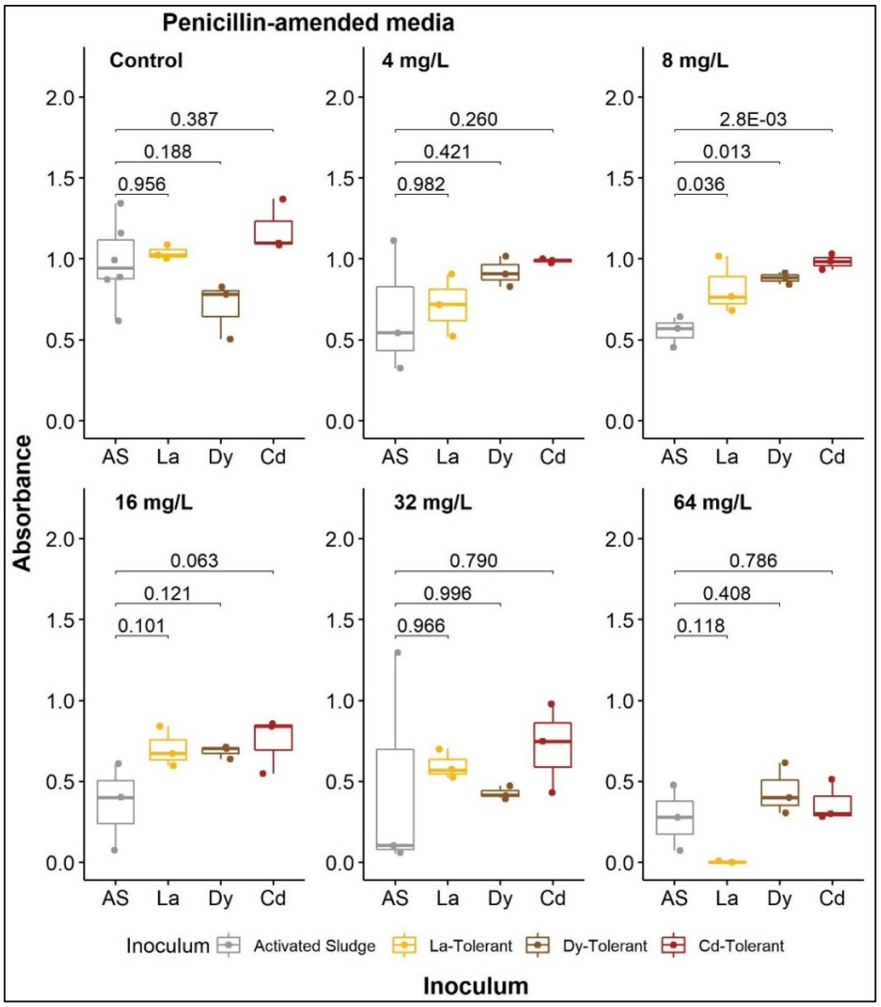

Figure 4.8 Absorbances of media amended with increasing concentration of penicillin with respect to growth of various inocula. Brackets depict Dunnett's test p-values between the mean absorbance of the activated sludge growth and the metal-resistant growth.

Absorbance of erythromycin-containing media inoculated with metal-resistant bacteria performed similarly to media inoculated with activated sludge up to the 2 mg/L concentration (Figure 4.9). All metal-resistant growth was significantly greater than growth with activated sludge at the 2 mg/L erythromycin concentration (Figure 4.9). While absorbance of media

inoculated with cadmium and dysprosium-resistant cells greatly decreased at the 4 mg/L concentration when compared to the absorbances at 2 mg/L, absorbance of media with lanthanum-resistant growth remained significantly higher than the media inoculated with activated sludge (Figure 4.9). This suggests that metal-resistant bacteria may exhibit resistance to erythromycin, and that lanthanum-resistant bacteria show greater resistance than cadmium- and dysprosium-resistant bacteria.

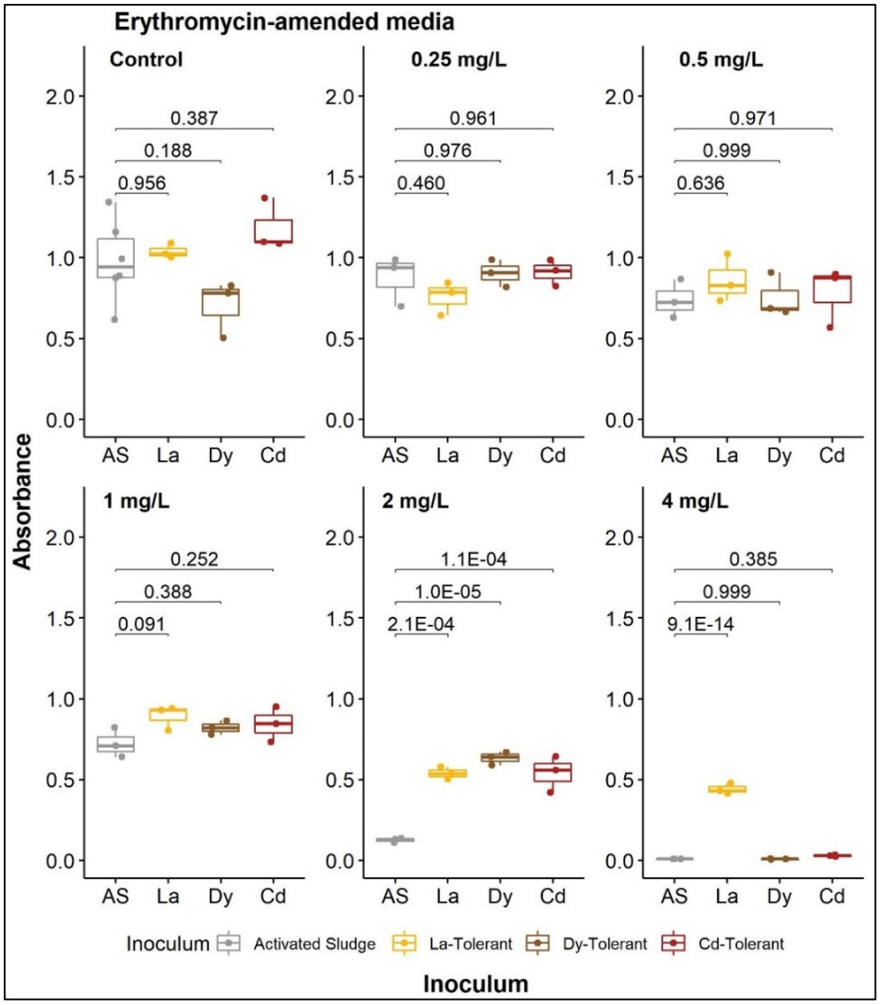

Figure 4.9 Absorbances of media amended with increasing concentration of erythromycin with respect to growth of various inocula. Brackets depict Dunnett's test p-values between the mean absorbance of the activated sludge growth and the metal-resistant growth.

The multi-resistant culturing experiment suggests that REE-resistant growth is similar to, or greater than, unamended activated sludge growth in antibiotic-amended media. A similar multi-resistant culturing experiment was performed on agar plates to evaluate metal-resistant

growth in the presence of antibiotics under different growth conditions.

4.2.3 Growth of Multi-Resistant Cells on Agar Plates

Metal-resistant cells were cultured on unamended agar plates embedded with antibiotic discs to investigate the relationship between metal resistance and antibiotic resistance on solid media. Seven of the nine antibiotics tested are shown in the results below. There were no inhibition zones around penicillin and nalidixic acid discs on any plates, regardless of metal resistance. A small inhibition zone indicates increased resistance, while a large inhibition zone indicates increased susceptibility to the antibiotic. Duplicates of the chloramphenicol discs showed a 25% variability in size of inhibition zone across plates.

Literature reports that cadmium resistance has been associated with antibiotic resistance [82, 83]. Cadmium served as a positive control to compare to rare earths lanthanum and dysprosium. Inhibition zone diameters are summarized in Table 4.5. In general, cadmium-resistant cells showed increased resistance to all antibiotics with the exception of streptomycin. For some antibiotics, like chloramphenicol and tetracycline, inhibition zones decrease with increasing cadmium resistance until a certain concentration, where antibiotic resistance decreases.

Table 4.5 Inhibition zone diameters (mm) around each antibiotic disc on plates inoculated with cells exposed to increasing concentrations of cadmium. Gray highlight depicts values within 25% of the no-cadmium control inhibition zone diameter. Yellow highlight depicts an increase in antibiotic resistance. Blue highlight depicts an increase in susceptibility to the antibiotic.

Antibiotic	**Cadmium concentration (μM)**				
	0	**100**	**250**	**500**	**1000**
Chloramphenicol	15.0	10.9	0.0	23.6	18.6
Erythromycin	10.0	0.0	0.0	10.9	8.6
Kanamycin	23.6	15.9	18.2	8.6	25.0
Nitrofurantoin	21.4	0.0	0.0	0.0	0.0
Streptomycin	9.6	13.6	10.9	15.9	11.4
Sulfamethoxazole	17.3	0.0	0.0	15.0	18.2
Tetracycline	15.9	0.0	0.0	0.0	24.1

Inhibition zones diameters were more variable on plates inoculated with lanthanum-resistant cells than plates inoculated with cadmium-resistant cells. Inhibition zone diameters are

summarized in Table 4.6. Similar to the cadmium-resistant results, increasing lanthanum resistance did not influence resistance to streptomycin. Increasing lanthanum resistance did not influence erythromycin resistance until lanthanum resistance increased to 1000 μM, where the cells were completely resistant to erythromycin. Increasing lanthanum resistance generally increased resistance to nitrofurantoin and tetracycline. Resistance was variable around chloramphenicol, kanamycin, and sulfamethoxazole.

Table 4.6 Inhibition zone diameters (mm) around each antibiotic disc on plates inoculated with cells exposed to increasing concentrations of lanthanum. Gray highlight depicts values within 25% of the no-lanthanum control inhibition zone diameter. Yellow highlight depicts an increase in antibiotic resistance. Blue highlight depicts an increase in susceptibility to the antibiotic.

Antibiotic	**Lanthanum concentration (μM)**				
	0	**100**	**250**	**500**	**1000**
Chloramphenicol	15.0	21.4	11.4	12.3	23.2
Erythromycin	10.0	10.0	11.8	9.6	0.0
Kanamycin	23.6	15.5	24.1	0.0	20.0
Nitrofurantoin	21.4	11.8	15.9	13.6	0.0
Streptomycin	9.6	8.6	8.6	10.0	11.8
Sulfamethoxazole	17.3	0.0	18.6	25.0	21.8
Tetracycline	15.9	11.8	0.0	0.0	20.0

Dysprosium-resistant cells were the most antibiotic resistant out of all three metals tested. Inhibition zone diameters are summarized in Table 4.7. Increasing dysprosium resistance was associated with increasing antibiotic resistance around all antibiotic discs, except for erythromycin.

The results from the multi-resistant culturing experiments in both liquid and agar media indicated the potential for REE-resistant bacteria to exhibit increased resistance to antibiotics when compared to unamended activated sludge. DNA sequencing was performed to gain a better understanding of the microbial community composition and the abundance and richness of antibiotic resistance genes (ARGs) in REE-resistant cultures.

Table 4.7 Inhibition zone diameters (mm) around each antibiotic disc on plates inoculated with cells exposed to increasing concentrations of dysprosium. Gray highlight depicts values within 25% of the no-dysprosium control inhibition zone diameter. Yellow highlight depicts an increase in antibiotic resistance. Blue highlight depicts an increase in susceptibility to the antibiotic.

Antibiotic	**Dysprosium concentration (μM)**				
	0	**100**	**250**	**500**	**1000**
Chloramphenicol	15.0	8.2	11.4	18.2	0.0
Erythromycin	10.0	10.5	9.6	10.5	12.3
Kanamycin	23.6	16.8	0.0	15.0	20.0
Nitrofurantoin	21.4	0.0	0.0	17.7	0.0
Streptomycin	15.4	9.0	0.0	8.7	0.0
Sulfamethoxazole	17.3	8.8	14.3	0.0	0.0
Tetracycline	15.9	0.0	0.0	0.0	8.6

4.2.4 Microbial Community Analysis

Cells resistant to lanthanum chloride ($LaCl_3$) or lanthanum oxide (La_2O_3) nanoparticles were cultured and sequenced to evaluate how lanthanum exposure affects the taxonomy and abundance of antibiotic resistant genes. Samples were collected from $LaCl_3$- or La_2O_3-resistant growth, and growth on antibiotic-amended plates inoculated with La-resistant cells. DNA extracted from the samples was sequenced and compared to sequences derived from a control sample of unamended activated sludge. Metagenomic sequencing was performed to identify predominant genera and resistance genes.

4.2.4.1 Taxonomy of Lanthanum-Resistant Cells

The top ten most abundant genera within each sample are shown in Figure 4.10. The top ten genera represented more than 80% of the total abundance in each sample. The control sample was dominated by *Acinetobacter*, *Aeromonas*, and *Peptostreptococcus*. Both *Acinetobacter* and *Aeromonas* are found in the environment, while *Peptostreptococcus* is part of the human microbiome [84, 85]. When cells were exposed to lanthanum, *Yersinia* became a predominant genus. *Yersinia* species are enteric (intestinal) bacteria that are often detected in activated sludge systems [84]. *Yersinia pestis*, the bacterium that causes plague, was detected in the sample resistant to lanthanum chloride and the sample resistant to both lanthanum oxide nanoparticles and antibiotics. Compared to the control, the La_2O_3-resistant sample had higher relative

abundances of *Pseudomonas* and *Shewanella*. When the lanthanum-resistant samples were also exposed to antibiotics, *Cronobacter* became an abundant genus.

The largest shift in microbial community composition occurred in the sample resistant to both lanthanum chloride and antibiotics. The sample was dominated by *Citrobacter*, *Morganella*, and *Enterobacter*, and had high abundances of enteric bacteria *Salmonella*, *Escherichia*, and *Serratia*. *Citrobacter* is an emerging concern due to its increasing resistance to commonly available antibiotics [86]. Liu et al. (2017) found that the majority of *Citrobacter* isolates collected from hospital patients were multidrug resistant. Transmission of *Citrobacter* infections has been linked to food, and infections often originate in hospitals [87]. *Morganella*, *Serratia*, and *Enterobacter* species are also known to exhibit resistance to a variety of widely-used antibiotics [88]. Interestingly, *Lambdavirus* was also a dominant genus in this sample. *Lambdavirus* is a genus of viruses in the order Caudovirales, and bacteria serve as natural hosts [89].

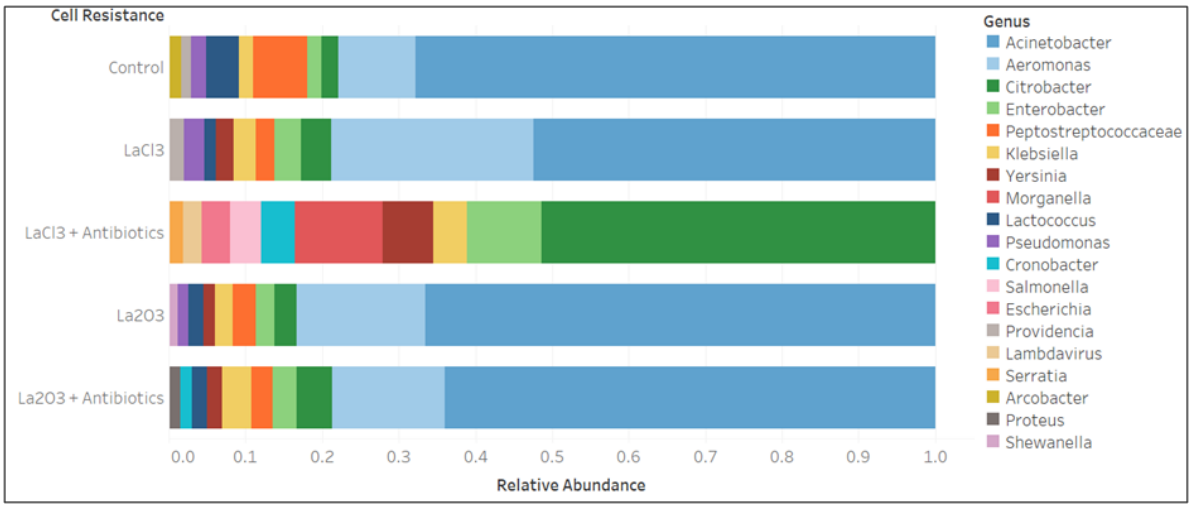

Figure 4.10 Relative abundance of the ten most abundant genera in each sample.

Multiple ESKAPE pathogens were detected in the five samples sequenced (Figure 4.11). ESKAPE pathogens made up 2.7% of the control sample. When exposed to lanthanum chloride and lanthanum oxide nanoparticles, the relative abundance of the ESKAPE pathogens increased by 36% and 3.6%, respectively, compared to the control. The greatest increase in ESKAPE pathogens occurred in the sample resistant to both lanthanum chloride and antibiotics, with a 211% increase in relative abundance compared to the control. The lanthanum oxide nanoparticle

and antibiotic-resistant sample had a 26% increase in the relative abundance of ESKAPE pathogens compared to the control.

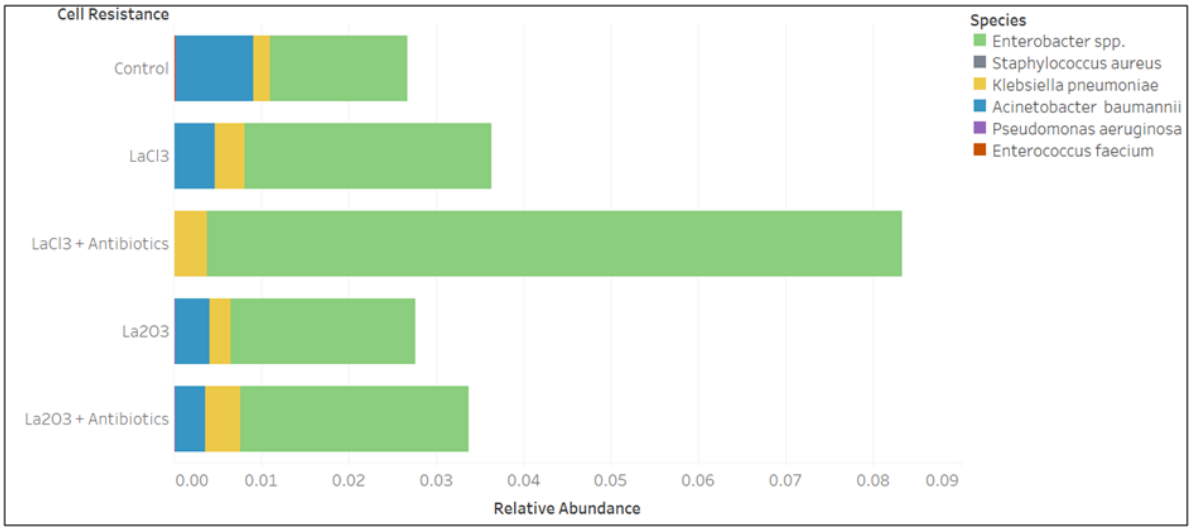

Figure 4.11 Relative abundance of ESKAPE pathogens in each sample.

Nitrifying families, Nitrosomonadaceae and Nitrospiraceae, made up a small fraction (0.047%) of the total genera in the control sample. The relative abundance of these families was 0.052%, 0.065%, and 0.049% in the samples resistant to lanthanum chloride, lanthanum oxide nanoparticles, and both lanthanum oxide nanoparticles and antibiotics, respectively. The relative abundance of nitrifying families decreased to 0.005% in the sample resistant to both lanthanum chloride and antibiotics.

4.2.4.2 Resistance Genes in Lanthanum-Resistant Samples

Over 130 different genes were identified in each sample. Shannon diversity and equitability results are shown in Table 4.8. Samples were not prepared in replicates; therefore, significance of the diversity and equitability results is difficult to determine. Of the five samples, the lanthanum oxide nanoparticle and antibiotic-resistant sample had the highest richness in genes , followed by lanthanum chloride-resistant cells, lanthanum oxide nanoparticle-resistant cells, and the control. The sample resistant to lanthanum chloride and antibiotics had the lowest diversity. This could be explained by the large community shift observed in this sample. The dominant species in this sample was *Citrobacter*, which is associated with multidrug resistance gene types. The dominant

species in the other four samples, *Acinetobacter*, was associated with multiple resistance gene types. The enrichment of *Citrobacter* species in the lanthanum chloride and antibiotic-resistant sample likely led to the selection of certain multidrug genes. The most abundant gene in this sample, *omp36*, made up 6.4% of the total genes in the sample, which was the highest relative abundance of the dominant gene in all five samples.

Table 4.8 Shannon diversity and equitability of the resistance genes found in each sample. Shannon diversity values are normalized to equitability values, which describe evenness of the distribution of genes on a scale of 0 to 1, with 1 representing complete evenness.

Sample	**Shannon Diversity Index**	**Shannon Equitability Index**
Control	4.16	0.822
$LaCl_3$	4.25	0.817
La_2O_3	4.19	0.860
$LaCl_3$ + Antibiotics	4.04	0.821
La_2O_3 + Antibiotics	4.36	0.848

The five most abundant resistance genes in each sample varied (Figure 4.12). In the control sample, the five most abundant genes were associated with multidrug, beta-lactam resistance, and aminoglycoside resistance genes, along with unclassified gene, *ArlR*. *ArlR* is involved in the regulation of multidrug resistance and virulence. Aminoglycoside, multidrug, and kasugamycin resistance genes were present in the aqueous lanthanum-resistant sample, along with unclassified gene, *H-NS*. *H-NS* has been shown to contribute to multidrug resistance by regulating the expression of multidrug exporter genes *acrEF* and *mdtEF* [90]. Lanthanum nanoparticle-resistant growth selected for similar genes to aqueous lanthanum, but also had *rosA*, which exhibits fosmidomycin resistance.

The dominant resistance genes in each sample were identified in certain genera. Genes associated with genera *Podoviridae*, *Peptostreptococcus*, and *Arcobacter* were only identified in the control sample. While all three samples had antibiotic resistance genes associated with genera like *Acinetobacter* and *Citrobacter*, dominant genes in the lanthanum-resistant samples were found in a variety of genera. Lanthanum-resistant samples contained genes associated with *Pseudomonas*, *Yersinia*, and *Cronobacter*, in addition to genera also identified in the control sample. Predominant aminoglycoside resistance gene, *aph(3')-I*, was associated with *Aggregatibacter* in

the aqueous lanthanum sample. In the lanthanum oxide nanoparticle sample, the *aph(3')-I* gene was associated with *Oxalobacter*, and fosmidomycin resistance gene, *rosA*, was identified with *Pectobacterium*.

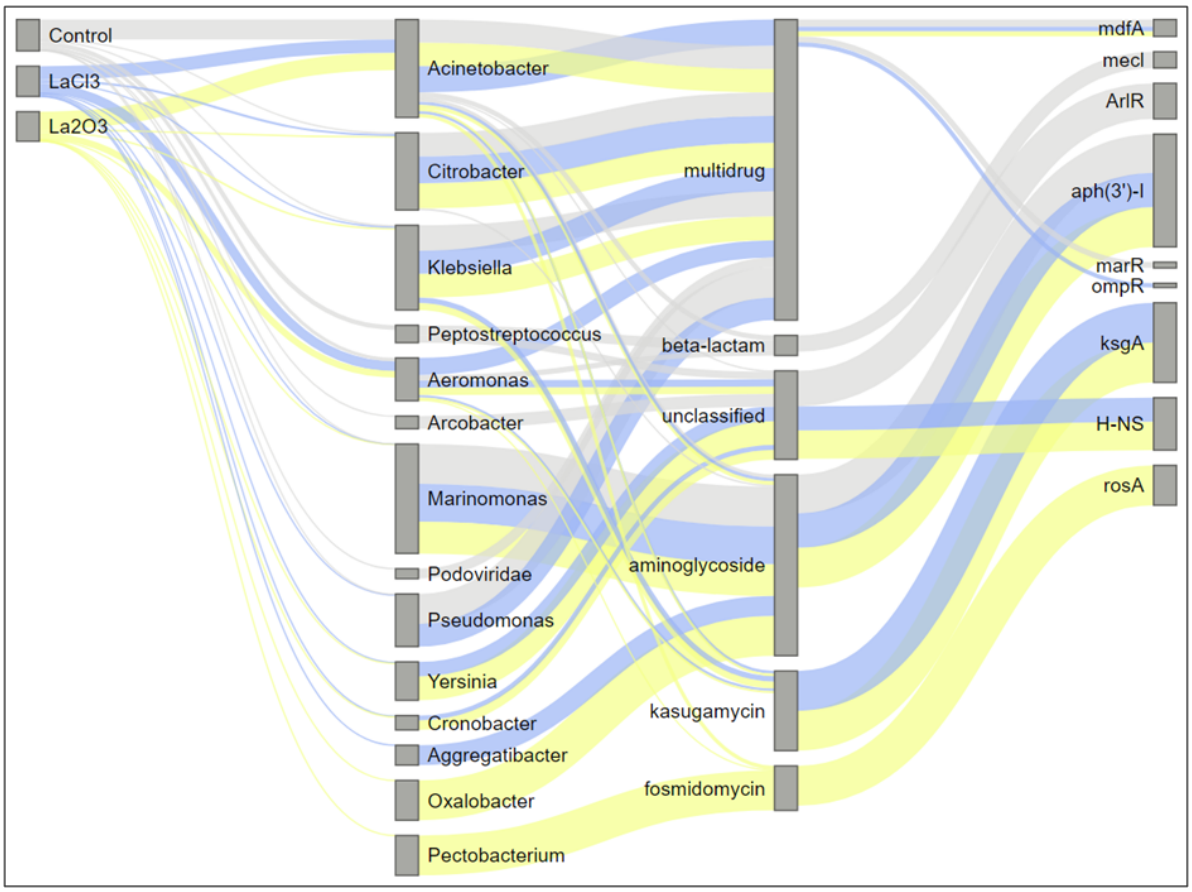

Figure 4.12 Five most abundant resistance genes in the control and lanthanum-resistant samples, along with their associated resistance types and genera. From right to left, the most abundant genes in each sample, the resistance type associated with the gene, the genera in which the gene was identified, and the media in which the cells were cultured. Gray, blue, and yellow connectors represent the control, $LaCl_3$-resistant, and La_2O_3-resistant samples, respectively. Connector thickness represents the relative abundance of the genera, resistance type, or gene from its source. Column height is a function of connector thickness, and depicts relative abundance.

The five most abundant genes varied even further when cells were exposed to antibiotics. Lanthanum chloride-resistant growth contained genes associated with aminoglycoside, kasugamycin, multidrug, and unclassified resistance. Figure 4.13 compares the control and aqueous lanthanum samples from Figure 4.12 to the aqueous lanthanum- and antibiotic-resistant sample. Growth resistant to lanthanum chloride and antibiotics contained genes associated with

multidrug and unclassified genes only (Figure 4.13). Additionally, the predominant genes were associated with additional genera when compared to the lanthanum chloride-resistant and control samples. These genes were associated with enteric genera like *Salmonella*, *Providencia*, and *Morganella*, as well as *Dickeya* and *Enterobacter*.

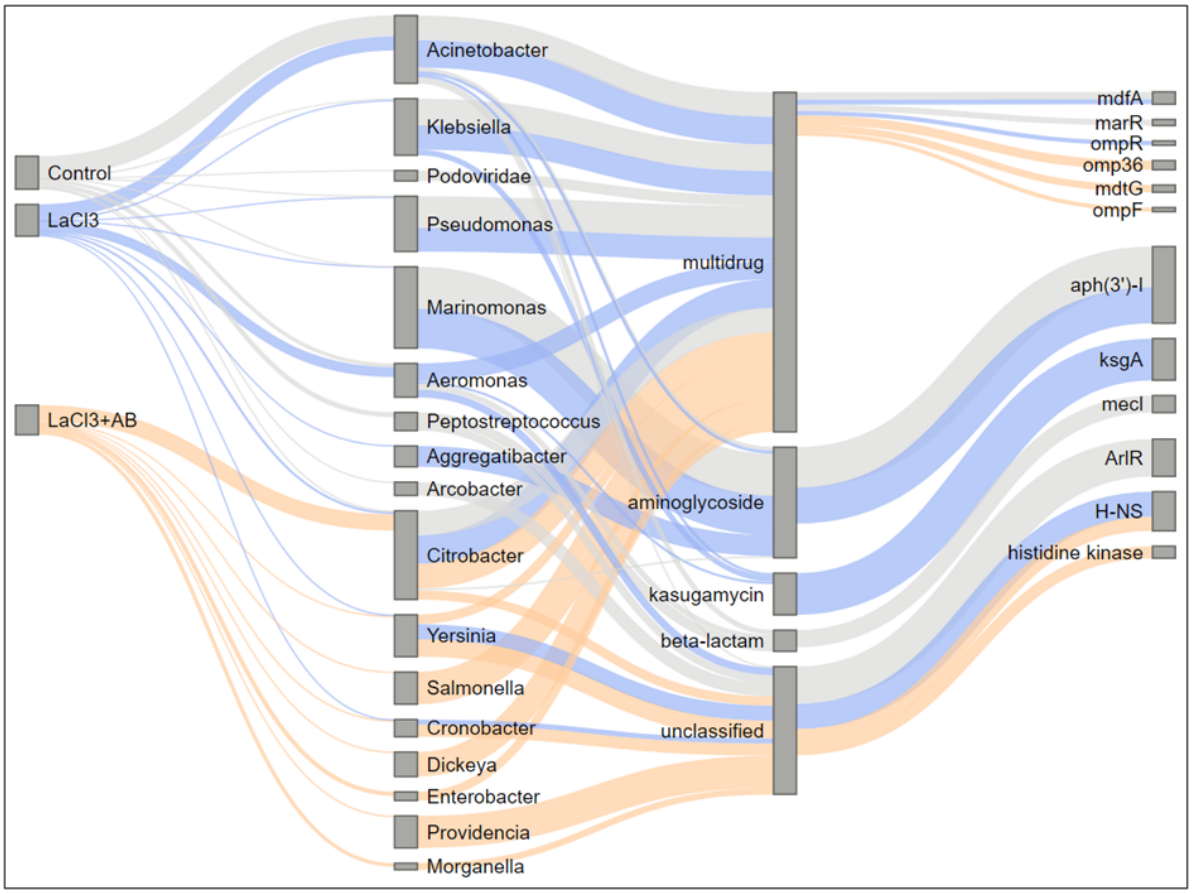

Figure 4.13 Five most abundant resistance genes in the control, lanthanum chloride-resistant, and lanthanum chloride and antibiotic-resistant samples, along with their associated resistance types and genera. From right to left, the most abundant genes in each sample, the resistance type associated with the gene, the genera in which the gene was identified, and the media in which the cells were cultured. Gray, blue, and orange connectors represent the control, $LaCl_3$-resistant, and $LaCl_3$ and antibiotic-resistant samples, respectively. Connector thickness represents the relative abundance of the genera, resistance type, or gene from its source. Column height is a function of connector thickness, and depicts relative abundance.

4.2.5 Discussion

The results from the liquid and plate culturing experiments cannot be directly compared due to the different growth conditions and antibiotic concentrations tested, but the overall trends are

assessed. Generally, rare earth-resistant cells have similar growth to, or greater growth than, unamended activated sludge in antibiotic-amended media. While the growth conditions are not representative of an activated sludge system, the culturing results provide insight on the growth of metal-resistant activated sludge inocula in the presence of antibiotics. Previous studies show heavy metal-resistant bacteria isolated from wastewater exhibiting multidrug resistance [91, 92]. Sludge from an electroplating wastewater treatment plant was found to have heavy metal-resistant bacterial strains belonging to the genera *Bacillus*, *Shewanella*, *Lysinibacillus*, and *Acinetobacter*. A *Shewanella decolorationis* strain collected from an aerobic tank was resistant to heavy metals copper, silver, and nickel, and also exhibited resistance to antibiotics erythromycin, chloramphenicol, tetracycline, kanamycin, and ampicillin. [92] In the current study, *Shewanella decolorationis* was identified in the control sample, lanthanum chloride-resistant sample, and the lanthanum oxide nanoparticle-resistant sample. It contained multidrug, beta-lactam, and macrolide-resistance genes. Interestingly, *S. decolorationis* was not identified in the samples resistant to both lanthanum and antibiotics.

The activated sludge microbial community is diverse, consisting of a variety of bacteria, viruses, and eukarya. The community composition is dynamic and is influenced by factors such as temperature and influent source, which can change the community structure seasonally [93, 94]. Though community composition differs slightly over time, predominant microorganisms stay relatively consistent despite seasonal changes [93, 94]. To attempt to portray a representative activated sludge community in our experiment, initial culture tubes were prepared in triplicate. Prior to inoculating the second round of amended media, the triplicate cultures were combined and mixed, in case selective growth occurred in a single culture tube. While the relative abundance of specific genera and resistance genes may shift based on variations in sampling, the results from the studies are consistent and establish the potential for REEs to co-select for antibiotic resistance in wastewater microbes.

The DNA sequencing results show that cells exposed to different forms of lanthanum have varying dominant genera, resistance types, and genes. When lanthanum-resistant cells were further exposed to antibiotics, the variation is even more distinct. Ding et al. (2019) also observed a compounded effect of heavy metals and the antibiotic oxytetracycline when looking at the relative abundance of ARGs in gut microbiota. While heavy metals showed a co-selection for

ARGs, the combined effects of heavy metals and oxytetracycline were greater than the effect of heavy metals or oxytetracycline alone [95]. The presence of both metals and antibiotics provides a greater selective pressure than metals alone. Literature reports the co-occurrence of heavy metal and antibiotic-resistant genes in soils, wastewater, and surface waters [96–98]. While the DNA sequencing analysis did not include identification of heavy metal-resistance genes, determining co-location of metal and antibiotic resistance genes is an important next step in future research into REE resistance co-selecting for antibiotic resistance.

The antibiotic investigation indicates that wastewater microbes exposed to REEs may show increased antibiotic resistance. Microbes resistant to dysprosium or lanthanum were able to grow in the presence of high concentrations of antibiotics in the culturing experiments. Cells exposed to lanthanum showed shifts in both microbial community composition and richness of ARGs. Lanthanum chloride had a greater impact on the microbial community than lanthanum oxide nanoparticles. The relative abundance of multidrug resistance genes increased by 16% in cells resistant to lanthanum chloride, compared to the control. When cells were resistant to both lanthanum chloride and antibiotics, a substantial shift in microbial community was observed, along with an 89% decrease in abundance of nitrifying microorganisms. This is important for wastewater treatment, as lanthanum chloride solutions have been added to treatment facilities as a phosphate reduction strategy [32]. The combined effect of lanthanum and the antibiotics present in wastewater influents has the potential to alter the microbial community and facilitate the spread of ARGs. A decrease in nitrifying microorganisms is especially noteworthy, as nitrification is an essential component of wastewater treatment, and potential impacts of lanthanum to nitrifying microorganisms requires further investigation.

4.3 Acute Impacts to Nitrification in Batch Reactors

Glass serum bottles inoculated with activated sludge from a local WRRF were prepared to evaluate the acute impact of REEs on nitrification. Inhibition of nitrification was assessed through ammonia, nitrite, and nitrate measurements taken throughout the experiment. The experiment was conducted multiple times and included reactors treated with aqueous lanthanum chloride, lanthanum oxide nanoparticles, aqueous dysprosium chloride, and aqueous cupric chloride. The average TSS of the reactors was 3,100 mg/L, which is within the typical TSS range

of 1,000-4,000 mg/L seen in activated sludge systems [99].

4.3.1 Ammonia Removal

Ammonia was completely removed from all reactors amended with lanthanum oxide nanoparticles. AUR was not significantly impacted by lanthanum oxide additions (Figure 4.14). Results indicate that acute additions of lanthanum oxide nanoparticles do not adversely impact nitrification in microcosms inoculated with activated sludge.

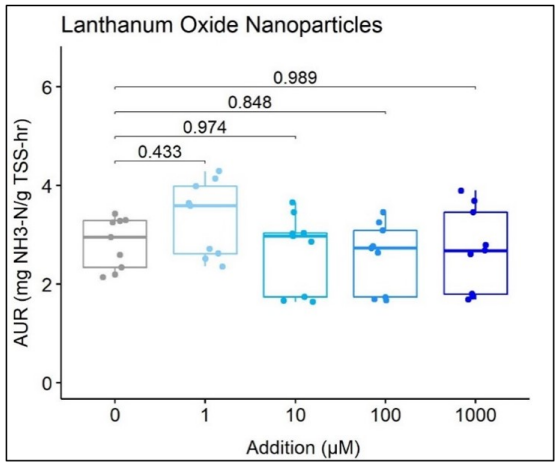

Figure 4.14 AUR in reactors amended with increasing concentrations of lanthanum oxide nanoparticles. Brackets depict Dunnett test p-values between the mean AUR of the control and amended reactors.

Unlike the reactors amended with nanoparticles, aqueous metals exhibited an inhibitory effect on nitrification at the 1000 µM treatment level. In reactors amended with aqueous lanthanum chloride, dysprosium chloride, and copper chloride, all completely removed ammonia except the 1000 µM amendment. In addition to overall ammonia removal, the AUR for the 1000 µM amendment was noticeably lower than the control (Figure 4.15). All other amendment concentrations were comparable to the control, suggesting that aqueous lanthanum, dysprosium, and copper exhibit acute impacts to nitrification at 1000 µM.

The different forms of lanthanum had varying effects on ammonia oxidation. Figure 4.16 clearly shows a reduction in ammonia removal at the 1000 µM treatment concentration of aqueous lanthanum. In the reactors amended with lanthanum oxide nanoparticles, ammonia was completely removed, or nearly completely removed, by the 90^{th} minute sampling event. In the

reactors amended with aqueous lanthanum chloride, ammonia was completely removed in all reactors, except for the reactors amended with 1000 µM, by the 90^{th} minute sampling event.

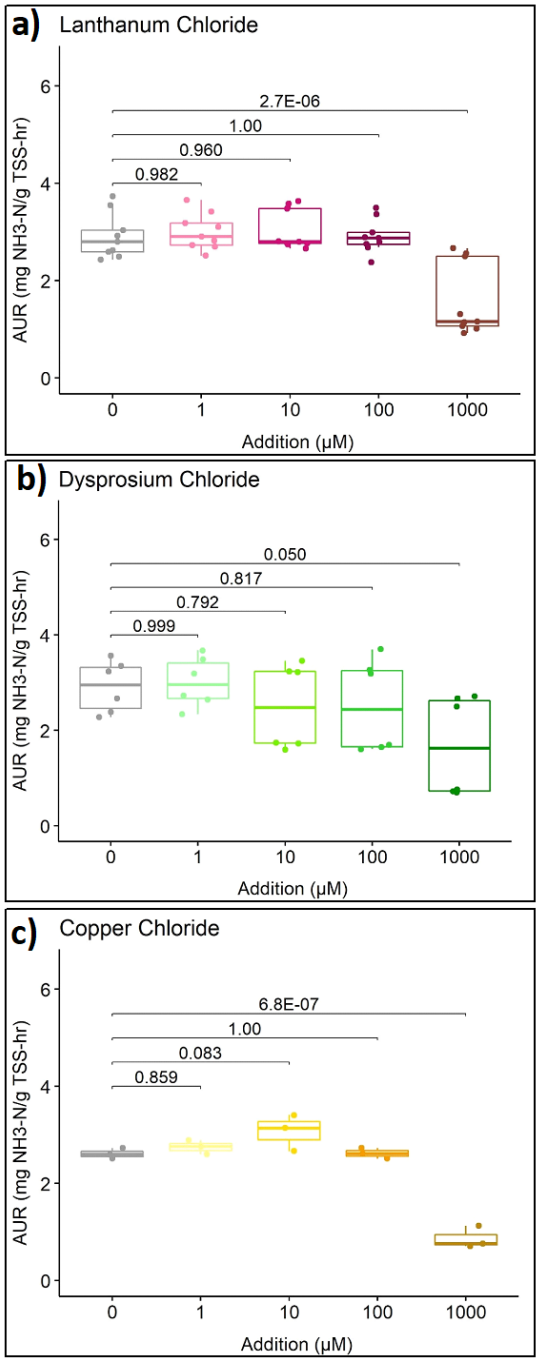

Figure 4.15 AUR in reactors amended with increasing concentrations of a) lanthanum chloride, b) dysprosium chloride, and c) copper chloride. Brackets depict Dunnett test p-values between the mean AUR of the control and amended reactors.

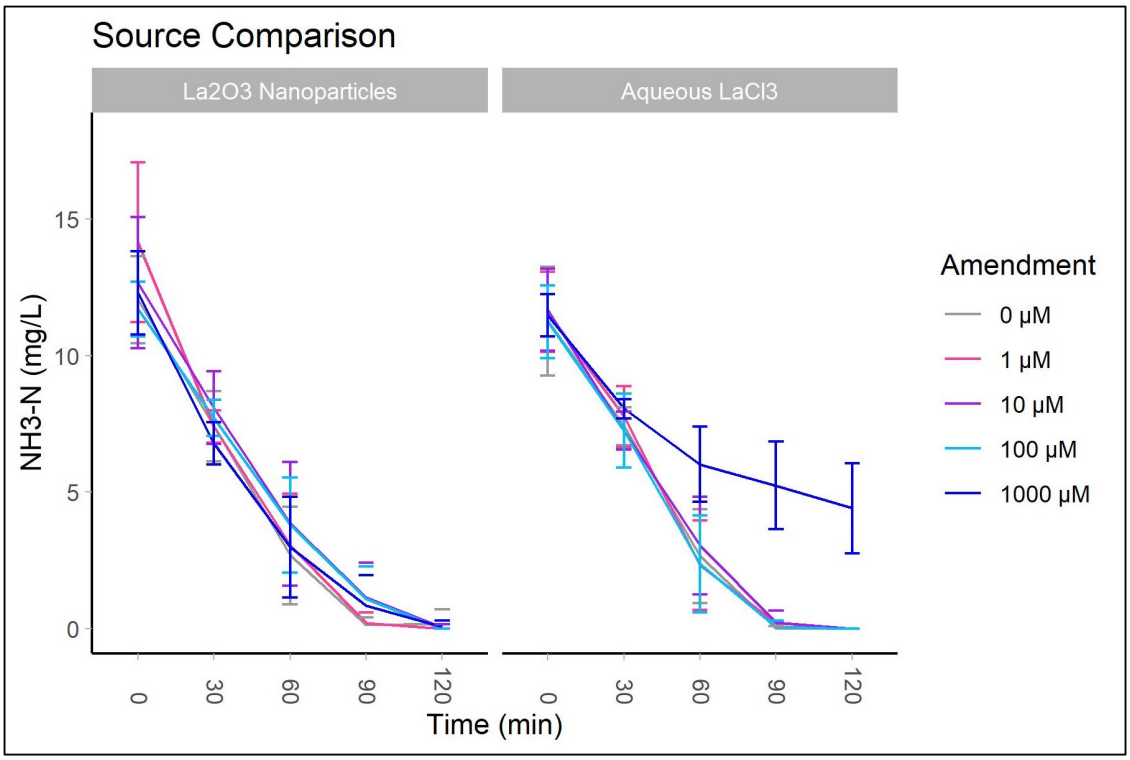

Figure 4.16 Ammonia (as nitrogen) concentration over time in reactors amended with increasing concentrations of lanthanum, as lanthanum oxide nanoparticles and aqueous lanthanum chloride. Error bars show the standard deviation in ammonia concentrations of replicate reactors.

4.3.2 Nitrogen Mass Balance

During the experiments, initial ammonia (as N) concentrations were not recovered as nitrate (as N) at the final sampling event. To reconcile the mass balance, nitrite measurements were also taken, but nitrite values were found to be negligible. Time series measurements of individual nitrogen species (NH_3-N, NO_2-N, NO_3-N) in reactors amended with lanthanum chloride, lanthanum oxide, dysprosium chloride, and copper (II) chloride are shown in Figure A.1, Figure A.2, Figure A.3, and Figure A.4, respectively, in Appendix A. Figure 4.17 shows the percent recovery of the initial sum of measured nitrogen at each sampling event throughout the two hour experiment.

In all metal treatments, the sum of measured nitrogen gradually decreased as the experiment progressed. The slow decline in measured nitrogen occurred in almost every treatment concentration, even the control. The only treatment concentration that maintained a near 100%

total nitrogen recovery at every sampling event was reactors amended with 1000 µM Cu. Interestingly, ammonia oxidation was noticeably inhibited at this treatment concentration (Figure 4.17). Similar nitrogen recovery also occurs in reactors amended with 1000 µM La (as $LaCl_3$) and Dy. Of all treatment concentrations in their respective amendments, the reactors treated with 1000 µM REE had the highest percentage of measured nitrogen recovery.

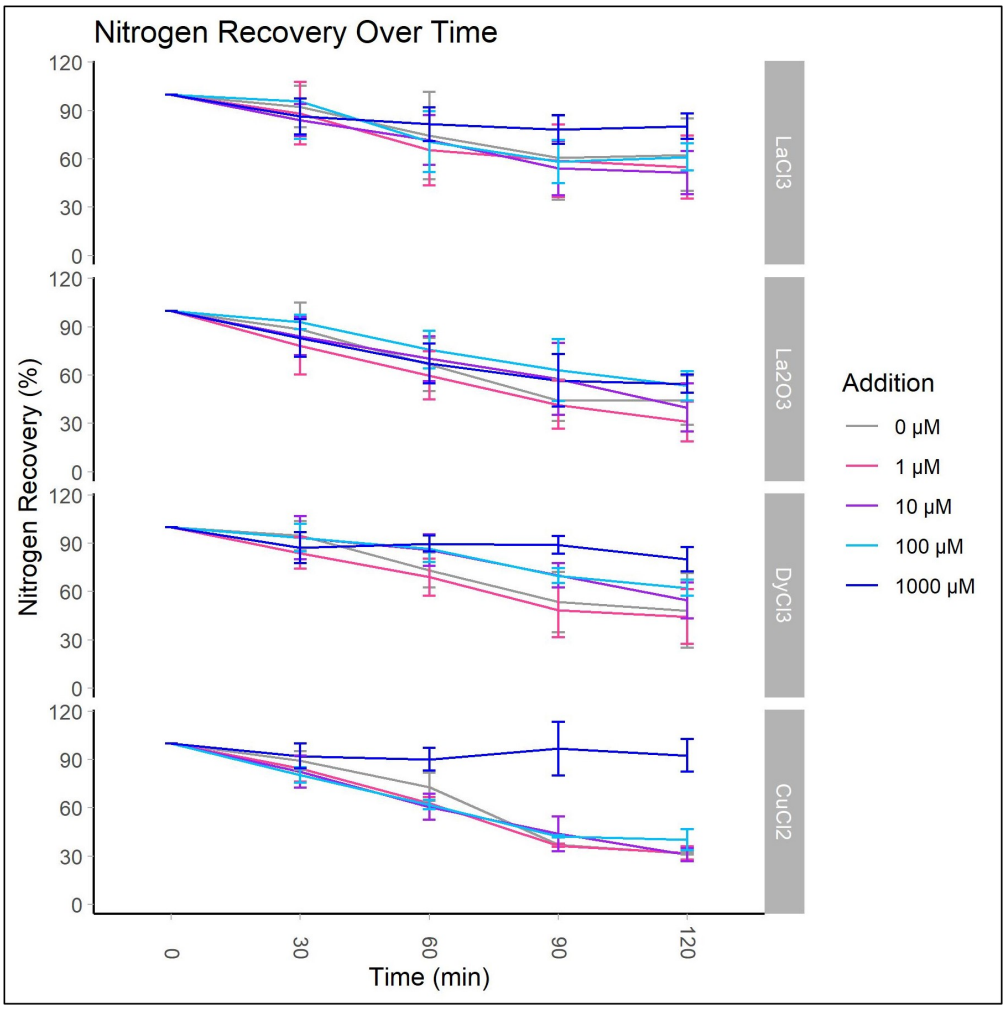

Figure 4.17 Percent of the initial nitrogen (NH_3-N, NO_2-N, NO_3-N) measured at each sampling time. Error bars depict the standard deviation in nitrogen measurements from replicate reactors.

4.3.3 Discussion

Acute effects on nitrification in batch reactor results are not believed to be representative of a full-scale activated sludge environment. At two hours, this experiment was relatively short compared to the time wastewater spends in an aeration basin. Hydraulic retention time (HRT),

the time that wastewater spends in a reactor, is dependent on flow rate and basin volume. In full-scale WRRFs, HRT in a complete mix activated sludge system can range from 3 to 5 hours [100]. Though AUR decreased in reactors amended with 1000 μM La (as lanthanum chloride), complete ammonia oxidation is expected over a time period longer than two hours. The HRT required to achieve 95% ammonia removal was calculated based on initial ammonia concentrations in the reactors and respective ammonia uptake rates for each amendment. The removal of 95% of initial ammonia would have taken approximately 7.1, 6.8, and 13.2 hours in reactors amended with 1000 μM of lanthanum chloride, dysprosium chloride, and cupric chloride, respectively. In a WRRF with a relatively long HRT, 1000 μM La (as lanthanum chloride) is not expected to affect overall ammonia removal.

The reason for the lack of reconciliation of the mass balance of measured nitrogen was unclear during these experiments. The gradual loss of total nitrogen in all reactors, except for the reactors that showed inhibition of AUR, suggests that another process, in addition to nitrification, may be occurring. The reactors were not aerated during the experiment; they were placed on a shaker that was intended to promote aeration. The reactors were also capped with a piece of aluminum foil. It is possible that the oxygen transfer was not sufficient to maintain aerobic conditions and that the low dissolved oxygen conditions promoted denitrification. This would explain the reduction in total nitrogen in the uninhibited reactors, as nitrogen gas (the product of denitrification) was not measured during the experiment. As ammonia oxidation was inhibited in some reactors, complete nitrification did not occur, and denitrification would not have transpired, resulting in a higher total nitrogen recovery for the measured nitrogen species. Alleman and Irvine (1980) observed denitrification in sequencing batch reactors when they were stirred but not aerated [101]. Zeng et al. (2003) observed a similar decline in total nitrogen species (NH_4-N, NO_2-N, NO_3-N) under aerobic conditions in a sequencing batch reactor. Simultaneous nitrification-denitrification was observed at DO concentrations of 0.5, 1.5, and 2.5 mg/L. [102] Dissolved oxygen measurements during our experiment ranged from 0.7 to 2.3 mg/L. It is possible that denitrification occurred in the batch reactors, explaining the gradual loss in total nitrogen of the measured nitrogen species. Sampling and measuring nitrogen gas (N_2, N_2O and NO) would shed light on the possible denitrification activity occurring during the acute batch experiments. An air-tight batch reactor with an off-gas system would allow the continuous

monitoring of N_2, N_2O, and NO concentrations during the experiment.

The acute batch reactor experiments indicate an adverse impact on ammonia oxidation when microbes are exposed to 1000 μM of aqueous metals. Interestingly, lanthanum oxide nanoparticles did not induce inhibition of nitrification. While AUR decreased in reactors amended with 1000 μM aqueous metals and complete ammonia oxidation did not occur within the two hour experiment, it is possible that complete nitrification could occur in a full-scale WRRF with a HRT of more than 7 hours. The acute experiments indicate that biological nitrification in full-scale WRRFs may be impacted by high concentrations of REEs, and it is important to understand how the microbial community itself is affected. Nitrifying microorganisms are slow-growing, and growth is affected by factors like temperature, pH, nitrogen concentrations, and oxygen concentration [103]. Any inhibition of nitrification may make retention of nitrifiers even more challenging.

4.4 Recovery of Microbial Community Composition and Function After REE-Induced Inhibition of Nitrification

Microbial community composition in bioreactors during and after long-term exposure to REEs yttrium (Y) and gadolinium (Gd) was evaluated through sequencing of 16S rRNA genes from bioreactor samples. Sequencing results were used to evaluate shifts in the microbial community and relative abundances of nitrifiers in response to amendment type and treatment concentration.

4.4.1 Shift in Microbial Community

Principal coordinate analysis (PCoA) from weighted UniFrac distance matrices is shown in Figure 4.18. Samples from all reactors started off in a cluster, indicating similarity. The samples deviated as the experiment proceeded. A clear shift is observed in samples collected from the Y-amended reactors, starting during the 25 ppm additions. The samples shifted further during the 50 ppm additions. The samples collected from the Gd-amended reactor had a less noticeable shift but did slightly deviate from untreated samples at 50 ppm Gd. Interestingly, samples collected from the Y-amended reactor during the recovery period appeared to shift back towards the untreated samples.

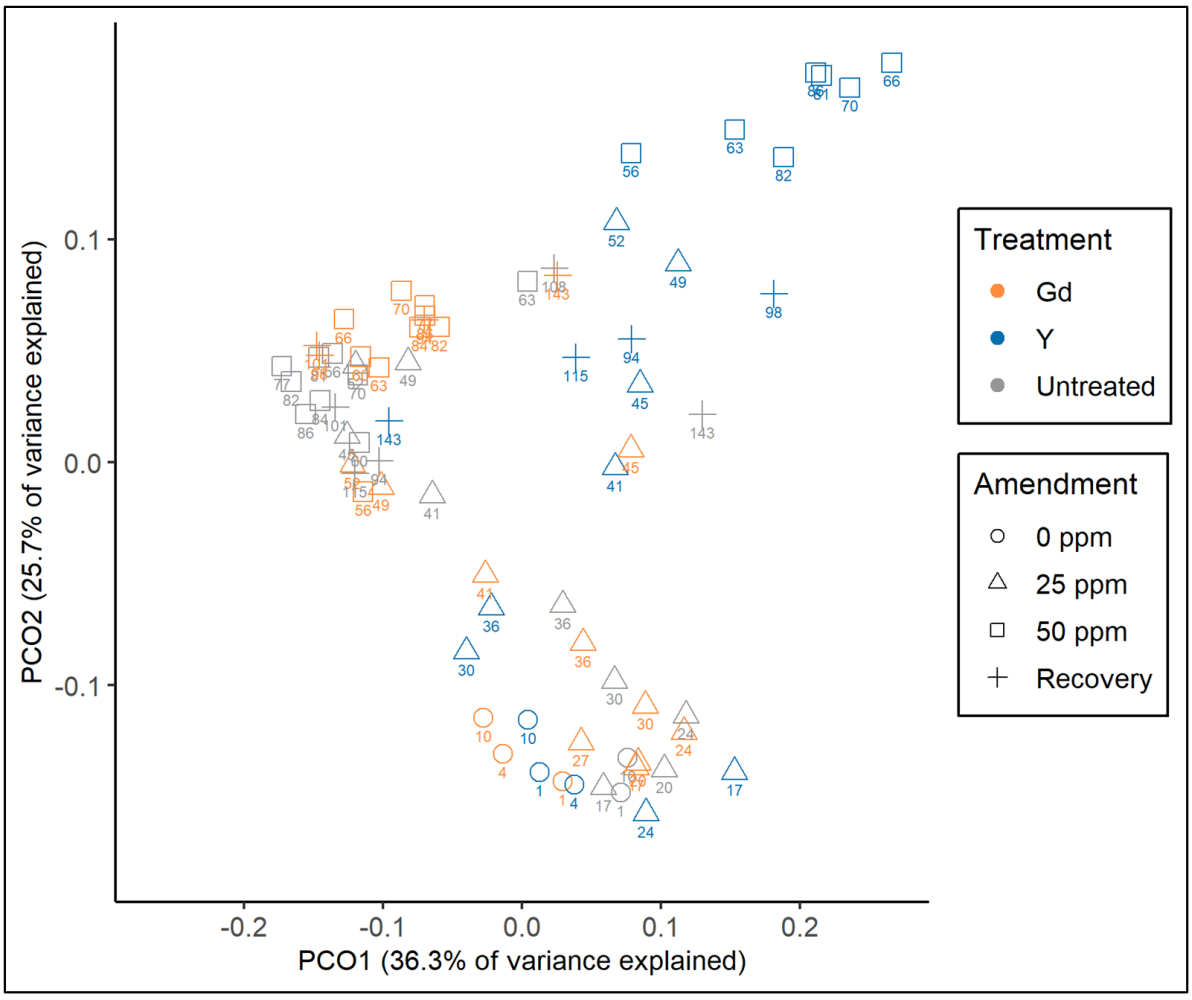

Figure 4.18 UniFrac PCoA analysis on all reactors during REE additions and the recovery period. Numbers below points show days from the start of the experiment. In the untreated reactor, points at 25 ppm and 50 ppm relate to time periods of amendments; the untreated reactor did not receive any amendments.

Statistical analysis of the UniFrac distance matrices was conducted using permutational multivariate analysis of variance (PERMANOVA) and beta dispersion. PERMANOVA tests if the centroids of each group are significantly different from one another. PERMANOVA results indicate that the Y-amended reactor was significantly different from the control and Gd-amended reactor (Table 4.9). Beta dispersion analysis tests if the dispersion, or variance, of groups is significantly different. Beta dispersion results suggest that the Y-amended reactor had a significantly different dispersion than the other two reactors (Table 4.10). This is clearly shown in Figure 4.18, where the Y-amended reactor displayed a larger dispersion than the relatively tightly

clustered Gd-amended and control reactors. R^2 values represent the percentage of the variance that can be attributed to each group, and a low R^2 value suggests that the majority of the variation in distance is unexplained.

Table 4.9 PERMANOVA analysis evaluating the differences in the centroids of each reactor. Significant p-values are bolded.

Comparison	**R^2**	**p-value**
Untreated vs Gd	0.024	0.274
Untreated vs Y	0.143	**0.002**
Gd vs Y	0.161	**0.002**

Table 4.10 Beta dispersion analysis on UniFrac distance matrices for each reactor. Significant p-values are bolded.

	Control	Gd	Y
Control	X	0.851	**0.005**
Gd	0.843	X	**0.001**
Y	**0.005**	**0.001**	X

4.4.2 Abundances of Nitrifying Microorganisms

The nitrifying community was analyzed by the relative abundance of nitrifying families, Nitrosomonadaceae and Nitrospiraceae. These two families include genera *Nitrosomonas* and *Nitrospira*, respectively. *Nitrosomonas* is important in wastewater treatment as an ammonia-oxidizing bacteria, while *Nitrospira* are nitrite-oxidizing bacteria and help complete the nitrification process in wastewater treatment. Figure 4.19 shows the relative abundance of both Nitrosomonadaceae and Nitrospiraceae during REE-induced inhibition of nitrification. A decrease in the relative abundance of nitrifying bacteria occurred simultaneously with a reduction in ammonia oxidation. The relative abundance of nitrifiers increased as nitrification recovered after additions were stopped in the Y-amended reactor, but not in the Gd-amended reactor (Figure 4.19).

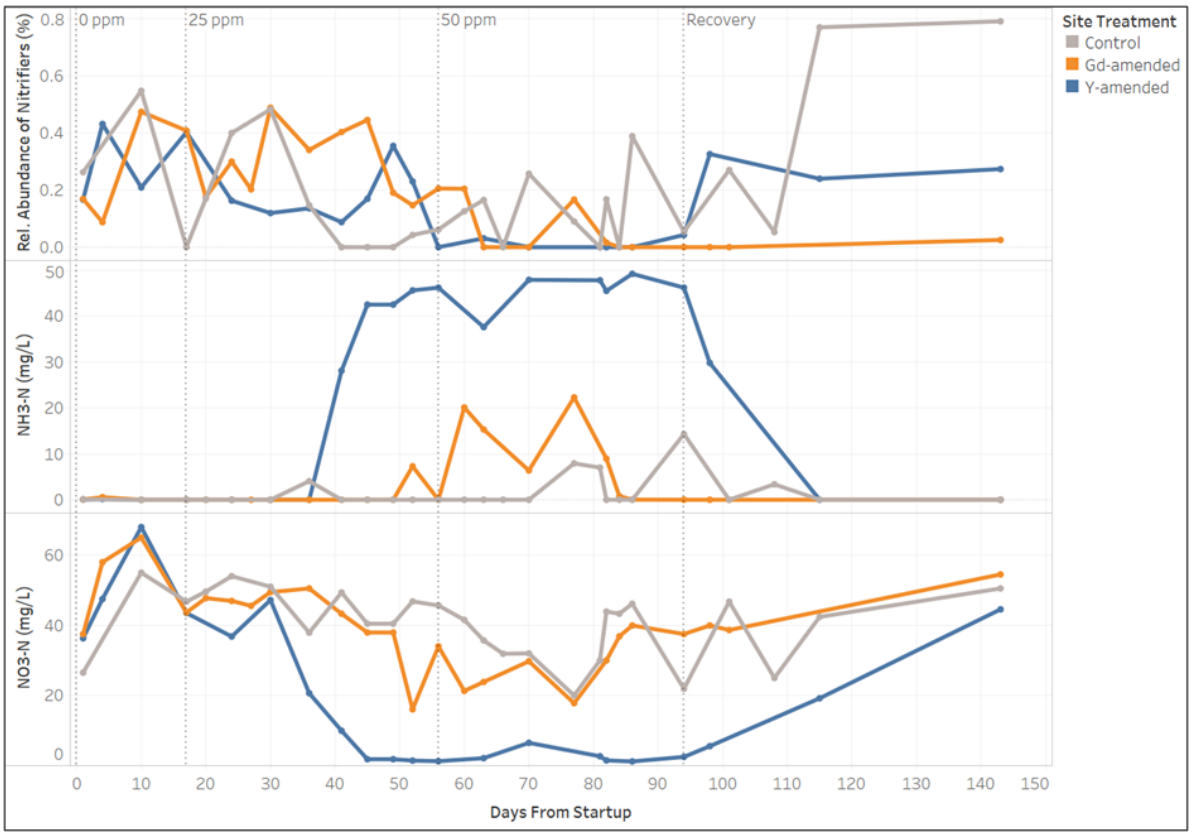

Figure 4.19 Relative abundance of nitrifying bacteria, Nitrosomonadaceae and Nitrospiraceae, and measured nitrogen species in response to gadolinium and yttrium additions.

Relative abundance of Nitrosomonadaceae fluctuated in all reactors during the stabilization period and 25 ppm addition (Figure 4.20). Relative abundance noticeably dropped in all reactors at the 50 ppm addition period. While abundances fluctuated between 0 and 0.2% in the control and Gd-amended reactors, abundance in the Y-amended reactor stayed between 0 and 0.04%. The relative abundance of Nitrosomonadaceae increased in the control reactor during the recovery period. Relative abundance initially recovered in the Y-amended reactor before dropping. Recovery of Nitrosomonadaceae was slower in the Gd-amended reactor but was gradually increasing when the experiment was stopped. Focusing in at the genus level, the abundance of amplicon sequence variants (ASV), or single DNA sequences, of *Nitrosomonas* was affected by 25 and 50 ppm of both Gd and Y. ASV abundance recovered to pre-treatment levels in the Y-amended reactor, but remained significantly lower than the original ASV abundance in the Gd-amended reactor (Table 4.11).

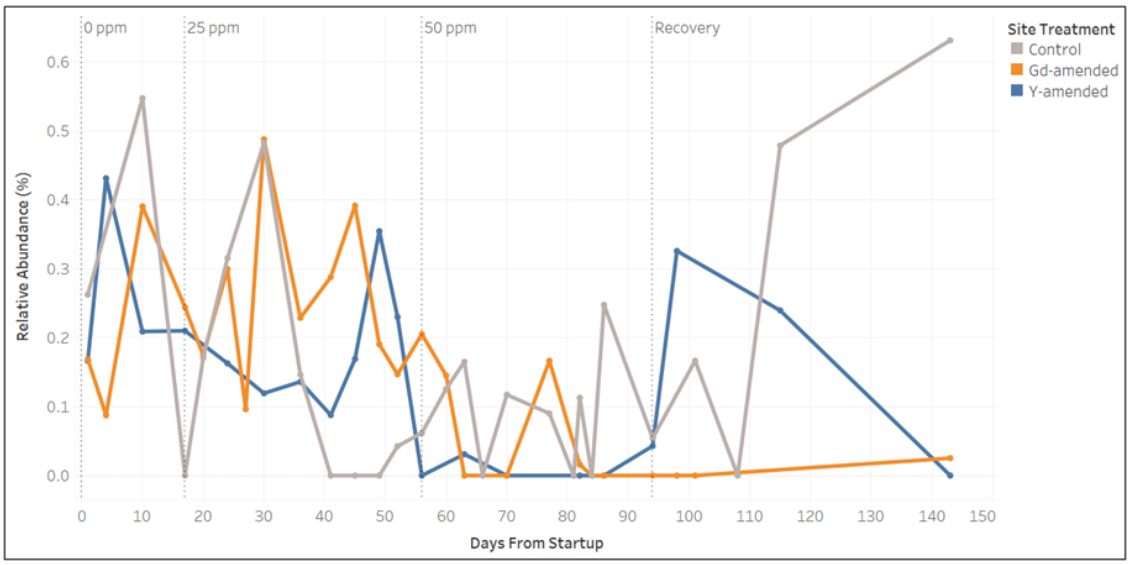

Figure 4.20 Relative abundance of Nitrosomonadaceae in all reactors over the course of the experiment.

Table 4.11 Average ASV abundance of *Nitrosomonas* at each REE addition concentration. Mean ASV values significantly different ($p<0.05$) from the starting mean ASV abundance are bolded.

Reactor	REE Addition (ppm)			
	0	25	50	0 (Recovery)
Control	12.7	3.1	2.51	14.2
Gd	6.75	**2.00**	**0.54**	**0.24**
Y	7.34	**0.36**	**0**	3.14

Like Nitrosomonadaceae, the relative abundance of Nitrospiraceae fluctuated in all reactors during the stabilization period and 25 ppm addition period (Figure 4.21). Relative abundance in the control and Y-amended reactors dropped roughly halfway into the 25 ppm addition period. During the 50 ppm addition period, relative abundance continued to fluctuate between 0 and 0.15% in the control reactor but remained low in both treated reactors. While relative abundance of Nitrospiraceae increased in the Y-amended reactor during the recovery period, relative abundance remained low in the Gd-amended reactor. The ASV abundance of *Nitrospira* was not significantly impacted by either Gd or Y at any metal addition concentration (Table 4.12).

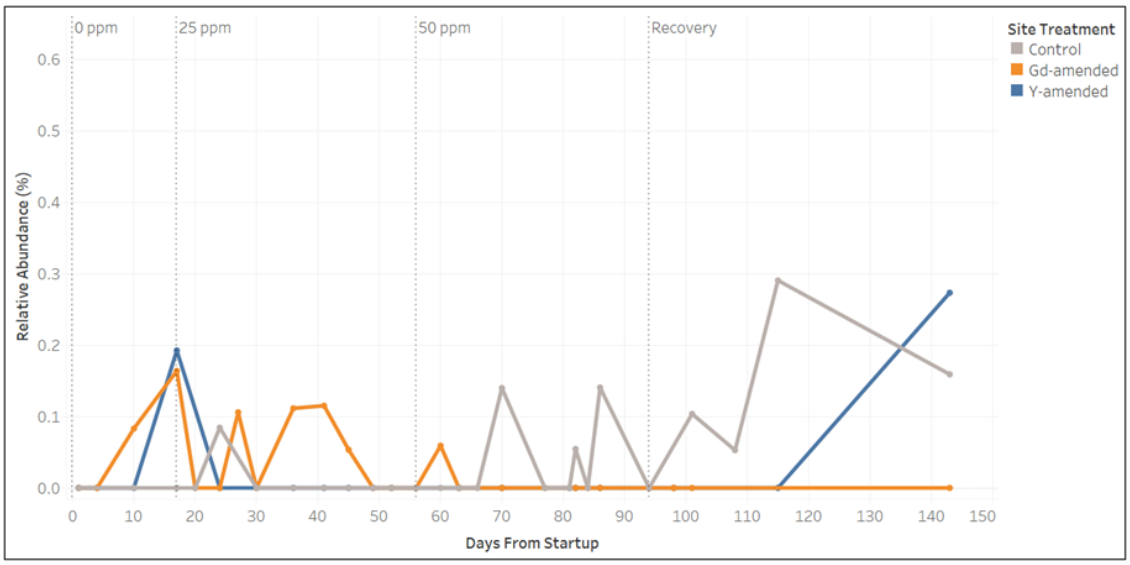

Figure 4.21 Relative abundance of Nitrospiraceae in all reactors over the course of the experiment.

Table 4.12 Average ASV abundance of *Nitrospira* at each REE addition concentration. Mean ASV values significantly different ($p<0.05$) from the starting mean ASV abundance are bolded.

Reactor	REE Addition (ppm)			
	0	25	50	0 (Recovery)
Control	2.85	2.25	1.99	7.8
Gd	1.04	2.59	0.45	0.8
Y	0.96	0.9	0.0	2.54

4.4.3 Discussion

The impacts to nitrification observed during REE amendments are supported by a shift in microbial community in the Y-amended reactor that was observed shortly after 25 ppm additions began. Time series analysis suggests that a decline in nitrifiers could play a role in the noticeable community shift of the Y-amended reactor. The relative abundance of Nitrosomonadaceae and the ASV abundance of ammonia-oxidizer *Nitrosomonas* substantially decreased during the 25 and 50 ppm Y additions. Su et al. (2020) also observed a dramatic decrease in ammonia nitrogen consumption when Y concentrations increased to 20 ppm in activated sludge batch reactors [104]. Microbial shifts in response to yttrium have also been observed in soil. When soils were amended with yttrium, soil microbial diversity decreased, and the relative abundance of soil microbes

changed. Principal component analysis of soil genera showed a large distance between Y-amended soils and control soil, similar to what was observed in the Y-amended reactor in our PCoA analysis. [105]

Nitrification recovered after REE additions were stopped, and microbial community began to recover as well. The PCoA analysis showed that, once additions were stopped, the microbial community in the Y-amended reactor began to shift towards the cluster that contained the Gd-amended and control reactor dispersions (Figure 4.18). During the recovery period, the relative abundances of nitrifying bacteria increased in the Y-amended reactor. The ASV abundance of *Nitrosomonas* increased to pre-treatment levels once additions were stopped. The Gd-amended reactor behaved slightly differently. The relative abundances of nitrifying bacteria did not recover as quickly as they did in the Y-amended reactor. Similarly, the ASV abundance of *Nitrosomonas* did not increase to pre-treatment levels during the recovery period. Y-amended reactors recovered to pre-treatment conditions relatively quickly, while nitrifying microbes in the Gd-amended reactors did not fully recover within the 49-day recovery period. Additional study is needed to understand the time frame of a full recovery of a Gd-amended reactor. Because complete nitrification was observed shortly after Gd additions stopped, it is possible that other genera, besides *Nitrosomonas*, were able to carry out ammonia oxidation (Figure 4.19). *Nitrospira* are typically nitrite-oxidizing microorganisms, but have been shown to carry out complete ammonia oxidation (comammox) in sequencing batch reactors and soil [106, 107]. The ASV abundance of *Nitrospira* in our aerobic bioreactor experiment was not impacted by gadolinium or yttrium additions. Though the ASV abundance of *Nitrospira* was relatively low compared to the ASV abundance of *Nitrosomonas*, the *Nitrospira* population remained steady throughout the experiment. It is possible that, without the stress of Gd additions, the reduced *Nitrosomonas* population may have been able to carry out ammonia oxidation, and may have been supplemented by *Nitrospira*.

The different recoveries of Gd and Y may be due to the mechanism of REE toxicity in cells. Literature has recognized K^+ channels as targets for REEs [104, 108]. Su et al. (2020) found that Y-induced inhibition of ammonium oxidation was likely due to the impact to potassium (K^+) channels. As Y concentration increased, the mass fraction of potassium in sludge decreased [104]. Y inhibited the activity of the K^+ channel protein, which affected the absorption of potassium by

ammonium-oxidizing bacteria, leading to inhibition. In human kidney cells, La and terbium (Tb) formed coordination bonds with the K^+ channel protein, affecting protein structure and channel properties, and decreasing the channel current. Cells could recover from the damaged caused by the light REE, La, but not from the damage caused by the heavy REE, Tb. The coordination of the REE and the K^+ channel protein influenced their respective cytotoxicities. [108] The distinct properties of Gd and Y may have impacted activated sludge K^+ channels differently, leading to varying recovery responses of nitrifying microbes. Gadolinium is a heavy REE with similar properties to terbium, and the lack of recovery from K^+ channels impacted by Tb may provide insight on the slow resurgence of nitrifying microbes in the Gd-amended reactor. Yttrium has a low atomic weight compared to other REEs, but it is grouped with heavy REEs due to similar chemical properties. Further investigation into the relationshihp and bonds between K^+ channel proteins and Gd or Y may shed light on the discrepancy between microbial recovery responses.

Results from the microbial community analysis indicate that exposure to relatively high concentrations of Gd or Y altered the microbial community structure and reduced the relative abundance of nitrifying microbes during inhibition of nitrification. Microbial community changes were more pronounced in the Y-amended reactor than the Gd-amended reactor. Though the nitrification process recovered almost immediately after REE additions were stopped, increasing the relative abundance of nitrifiers to pre-treatment levels may take an extended period of time. These findings are useful for WRRFs receiving REE-impacted wastewater. The presence of REEs at 25 ppm significantly impacted the ammonium-oxidizer *Nitrosomonas*. Though nitrification recovered after REE additions were stopped, the nitrifying microbial population did not recover to pre-treatment levels in the Gd-amended reactor. REE-impacted wastewater has the potential to impact biological treatment, and WRRF operators must ensure the retention of nitrifying microbes to maintain the efficacy of the water treatment process.

CHAPTER 5

CONCLUSIONS AND RECOMMENDATIONS

These experiments were performed to investigate the effect of rare earth elements (REEs) on wastewater microbes, specifically their growth, community structure, metal and antibiotic resistance, and performance. An additional goal of the research was to investigate shifts in microbial community composition during, and after, REE-induced inhibition of nitrification in long-term, bench-scale aerobic bioreactor experiments. By evaluating both the composition and performance of the wastewater microbial community in response to REEs, we hope to inform REE waste generators and water resource reclamation facility (WRRF) operators.

5.1 Conclusions

We hypothesized, based on literature that identified notable effects of REEs on soil and wastewater microbes, that REEs, at relatively high concentrations, would impact the performance and composition wastewater microbial communities. This hypothesis was supported by culturing studies, batch reactor experiments, and DNA sequencing.

Aerobic culture plates amended with REE recycling waste and inoculated with activated sludge from a local WRRF showed inhibition of colony growth on plates amended with 5% v/v of acidic waste. Cell growth was not inhibited on plates amended with neutral waste, or at the 2.5% v/v dilution. When control and amended plates were acidified to the pH of the 5% v/v plates, cell growth was completely inhibited on the plates amended with both dilutions of Waste 2A. While acidity of the waste is likely the main factor in cell growth inhibition, results suggest that constituents in Waste 2A also contribute to inhibition. Waste 2A contained relatively high concentrations of rare earths dysprosium and terbium, along with iron and copper. An investigation into the potential for REEs to co-select for antibiotic resistance in wastewater microbial communities indicate that growth of REE-resistant cells is similar to, or greater than, unamended activated sludge in the presence of antibiotics. In liquid cultures, cadmium-, dysprosium-, and lanthanum-resistant cells showed growth similar to activated sludge in both penicillin- and streptomycin-amended media. Metal-resistant cells, particularly

lanthanum-resistant cells, showed a higher growth than activated sludge in erythromycin-amended media. While results were not as distinct in plate cultures as liquid cultures, a similar trend was observed. While increased susceptibility was observed around a few antibiotic discs, metal-resistant cells generally showed comparable or greater resistance to antibiotics compared to activated sludge, especially on plates inoculated with Dy-resistant cells. Additionally, different predominant antibiotic resistance genes were identified in cells exposed to different lanthanum sources (aqueous vs. nanoparticle). This shift was even more pronounced when cells were exposed to both lanthanum and antibiotics. In cells exposed to both aqueous lanthanum and antibiotics, the majority of predominant genes were multidrug resistant. A shift in predominant genera was observed as well. In cells exposed to both aqueous lanthanum and antibiotics, the relative abundance of *Citrobacter* substantially increased, along with genera *Enterobacter*, *Morganella*, and *Yersinia*.

An evaluation of biological nitrification performance parameters was conducted on batch reactors amended with increasing concentrations of metals. Inhibition of nitrification was observed in reactors amended with 1000 µM of aqueous metals. Interestingly, reactors amended with lanthanum oxide nanoparticles did not exhibit inhibitory effects. The acute batch reactor experiments indicate that ammonia uptake rate decreases in the presence of high concentrations of aqueous metals, and effects of REEs are comparable to the heavy metal copper. Since inhibition of nitrification occurred, it is possible that nitrifying microbial populations were impacted as well. Long-term performance may be affected by acute exposure to REEs, as the retention of nitrifiers is essential in the efficacy of the treatment process.

DNA sequencing of sludge pellets collected before, during, and after REE-induced inhibition of nitrification in bench-scale aerobic sequencing batch bioreactors indicated a shift in microbial community composition in reactors exposed to 25 ppm yttrium and 50 ppm gadolinium. The shift was more pronounced in the yttrium-amended reactor. A decrease in relative abundance of nitrifying bacteria was also observed during inhibition of nitrification in amended reactors. Abundance of nitrifying microbes returned to pre-treatment levels once additions were stopped in the yttrium-amended reactor, but not in the gadolinium-amended reactor.

The results of this research have implications for REE waste generators, WRRFs receiving REE-impacted waste, and regulators. Inhibition of colony growth was observed on plates

amended with acidic wastes at 5% v/v dilutions, but inhibition was not observed at 2.5% v/v dilutions or when the waste was neutralized. Ammonia utilization rate decreased in batch reactors amended with high concentrations of aqueous metals, and potential impacts to nitrifiers may results in long-term inhibitory effects. Antibiotic studies suggest that exposure to REEs may lead to increased antibiotic resistance in wastewater microbes. Additionally, a notable microbial shift, and a decrease in nitrifying microbes, was observed in reactors amended with increasing concentrations of REEs. Overall, our results indicate that caution needs to be taken when considering biological treatment of REE-laden wastewater or adding REE solutions to WRRFs. Results suggest that REE recycling waste must be neutralized or highly diluted prior to dicharge to WRRFs, and elevated concentrations of REEs may adversely affect nitrifying microbes.

5.2 Recommendations for Future Work

The research identified many avenues to expand upon our findings. Plate assays indicated that constituents in Waste 2A contributed to inhibition of colony growth. Waste 2A contained a variety of REE, and future work into the main components of Waste 2A, like dysprosium and terbium, would more precisely determine the mechanism of toxicity in those assays.

The antibiotic investigation showed the potential for REEs to co-select for antibiotic resistance, but there are opportunities to expand upon this research. Our analysis evaluated antibiotic resistance genes but not metal resistance genes. Because co-selection is believed to occur on mobile genetic elements, future work should focus on identifying the locations of metal and antibiotic resistance genes along with associated mobile genetic elements. Future DNA sequencing efforts should also investigate different REEs along with heavy metals that are known to co-select for antibiotic resistance. These data would clarify the mechanism of co-selection of REE resistance and antibiotic resistance and indicate whether heavy metals and REEs affect the resistance of microbes in a comparable way. Additionally, it is important to quantify the magnitude of antibiotic resistant bacteria (ARB) in biosolids collected from WRRFs, as they are used as fertilizer on agricultural fields. With the spread of antibiotic resistance becoming a more urgent public health threat, it is necessary to assess the contributions of biosolids. Identifying ARB in the biosolids, applied fertilizer, and the receiving soil over time would shed light on the fate and potential hot spots of ARB. It could also introduce a possible positive feedback loop for

resistance development, from farms, to humans, to WRRFs, and back to farms.

The acute bioreactor experiment could be expanded upon to identify the time required for the nitrification process to be completed in reactors amended with higher concentrations of aqueous metals. Ammonia was not completely removed in reactors amended with 1000 µM aqueous metals and understanding the time frame for complete nitrification would be useful to evaluate hydraulic residence time (HRT) for facilities receiving impacted wastewater. In addition, the possible denitrification in the unaffected reactors needs to be better understood. Sampling for nitrogen gas species (N_2, N_2O) throughout the experiment could rectify the nitrogen mass balance. Denitrification products have previously been measured in the off-gas of sequencing batch reactors [102, 109].

Additional work is also needed to investigate the acute effect of REEs on nitrifying microbes and the recovery of microbes impacted by chronic exposure to REEs. Because ammonia oxidation was inhibited in the acute experiment and nitrifying microbes are slow-growing and sensitive to stressors, community analysis would provide insight to whether acute exposure to REEs adversely affects community composition. Similarly, the microbial community recovery following REE-induced inhibition could be expanded upon. Nitrifying microbes in yttrium-amended reactors recovered to pre-treatment levels, but not in the gadolinium-amended reactor. Because ntirification recovered shortly after REE additions were stopped, it is possible that other genera, besides *Nitrosomonas*, carried out ammonia oxidation. A longer recovery period would determine whether or not the nitrifying microbes in the gadolinium-amended reactor are able to return to pre-treatment levels. Since WRRFs need to retain nitrifying microbes to ensure the efficacy of water treatment, an understanding of the lasting impacts of REE exposure on the wastewater microbial community is essential.

REFERENCES

[1] Bradley S Van Gosen, Philip L Verplanck, Robert R Seal II, Keith R Long, and Joseph Gambogi. Rare-earth elements. Technical Report 1802-O, US Geological Survey, 2017.

[2] MP Materials. History, 2020. URL http://mpmaterials.com/about/#history.

[3] United States Environmental Protection Agency. Primer for municipal wastewater treatment systems. Technical Report 832-R-04-001, United States Environmental Protection Agency, Washington DC (United States), 2004.

[4] Prachi Kulkarni, Nathan D Olson, Greg A Raspanti, Rachel E Rosenberg Goldstein, Shawn G Gibbs, Amir Sapkota, and Amy R Sapkota. Antibiotic concentrations decrease during wastewater treatment but persist at low levels in reclaimed water. *International journal of environmental research and public health*, 14(6):668, 2017.

[5] Manlin Qi, Wen Li, Xufeng Zheng, Xue Li, Yue Sun, Yu Wang, Chunyan Li, and Lin Wang. Cerium and its oxidant-based nanomaterials for antibacterial applications: a state-of-the-art review. *Frontiers in Materials*, 7:213, 2020.

[6] L Rizzo, C Manaia, C Merlin, T Schwartz, C Dagot, MC Ploy, I Michael, and Despo Fatta-Kassinos. Urban wastewater treatment plants as hotspots for antibiotic resistant bacteria and genes spread into the environment: a review. *Science of the total environment*, 447:345–360, 2013.

[7] Tucker R Burch, Michael J Sadowsky, and Timothy M LaPara. Aerobic digestion reduces the quantity of antibiotic resistance genes in residual municipal wastewater solids. *Frontiers in microbiology*, 4:17, 2013.

[8] Centers for Disease Control and Prevention. Antibiotic resistance threats in the united states, 2019. Technical report, US Department of Health and Human Services, 2019.

[9] C Lee Ventola. The antibiotic resistance crisis: part 1: Causes and threats. *Pharmacy and therapeutics*, 40(4):277, 2015.

[10] Timothy M Rawson, Luke SP Moore, Nina Zhu, Nishanthy Ranganathan, Keira Skolimowska, Mark Gilchrist, Giovanni Satta, Graham Cooke, and Alison Holmes. Bacterial and fungal coinfection in individuals with coronavirus: a rapid review to support covid-19 antimicrobial prescribing. *Clinical Infectious Diseases*, 71(9):2459–2468, 2020.

[11] Alvaro Goncalves Mendes Neto, Kevin Bryan Lo, Ammaar Wattoo, Grace Salacup, Jerald Pelayo, Robert DeJoy III, Ruchika Bhargav, Fahad Gul, Eric Peterson, Jeri Albano, et al. Bacterial infections and patterns of antibiotic use in patients with covid-19. *Journal of medical virology*, 93(3):1489–1495, 2021.

[12] Sirijan Santajit and Nitaya Indrawattana. Mechanisms of antimicrobial resistance in eskape pathogens. *BioMed research international*, 2016, 2016.

[13] Craig Baker-Austin, Meredith S Wright, Ramunas Stepanauskas, and JV McArthur. Co-selection of antibiotic and metal resistance. *Trends in microbiology*, 14(4):176–182, 2006.

[14] Amalesh Samanta, Paramita Bera, MAHAMUDA Khatun, Chandrima Sinha, Pinaki Pal, Asif Lalee, and Anurup Mandal. An investigation on heavy metal tolerance and antibiotic resistance properties of bacterial strain bacillus sp. isolated from municipal waste. *Journal of Microbiology and Biotechnology Research*, 2(1):178–189, 2012.

[15] Daloha Rodríguez-Molina, Petra Mang, Heike Schmitt, Mariana Carmen Chifiriuc, Katja Radon, and Laura Wengenroth. Do wastewater treatment plants increase antibiotic resistant bacteria or genes in the environment? protocol for a systematic review. *Systematic reviews*, 8(1):1–8, 2019.

[16] Edward Peltier, Joshua Vincent, Christopher Finn, and David W Graham. Zinc-induced antibiotic resistance in activated sludge bioreactors. *water research*, 44(13):3829–3836, 2010.

[17] Tokumitsu Wakabayashi, Ayumi Ymamoto, Akira Kazaana, Yuta Nakano, Yui Nojiri, and Moeko Kashiwazaki. Antibacterial, antifungal and nematicidal activities of rare earth ions. *Biological trace element research*, 174(2):464–470, 2016.

[18] Lin Qi, Yuan Ge, Tian Xia, Ji-Zheng He, Congcong Shen, Jianlei Wang, and Yong-Jun Liu. Rare earth oxide nanoparticles promote soil microbial antibiotic resistance by selectively enriching antibiotic resistance genes. *Environmental Science: Nano*, 6(2):456–466, 2019.

[19] Ralf Kaegi, Alexander Gogos, Andreas Voegelin, Stephan J Hug, Lenny HE Winkel, Andreas M Buser, and Michael Berg. Quantification of individual rare earth elements from industrial sources in sewage sludge. *Water research X*, 11:100092, 2021.

[20] Urs F Uehlinger, Karl M Wantzen, Rob S Leuven, and Hartmut Arndt. *The Rhine river basin*. 2009.

[21] Serkan Kulaksız and Michael Bau. Anthropogenic dissolved and colloid/nanoparticle-bound samarium, lanthanum and gadolinium in the rhine river and the impending destruction of the natural rare earth element distribution in rivers. *Earth and Planetary Science Letters*, 362:43–50, 2013.

[22] Philip L Verplanck, Edward T Furlong, James L Gray, Patrick J Phillips, Ruth E Wolf, and Kathleen Esposito. Evaluating the behavior of gadolinium and other rare earth elements through large metropolitan sewage treatment plants. *Environmental science & technology*, 44(10):3876–3882, 2010.

[23] Pooria Ebrahimi and Maurizio Barbieri. Gadolinium as an emerging microcontaminant in water resources: threats and opportunities. *Geosciences*, 9(2):93, 2019.

[24] Klaus Kümmerer and Eckard Helmers. Hospital effluents as a source of gadolinium in the aquatic environment. *Environmental science & technology*, 34(4):573–577, 2000.

[25] Lena Telgmann, Christoph A Wehe, Marvin Birka, Jens Kunnemeyer, Sascha Nowak, Michael Sperling, and Uwe Karst. Speciation and isotope dilution analysis of gadolinium-based contrast agents in wastewater. *Environmental science & technology*, 46 (21):11929–11936, 2012.

[26] Francisco Gómez-Rivera, James A Field, Dustin Brown, and Reyes Sierra-Alvarez. Fate of cerium dioxide (ceo2) nanoparticles in municipal wastewater during activated sludge treatment. *Bioresource technology*, 108:300–304, 2012.

[27] Alexander Gogos, Jonas Wielinski, Andreas Voegelin, Frank von der Kammer, and Ralf Kaegi. Quantification of anthropogenic and geogenic ce in sewage sludge based on ce oxidation state and rare earth element patterns. *Water research X*, 9:100059, 2020.

[28] F Henry Firsching. Solubility products of the trivalent rare-earth arsenates. *Journal of Chemical and Engineering Data*, 37(4):497–499, 1992.

[29] Howard Leonard Recht and Masood Ghassemi. *Phosphate removal from wastewaters using lanthanum precipitation*. US Federal Water Quality Administration, 1970.

[30] Eugene V. Kleber and Howard L. Recht. Removal of phosphate from waste water, 1970. URL https://patentimages.storage.googleapis.com/e0/45/4b/ad16e40a7f79c5/US3956118.pdf. US Patent US3956118A.

[31] Neo Chemicals and Oxides. Phosphorus removal, 2020. URL http://neowatertreatment.com/phosphorus-removal.

[32] Mason Reames Haneline and James Frederic Gallman. Rare earth clarifying agent and method for use in primary treatment of wastewater. URL https: //patentimages.storage.googleapis.com/cf/4c/48/8972cf19173c57/WO2019089954A1.pdf. WIPO Patent WO2019089954A1.

[33] Anitha Kunhikrishnan, Md Aminur Rahman, Dane Lamb, Nanthi S Bolan, Surinder Saggar, Aravind Surapaneni, and Chengrong Chen. Rare earth elements (ree) for the removal and recovery of phosphorus: A review. *Chemosphere*, page 131661, 2021.

[34] Li Wang, Jingyi Wang, Chi He, Wei Lyu, Wenlong Zhang, Wei Yan, and Liu Yang. Development of rare earth element doped magnetic biochars with enhanced phosphate adsorption performance. *Colloids and Surfaces A: Physicochemical and Engineering Aspects*, 561:236–243, 2019.

[35] Willis Gwenzi, Lynda Mangori, Concilia Danha, Nhamo Chaukura, Nothando Dunjana, and Edmond Sanganyado. Sources, behaviour, and environmental and human health risks of high-technology rare earth elements as emerging contaminants. *Science of the Total Environment*, 636:299–313, 2018.

[36] Chrystelle NH Atinkpahoun, Marie-Noëlle Pons, Pauline Louis, Jean-Pierre Leclerc, and Henri H Soclo. Rare earth elements (ree) in the urban wastewater of cotonou (benin, west africa). *Chemosphere*, 251:126398, 2020.

[37] Simon M Jowitt, Timothy T Werner, Zhehan Weng, and Gavin M Mudd. Recycling of the rare earth elements. *Current Opinion in Green and Sustainable Chemistry*, 13:1–7, 2018.

[38] Didier Técher, Nicolas Grosjean, Bénédicte Sohm, Damien Blaudez, and Marie Le Jean. Not merely noxious? time-dependent hormesis and differential toxic effects systematically induced by rare earth elements in escherichia coli. *Environmental Science and Pollution Research*, 27(5):5640–5649, 2020.

[39] Yoshiko Fujita, Joni Barnes, and Sandra Fox. Rare earth element impacts on biological wastewater treatment. Technical report, Idaho National Lab.(INL), Idaho Falls, ID (United States), 2016.

[40] I Kamika and M Tekere. Impacts of cerium oxide nanoparticles on bacterial community in activated sludge. *AMB Express*, 7(1):1–11, 2017.

[41] Yan Yue, Lin Qi, Yan Li, Jichen Wang, Congcong Shen, and Yuan Ge. Negative effects of rare earth oxide nanoparticles of la2o3, nd2o3, and gd2o3 on the ammonia-oxidizing microorganisms. *Journal of Soils & Sediments: Protection, Risk Assessment, & Remediation*, 20(8), 2020.

[42] Jill E Clarridge III. Impact of 16s rrna gene sequence analysis for identification of bacteria on clinical microbiology and infectious diseases. *Clinical microbiology reviews*, 17(4): 840–862, 2004.

[43] Bo Yang, Yong Wang, and Pei-Yuan Qian. Sensitivity and correlation of hypervariable regions in 16s rrna genes in phylogenetic analysis. *BMC bioinformatics*, 17(1):1–8, 2016.

[44] Eduard Fadeev, Magda G Cardozo-Mino, Josephine Z Rapp, Christina Bienhold, Ian Salter, Verena Salman-Carvalho, Massimiliano Molari, Halina E Tegetmeyer, Pier Luigi Buttigieg, and Antje Boetius. Comparison of two 16s rrna primers (v3–v4 and v4–v5) for studies of arctic microbial communities. *Frontiers in microbiology*, 12:283, 2021.

[45] Ryan R Wick, Louise M Judd, Claire L Gorrie, and Kathryn E Holt. Completing bacterial genome assemblies with multiplex minion sequencing. *Microbial genomics*, 3(10), 2017.

[46] You Che, Yu Xia, Lei Liu, An-Dong Li, Yu Yang, and Tong Zhang. Mobile antibiotic resistome in wastewater treatment plants revealed by nanopore metagenomic sequencing. *Microbiome*, 7(1):1–13, 2019.

[47] Maciej Białasek and Aleksandra Miłobedzka. Revealing antimicrobial resistance in stormwater with minion. *Chemosphere*, 258:127392, 2020.

[48] Anders B Nygaard, Hege S Tunsjø, Roger Meisal, and Colin Charnock. A preliminary study on the potential of nanopore minion and illumina miseq 16s rrna gene sequencing to characterize building-dust microbiomes. *Scientific Reports*, 10(1):1–10, 2020.

[49] Yu Xia, An-Dong Li, Yu Deng, Xiao-Tao Jiang, Li-Guan Li, and Tong Zhang. Minion nanopore sequencing enables correlation between resistome phenotype and genotype of coliform bacteria in municipal sewage. *Frontiers in microbiology*, 8:2105, 2017.

[50] Amrita Srivathsan, Emily Hartop, Jayanthi Puniamoorthy, Wan Ting Lee, Sujatha Narayanan Kutty, Olavi Kurina, and Rudolf Meier. Rapid, large-scale species discovery in hyperdiverse taxa using 1d minion sequencing. *BMC biology*, 17(1):1–20, 2019.

[51] Sophie George, Louise Pankhurst, Alasdair Hubbard, Antonia Votintseva, Nicole Stoesser, Anna E Sheppard, Amy Mathers, Rachel Norris, Indre Navickaite, Chloe Eaton, et al. Resolving plasmid structures in enterobacteriaceae using the minion nanopore sequencer: assessment of minion and minion/illumina hybrid data assembly approaches. *Microbial genomics*, 3(8), 2017.

[52] LARS Sandlund, MIRKA Fahlander, TORD Cedell, AE Clark, JB Restorff, and M Wun-Fogle. Magnetostriction, elastic moduli, and coupling factors of composite terfenol-d. *Journal of Applied Physics*, 75(10):5656–5658, 1994.

[53] Zhu Houqing, Liu Jianguo, Wang Xiurong, Xing Yanhong, and Zhang Hongping. Applications of terfenol-d in china. *Journal of Alloys and Compounds*, 258(1-2):49–52, 1997.

[54] Priya Choudhry. High-throughput method for automated colony and cell counting by digital image analysis based on edge detection. *PloS one*, 11(2):e0148469, 2016.

[55] Torsten Hothorn, Frank Bretz, and Peter Westfall. Simultaneous inference in general parametric models. *Biometrical Journal*, 50(3):346–363, 2008.

[56] Melvin Weinstein, James S. Lewis II, April M. Bobenchik, Shelley Campeau, Marcelo F. Galas, Howard Gold, Romney M. Humphries, Thomas J. Kirn Jr., Brandi Limbago, Amy J. Mathers, Tony Mazzulli, Michael Satlin, Audrey N. Schuetz, Patricia J. Simner, and Pranita D. Tamma. Performance standards for antimicrobial susceptibility testing. Technical Report M100, Clinical and Laboratory Standards Institute, Wayne, PA (United States), 2020.

[57] Ya Hu, Lu Liu, Xiaoxia Zhang, Yu Feng, and Zhiyong Zong. In vitro activity of neomycin, streptomycin, paromomycin and apramycin against carbapenem-resistant enterobacteriaceae clinical strains. *Frontiers in microbiology*, 8:2275, 2017.

[58] Nagraj Mani, Christian H Gross, Jonathan D Parsons, Brian Hanzelka, Ute Muh, Steve Mullin, Yusheng Liao, Anne-Laure Grillot, Dean Stamos, Paul S Charifson, et al. In vitro characterization of the antibacterial spectrum of novel bacterial type ii topoisomerase inhibitors of the aminobenzimidazole class. *Antimicrobial agents and chemotherapy*, 50(4): 1228–1237, 2006.

[59] Paolo Madoni, Genoveva Esteban, and Gessica Gorbi. Acute toxicity of cadmium, copper, mercury, and zinc to ciliates from activated sludge plants. *Bulletin of environmental contamination and toxicology*, 49(6):900–905, 1992.

[60] Oxford Nanopore Technologies. Genomic dna by ligation (sqk-lsk110). Technical report, Oxford Nanopore Technologies, Oxford, UK, 2021. URL https://store.nanoporetech.net/ligation-sequencing-kit110.html.

[61] GA Arango-Argoty, Dongjuan Dai, Amy Pruden, P Vikesland, Lenwood S Heath, and Liqing Zhang. Nanoarg: a web service for detecting and contextualizing antimicrobial resistance genes from nanopore-derived metagenomes. *Microbiome*, 7(1):1–18, 2019.

[62] OECD. *Test No. 209: Activated Sludge, Respiration Inhibition Test (Carbon and Ammonium Oxidation)*. 2010. doi: https://doi.org/https://doi.org/10.1787/9789264070080-en. URL https://www.oecd-ilibrary.org/content/publication/9789264070080-en.

[63] L. Clesceri, A. Greenberg, and Eaton. A. *Standard methods for the examination of water and wastewater*. American Public Health Association, American Water Works Association, Water Environment Federation, Washington, DC, USA, 1999.

[64] Thongchai Panswad and Chadarut Anan. Specific oxygen, ammonia, and nitrate uptake rates of a biological nutrient removal process treating elevated salinity wastewater. *Bioresource Technology*, 70(3):237–243, 1999.

[65] Hadley Wickham. The split-apply-combine strategy for data analysis. *Journal of Statistical Software*, 40(1):1–29, 2011. URL http://www.jstatsoft.org/v40/i01/.

[66] Hadley Wickham, Mara Averick, Jennifer Bryan, Winston Chang, Lucy D'Agostino McGowan, Romain François, Garrett Grolemund, Alex Hayes, Lionel Henry, Jim Hester, Max Kuhn, Thomas Lin Pedersen, Evan Miller, Stephan Milton Bache, Kirill Müller, Jeroen Ooms, David Robinson, Dana Paige Seidel, Vitalie Spinu, Kohske Takahashi, Davis Vaughan, Claus Wilke, Kara Woo, and Hiroaki Yutani. Welcome to the tidyverse. *Journal of Open Source Software*, 4(43):1686, 2019. doi: 10.21105/joss.01686.

[67] Olivia Salmon. Impacts of rare earth elements on biological wastewater treatment processes. Master's thesis, Colorado School of Mines, Golden, CO, 2019.

[68] Blake W Stamps, Menu B Leddy, Megan H Plumlee, Nur A Hasan, Rita R Colwell, and John R Spear. Characterization of the microbiome at the world's largest potable water reuse facility. *Frontiers in microbiology*, 9:2435, 2018.

[69] Alma E Parada, David M Needham, and Jed A Fuhrman. Every base matters: assessing small subunit rrna primers for marine microbiomes with mock communities, time series and global field samples. *Environmental microbiology*, 18(5):1403–1414, 2016.

[70] Evan Bolyen, Jai Ram Rideout, Matthew R Dillon, Nicholas A Bokulich, Christian C Abnet, Gabriel A Al-Ghalith, Harriet Alexander, Eric J Alm, Manimozhiyan Arumugam, Francesco Asnicar, et al. Reproducible, interactive, scalable and extensible microbiome data science using qiime 2. *Nature biotechnology*, 37(8):852–857, 2019.

[71] Benjamin J Callahan, Paul J McMurdie, Michael J Rosen, Andrew W Han, Amy Jo A Johnson, and Susan P Holmes. Dada2: high-resolution sample inference from illumina amplicon data. *Nature methods*, 13(7):581–583, 2016.

[72] Elmar Pruesse, Christian Quast, Katrin Knittel, Bernhard M Fuchs, Wolfgang Ludwig, Jörg Peplies, and Frank Oliver Glöckner. Silva: a comprehensive online resource for quality checked and aligned ribosomal rna sequence data compatible with arb. *Nucleic acids research*, 35(21):7188–7196, 2007.

[73] Stefan Janssen, Daniel McDonald, Antonio Gonzalez, Jose A Navas-Molina, Lingjing Jiang, Zhenjiang Zech Xu, Kevin Winker, Deborah M Kado, Eric Orwoll, Mark Manary, et al. Phylogenetic placement of exact amplicon sequences improves associations with clinical information. *Msystems*, 3(3):e00021–18, 2018.

[74] Nam-phuong Nguyen, Siavash Mirarab, Bo Liu, Mihai Pop, and Tandy Warnow. Tipp: taxonomic identification and phylogenetic profiling. *Bioinformatics*, 30(24):3548–3555, 2014.

[75] Paul J McMurdie and Susan Holmes. phyloseq: an r package for reproducible interactive analysis and graphics of microbiome census data. *PloS one*, 8(4):e61217, 2013.

[76] Damian D Baldwin and Christine E Campbell. Short-term effects of low ph on the microfauna of an activated sludge wastewater treatment system. *Water Quality Research Journal*, 36(3):519–535, 2001.

[77] Özer Çinar. New tool for evaluation of performance of wastewater treatment plant: artificial neural network. *Process Biochemistry*, 40(9):2980–2984, 2005.

[78] Per Halkjær Nielsen, Bo Frølund, Stephan Spring, and Frank Caccavo Jr. Microbial fe (iii) reduction in activated sludge. *Systematic and applied microbiology*, 20(4):645–651, 1997.

[79] Jeppe L Nielsen and Per H Nielsen. Microbial nitrate-dependent oxidation of ferrous iron in activated sludge. *Environmental science & technology*, 32(22):3556–3561, 1998.

[80] Qiong Wu, Jie Chen, Malcolm Clark, and Yan Yu. Adsorption of copper to different biogenic oyster shell structures. *Applied surface science*, 311:264–272, 2014.

[81] Valeria Ochoa-Herrera, Glendy León, Qais Banihani, Jim A Field, and Reyes Sierra-Alvarez. Toxicity of copper (ii) ions to microorganisms in biological wastewater treatment systems. *Science of the total environment*, 412:380–385, 2011.

[82] Ghufranud Din, Asifa Farooqi, Wasim Sajjad, Muhammad Irfan, Sarah Gul, and Aamer Ali Shah. Cadmium and antibiotic-resistant acinetobacter calcoaceticus strain stp14 reported from sewage treatment plant. *Journal of Basic Microbiology*, 61(3):230–240, 2021.

[83] Ujjwal Jit Kaur, Simran Preet, and Praveen Rishi. Augmented antibiotic resistance associated with cadmium induced alterations in salmonella enterica serovar typhi. *Scientific reports*, 8(1):1–10, 2018.

[84] Daniela Numberger, Lars Ganzert, Luca Zoccarato, Kristin Mühldorfer, Sascha Sauer, Hans-Peter Grossart, and Alex D Greenwood. Characterization of bacterial communities in wastewater with enhanced taxonomic resolution by full-length 16s rrna sequencing. *Scientific reports*, 9(1):1–14, 2019.

[85] Eugene Rosenberg, Edward F DeLong, Stephen Lory, Erko Stackebrandt, and Fabiano Thompson. *The prokaryotes: Firmicutes and tenericutes*. Springer, 2014.

[86] Basavaraj C Metri, P Jyothi, and Basavaraj V Peerapur. Antibiotic resistance in citrobacter spp. isolated from urinary tract infection. *Urology annals*, 5(4):312, 2013.

[87] Liyun Liu, Ruiting Lan, Liqin Liu, Yonglu Wang, Yushi Zhang, Yiting Wang, and Jianguo Xu. Antimicrobial resistance and cytotoxicity of citrobacter spp. in maanshan anhui province, china. *Frontiers in microbiology*, 8:1357, 2017.

[88] Jan Hrbacek, Pavel Cermak, and Roman Zachoval. Current antibiotic resistance patterns of rare uropathogens: survey from central european urology department 2011–2019. *BMC urology*, 21(1):1–8, 2021.

[89] ViralZone. Lambdavirus, 2011. URL https://viralzone.expasy.org/512?outline=all_by_species.

[90] Kunihiko Nishino and Akihito Yamaguchi. Role of histone-like protein h-ns in multidrug resistance of escherichia coli. *Journal of bacteriology*, 186(5):1423–1429, 2004.

[91] Benmalek Yamina, Benayad Tahar, and Fardeau Marie Laure. Isolation and screening of heavy metal resistant bacteria from wastewater: a study of heavy metal co-resistance and antibiotics resistance. *Water Science and Technology*, 66(10):2041–2048, 2012.

[92] Xunchao Cai, Xin Zheng, Dunnan Zhang, Waheed Iqbal, Changkun Liu, Bo Yang, Xu Zhao, Xiaoying Lu, and Yanping Mao. Microbial characterization of heavy metal resistant bacterial strains isolated from an electroplating wastewater treatment plant. *Ecotoxicology and environmental safety*, 181:472–480, 2019.

[93] Sangwon Lee, Jil T Geller, Tamas Torok, Cindy H Wu, Mary Singer, Francine C Reid, Daniel R Tarjan, Terry C Hazen, Adam P Arkin, and Nathan J Hillson. Characterization of wastewater treatment plant microbial communities and the effects of carbon sources on diversity in laboratory models. *PloS one*, 9(8):e105689, 2014.

[94] Bing Guo, Zhiya Sheng, and Yang Liu. Evaluation of influent microbial immigration to activated sludge is affected by different-sized community segregation. *npj Clean Water*, 4 (1):1–5, 2021.

[95] Jing Ding, Xin Li An, Simon Bo Lassen, Hong Tao Wang, Dong Zhu, and Xin Ke. Heavy metal-induced co-selection of antibiotic resistance genes in the gut microbiota of collembolans. *Science of the Total Environment*, 683:210–215, 2019.

[96] Jesse C Thomas IV, Adelumola Oladeinde, Troy J Kieran, John W Finger Jr, Natalia J Bayona-Vásquez, John C Cartee, James C Beasley, John C Seaman, J Vuan McArthur, Olin E Rhodes Jr, et al. Co-occurrence of antibiotic, biocide, and heavy metal resistance genes in bacteria from metal and radionuclide contaminated soils at the savannah river site. *Microbial biotechnology*, 13(4):1179–1200, 2020.

[97] Andrea Di Cesare, Ester M Eckert, Silvia D'Urso, Roberto Bertoni, David C Gillan, Ruddy Wattiez, and Gianluca Corno. Co-occurrence of integrase 1, antibiotic and heavy metal resistance genes in municipal wastewater treatment plants. *Water Research*, 94:208–214, 2016.

[98] Bulent Icgen and Fadime Yilmaz. Co-occurrence of antibiotic and heavy metal resistance in kızılırmak river isolates. *Bulletin of environmental contamination and toxicology*, 93(6): 735–743, 2014.

[99] Pennsylvania Department of Environmental Protection. Wastewater treatment plant operator certification training instructor guide. Technical Report Module 16: The Activated Sludge Process Part II, Pennsylvania Department of Environmental Protection, Harrisburg, PA (United States), 2014.

[100] George Tchobanoglus, Franklin Burton, and H David Stensel. Wastewater engineering: Treatment and reuse. *American Water Works Association. Journal*, 95(5):201, 2003.

[101] James E Alleman and Robert L Irvine. Storage-induced denitrification using sequencing batch reactor operation. *Water Research*, 14(10):1483–1488, 1980.

[102] Raymond J Zeng, Romain Lemaire, Zhiguo Yuan, and Jürg Keller. Simultaneous nitrification, denitrification, and phosphorus removal in a lab-scale sequencing batch reactor. *Biotechnology and bioengineering*, 84(2):170–178, 2003.

[103] American Water Works Association. Nitrification. Technical report, United States Environmental Protection Agency, Washington, DC (United States), 2002. URL https://www.epa.gov/sites/default/files/2015-09/documents/nitrification_1.pdf.

[104] Hao Su, Dachao Zhang, Philip Antwi, Longwen Xiao, Zuwen Liu, Xiaoyu Deng, Akwasi Bonsu Asumadu-Sakyi, and Jianzheng Li. Effects of heavy rare earth element (yttrium) on partial-nitritation process, bacterial activity and structure of responsible microbial communities. *Science of The Total Environment*, 705:135797, 2020.

[105] Caigui Luo, Yangwu Deng, Jian Liang, Sipin Zhu, Zhenya Wei, Xiaobin Guo, and Xianping Luo. Exogenous rare earth element-yttrium deteriorated soil microbial community structure. *Journal of Rare Earths*, 36(4):430–439, 2018.

[106] Paul Roots, Yubo Wang, Alex F Rosenthal, James S Griffin, Fabrizio Sabba, Morgan Petrovich, Fenghua Yang, Joseph A Kozak, Heng Zhang, and George F Wells. Comammox nitrospira are the dominant ammonia oxidizers in a mainstream low dissolved oxygen nitrification reactor. *Water research*, 157:396–405, 2019.

[107] Shaoyi Xu, Baozhan Wang, Yong Li, Daqian Jiang, Yuting Zhou, Aqiang Ding, Yuxiao Zong, Xiaoting Ling, Senyin Zhang, and Huijie Lu. Ubiquity, diversity, and activity of comammox nitrospira in agricultural soils. *Science of The Total Environment*, 706:135684, 2020.

[108] Lihong Wang, Jingfang He, Ao Xia, Mengzhu Cheng, Qing Yang, Chunlei Du, Haiyan Wei, Xiaohua Huang, and Qing Zhou. Toxic effects of environmental rare earth elements on delayed outward potassium channels and their mechanisms from a microscopic perspective. *Chemosphere*, 181:690–698, 2017.

[109] Can Li, Shufeng Liu, Tao Ma, Maosheng Zheng, and Jinren Ni. Simultaneous nitrification, denitrification and phosphorus removal in a sequencing batch reactor (sbr) under low temperature. *Chemosphere*, 229:132–141, 2019.

APPENDIX A

ADDITIONAL DATA

Table A.1 Analyte concentrations in each recycling waste, determined from ICP analysis. BDL indicates a measurement below the instrument's detection limit.

Analyte	**Detection Limit (mM)**	**W1A**	**W1B**	**W2A**	**W2B**
		Concentration (mM)			
Al	2.96E-05	BDL	0.002	3.2	0.018
As	5.98E-04	0.046	4.4E-04	0.039	BDL
B	1.74E-04	1.86	0.018	BDL	0.053
Ba	3.65E-05	BDL	1.6E-05	BDL	1.7E-05
Be	1.39E-06	BDL	BDL	BDL	5.8E-04
Ca	1.02E-03	BDL	0.005	BDL	0.011
Cd	6.73E-05	BDL	3.0E-05	0.004	1.7E-05
Co	3.08E-05	0.007	3.1E-04	0.008	1.1E-04
Cu	3.62E-04	0.168	0.185	143	0.007
Cr	3.75E-05	BDL	0.001	BDL	5.1E-05
Fe	8.94E-05	67.8	0.058	212	0.010
K	4.23E-03	8.07	0.029	3.55	7.04
Li	3.42E-05	1.54	0.009	1.44	0.133
Mg	4.93E-04	0.333	1.38	BDL	0.005
Mn	9.28E-06	0.002	6.4E-05	0.003	1.6E-04
Mo	1.19E-04	BDL	8.5E-05	BDL	1.1E-04
Na	4.44E-04	300	2.63	429	417
Ni	8.52E-05	BDL	9.6E-04	BDL	0.001
P	2.86E-03	BDL	0.030	16.9	81.5
Pb	1.04E-03	BDL	9.9E-05	0.097	3.3E-04
S	4.76E-04	803	17.4	683	150
Sb	4.47E-04	BDL	BDL	BDL	BDL
Se	6.50E-04	0.031	5.5E-04	BDL	4.1E-04
Si	2.90E-03	BDL	0.010	2.64	0.079
Sn	6.42E-04	BDL	2.1E-04	BDL	BDL
Sr	2.57E-05	BDL	1.3E-05	0.004	2.2E-05
Ti	4.33E-06	BDL	3.9E-05	0.052	BDL
Tl	2.14E-03	BDL	BDL	0.016	BDL
V	1.95E-05	0.004	3.1E-05	BDL	1.3E-05
Zn	1.50E-04	0.012	8.6E-04	0.096	0.001

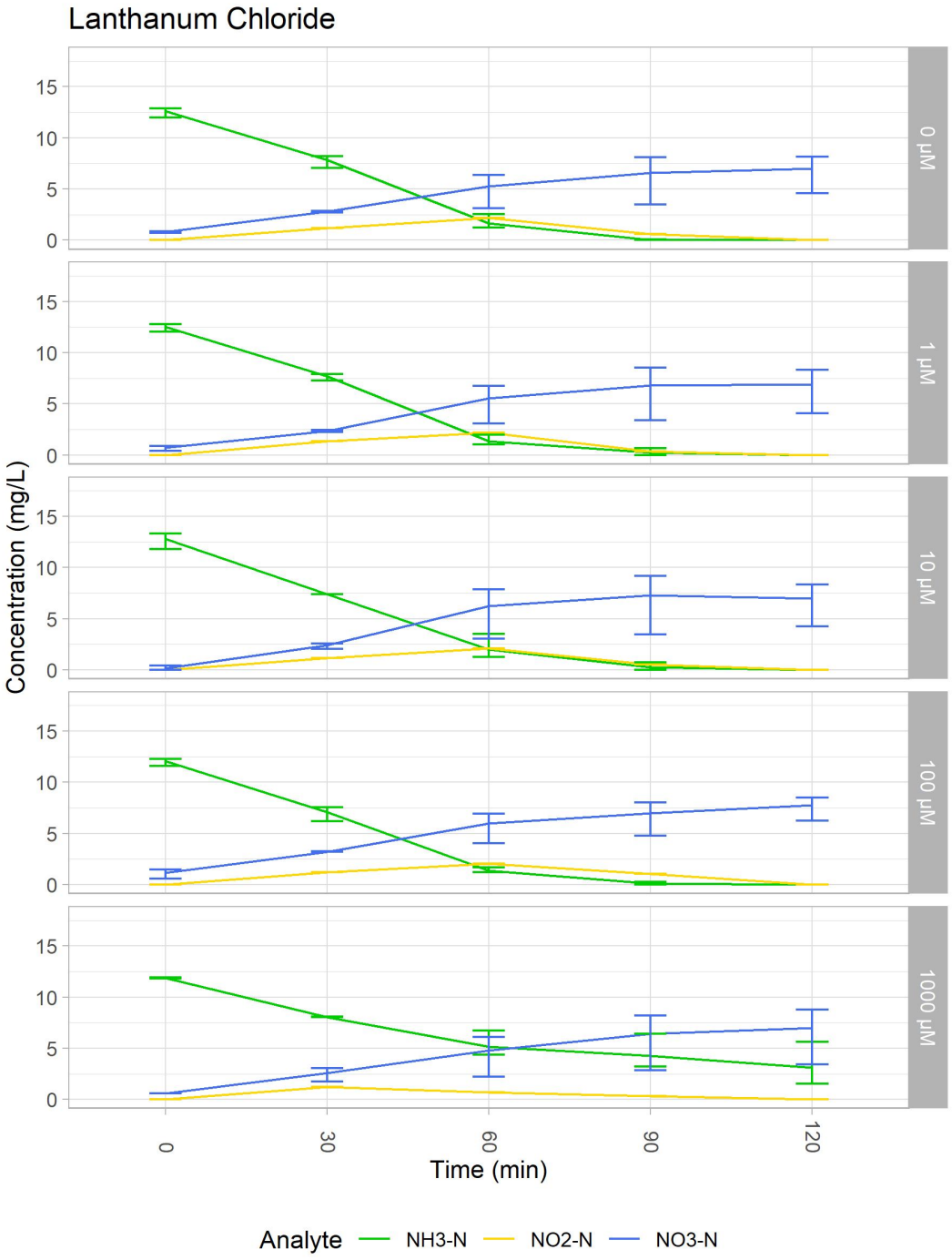

Figure A.1 Nitrogen species (NH_3-N, NO_2-N, NO_3-N) measurements in reactors amended with lanthanum chloride at each sampling time. Error bars show the standard deviation of measurements from replicate reactors.

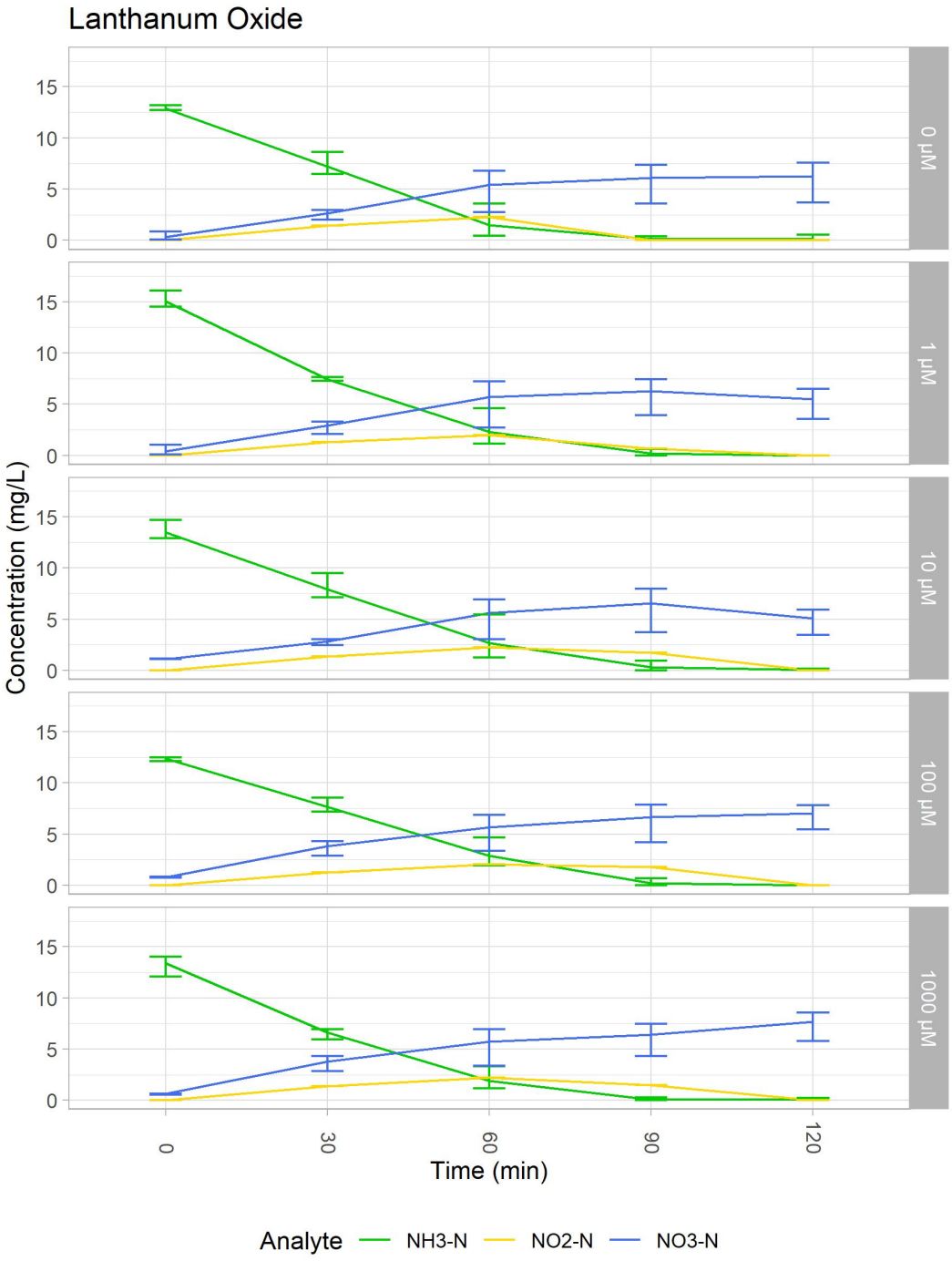

Figure A.2 Nitrogen species (NH_3-N, NO_2-N, NO_3-N) measurements in reactors amended with lanthanum oxide at each sampling time. Error bars show the standard deviation of measurements from replicate reactors.

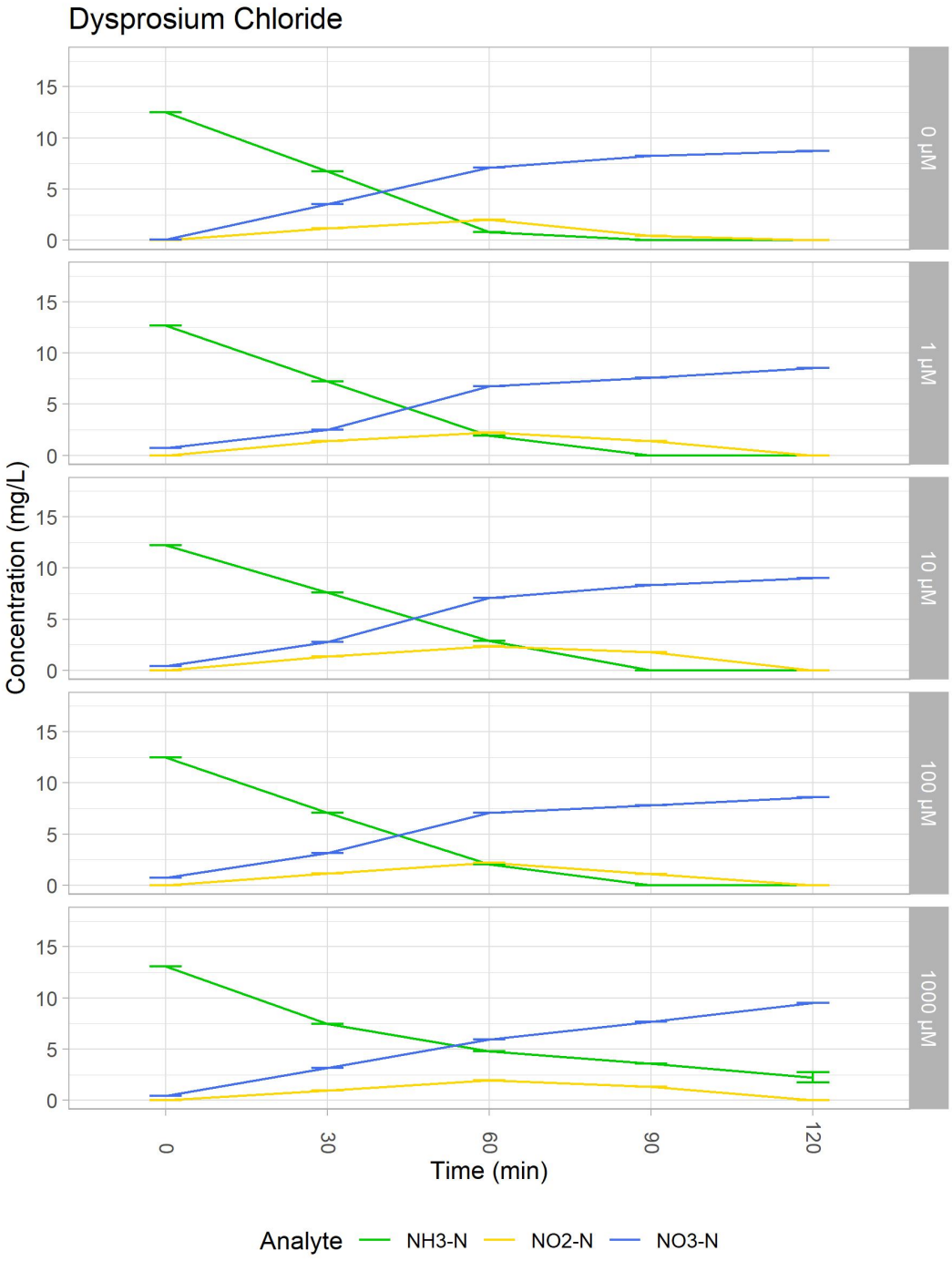

Figure A.3 Nitrogen species (NH_3-N, NO_2-N, NO_3-N) measurements in reactors amended with dysprosium chloride at each sampling time. Error bars show the standard deviation of measurements from replicate reactors.

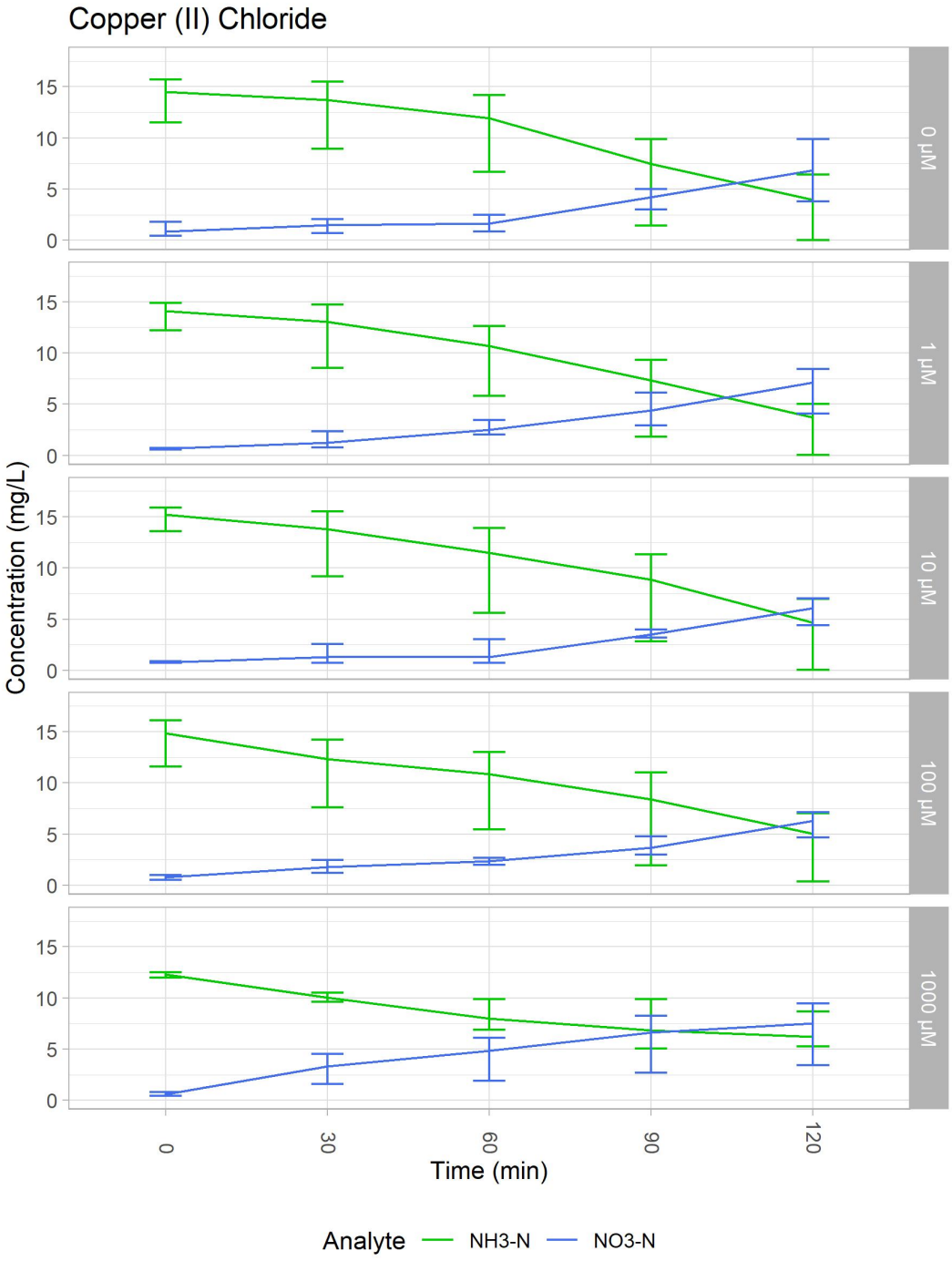

Figure A.4 Nitrogen species (NH_3-N, NO_3-N) measurements in reactors amended with copper (II) chloride at each sampling time. Copper (II) chloride-amended reactors were tested before nitrite (NO_2-N) measurements were added to the protocol. Error bars show the standard deviation of measurements from replicate reactors.

APPENDIX B

COPYRIGHT PERMISSIONS

B.1 Terfenol-D Recycling Process

Denis Prodius and Ikenna Nlebedim, of Ames Laboratory, provided Figure 3.1 and permitted use of the schematic for this thesis via email (Figure B.1).

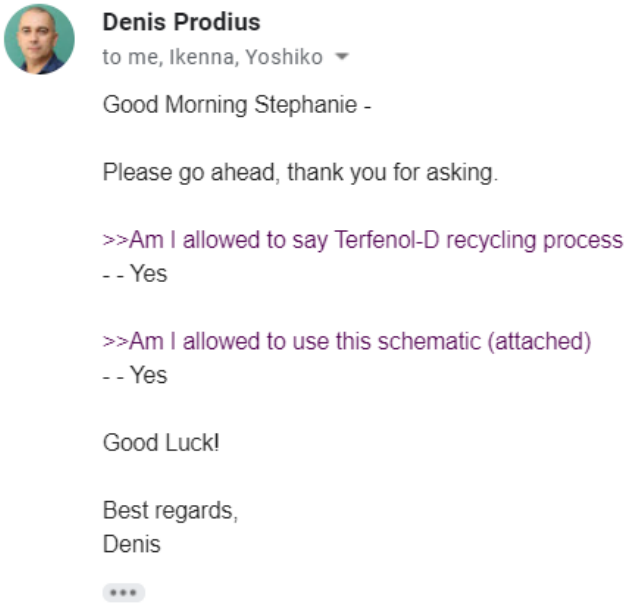

Denis Prodius
to me, Ikenna, Yoshiko

Good Morning Stephanie -

Please go ahead, thank you for asking.

>>Am I allowed to say Terfenol-D recycling process
- - Yes

>>Am I allowed to use this schematic (attached)
- - Yes

Good Luck!

Best regards,
Denis

Figure B.1 Approval for use of Terfenol-D schematic.

B.2 Oxford Nanopore

On their website, Oxford Nanopore provide press images of their products for public use (Figure B.2). An image of a MinION sequencing device was used to create Figure 3.3. I have confirmed the reuse of these images with representatives via email (Figure B.3).

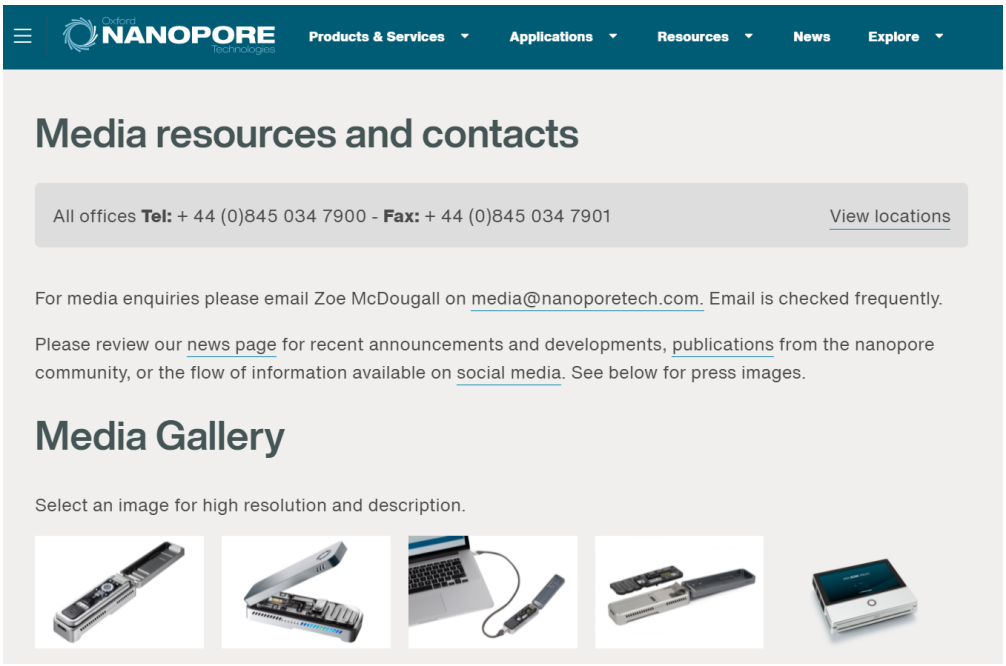

Figure B.2 Oxford Nanopore media gallery.

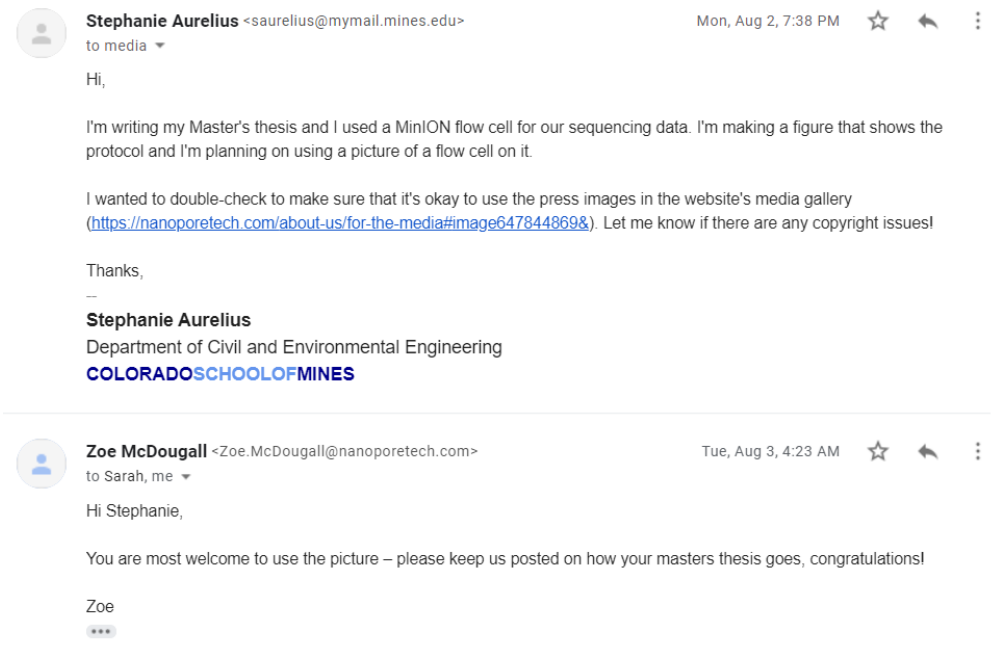

Figure B.3 Approval for use of Oxford Nanopore media.